Nordic Volcanological Institute 9901
University of Iceland

THE KRAFLA CENTER OF INFLATIONS AND DEFLATIONS DURING THE YEARS 1975 TO 1997

Based on analysis of tilt and distance measurements
made by
The Nordic Volcanological Institute, Reykjavík

by

Eysteinn Tryggvason

Reykjavík 1999

The author of this report worked at the Nordic Volcanological Institute, Reykjavík from 1977 to 1994. His principal duties during that period were to study ground deformation at active volcanoes in Iceland. The volcano Krafla in North Iceland went into an eruptive phase in 1975 and remained more or less active during the following 20 years. Because of this activity of Krafla, a large portion of the author's effort at the Nordic Volcanological Institute was related to ground deformation at that volcano. Extensive programs of measurements of ground tilt and electronic distance measurements were designed and carried out in addition to observations by electronic tiltmeters and lake level measurements. These measurements, together with measurements by several other institutions added very significantly to the knowledge of sub-surface processes and conditions which controlled the activity of Krafla, and maintained that activity for 20 years.

The great amount of observational data on ground deformation of Krafla, collected by the Nordic Volcanological Institute 1975 to 1995 still contain information which have not been analysed and published. This present report is an effort to use this data to investigate one special problem, that of location of the center of volcanic activity at Krafla. Although several authors have arrived at a location of the source of inflation and deflation at Krafla, it appeared of some importance to analyse long series of rather uniform observational data to investigate the stability with time of the source location, and also to investigate the capacity of the observational methods used at the Nordic Volcanological Institute to locate precisely a source of deformation.

November, 1998

Eysteinn Tryggvason
Ásgarðsvegi 10
640 Húsavík

CONTENTS

INTRODUCTION

The Krafla fires of 1975-1978 commenced with an event of great ground rifting along the Krafla fissure zone of North Iceland, an intense swarm of earthquakes, and a small volcanic eruption on December 20, 1975 (Björnsson et al. 1979). The continuation of this volcanic and tectonic activity included about 20 rifting events, when segments of the Krafla fissure swarm were widened by opening of old or new fissures, eight volcanic eruptions in addition to that of December 20, 1975, the last one on September 4 to 18, 1984, and repeated uplift and subsidence of the ground in the Krafla area (Tryggvason 1984). The observed ground deformation continued for several years after the eruptions ceased, and at the time of this writing in 1998, some ground deformation is still taking place.

This ground deformation was observed by measurements of various components of the deformation, using many different techniques. These included optical levelling to observe vertical ground displacements (Björnsson and Eysteinsson 1998, Spickernagel 1980, Czubik 1988) and ground tilt (Tryggvason 1995), electronic distance measurements (EDM) to observe horizontal ground displacements (Möller and Ritter 1980, Tryggvason 1993), lake level measurements (Tryggvason 1987), gravity measurements (Torge 1981) and various types of strain measurements.

During the period of most intense activity, from late 1975 to end of 1981, the vertical component of ground deformation consisted of periodic uplift and subsidence of a near circular area, centred near the center of the Krafla volcano. The uplift or inflation lasted for several months while the subsidence or deflation was much more violent and lasted for a few hours to several days.

Outside of the Krafla volcano proper, the vertical component of ground deformation consisted of subsidence of a narrow strip of land extending along the N13°E trending Krafla fissure zone, while the flanks of this strip were uplifted, this uplift decreasing gradually with distance from the fissure zone. The subsided strip is about one km wide in the vicinity of Krafla, but its northern part is wider, probably about 4 km near the north coast of Iceland. This vertical ground displacements along the fissure zone coincided in time with the deflations of the Krafla volcano.

The rate of ground deformation decreased markedly after 1981 and especially after 1984. Sometimes no deformation was observed for many months (Tryggvason 1994), and the rate of deformation varied irregularly. A significant change in the progress of ground deformation occurred in 1989, probably early that year, when slow inflation, which had been in progress more or less continuously, ceased altogether, and slow deflation of the Krafla volcano commenced. This slow deflation has continued until the time of this writing in 1998 at slowly decreasing rate.

The horizontal component of ground deformation during the period of the Krafla fires was observed along the Krafla fissure zone as displacements of its flanks away from each other during rifting events, signifying widening of the fissure zone. This displacement of the flanks away from the fissure zone, decreases gradually with distance from the fissure zone. Thus the fissure zone did expand in east-west direction, perpendicular to its strike, while the flanks were contracted in east-west direction. Furthermore, horizontal component of ground deformation of the Krafla volcano proper include gradual ground displacement away from the center of the volcano during periods of inflation, and rapid displacements towards the center of the volcano during deflation events.

The rifting events always coincided with subsidence of the Krafla region, but some small subsidence events were not associated with any observed ground rifting. Further, all eruptions of Krafla coincide with deflation events, although many deflation events were not associated with any eruptions.

The aim of the present report is to use repeated tilt and EDM observations to determine the precise location of the source of the near circular inflations and deflations which were observed repeatedly at Krafla from 1975 to 1995, and to investigate if the source location was stationary throughout this period. Most of the observational data for this study was obtained by the Nordic Volcanological Institute.

The tilt observations were initiated in 1976 at several optical levelling tilt stations. Most of these tilt stations consist of 5 permanent markers arranged in a circular array of 25 m radius. More tilt stations were constructed in 1977, 1981 and 1984 (Table I,1 and Fig. I,1). These tilt stations were initially occupied several times each year, but frequency of observations was gradually decreased to once per year after 1988.

The electronic distance measurements (EDM) were initiated in early 1977 when about 40 permanent markers were constructed and more markers were added later (Table I,2 and Fig. I,1). Measurements of distances between these markers were usually made once or twice each year. The present study used only distance measurements between markers within about 7 km distance from the suggested center of deformation.

It is assumed that the inflations were the result of increased pressure in the source region, caused by influx of molten magma into a hypothetical magma chamber and that deflations are caused by pressure drop in the source region because of flow of magma out of the same magma chamber.

The use of surface observations to detect sub-surface processes requires the use of models to predict which type of processes will produce the observed surface deformation. Ewart et al. (1991) made an extensive model study of the source of deformation at Krafla by using some of the same observational data as are used in the present study, in addition to extensive levelling data obtained by the National Energy Authority. They found that double-sphere or ellipsoid models did fit the observations better than did single sphere models and that vertical displacement observations agreed better with the models, than did distance measurements or tilt.

The present study uses the single point source Mogi (1958) model to study consistency and possible change with time of the source of deformation. The tilt observations deviate significantly from that predicted by a single point source model, but the deviations are rather systematic (Tryggvason 1995). The observed tilt at any tilt station has tendency to always deviate in the same manner from the tilt predicted by the Mogi model. Although the cause of these systematic deviations are not known, it is strongly suggested that station locations are somehow responsible. Possible causes are inhomogeneity of elastic properties of the underlying formations, near surface fissures and topography.

Although the observed tilt at several tilt stations deviates significantly from the predicted by the Mogi model, the tilt observations are considered as rather reliable as a tool to study possible variation of source location with time.

Deviations of distance measurements from models are also significantly greater than the estimated observational errors. The cause of this is assumed to be the same as that of systematic deviation of tilt observations from the models, that local irregularities in elastic properties of the underlying formations causes irregularity of the displacement field.

The geographic coordinates used for most of the calculations presented in this report are rectangular coordinates in kilometers of transverse Mercator projection, international spheroid, zone 28, horizontal reference datum Reykjavík. The results which are presented in tables and figures were modified to agree with the World Geodetic System 1984 horizontal datum. However, the contoures of maps in this report use Hjörsey horizontal reference datum.

Table I,1

Optical levelling tilt stations in the southern section of the Krafla area.

Station Identification	East coordinate km	North coordinate Km	Time when established	Type of tilt station. *)
Námaskarð	17.434	82.091	Jan 1976	L, 5
0000	18.188	85.767	July 1976	O, 6
0010	18.153	89.948	July 1976	O, 5
0020	10.963	82.863	July 1976	O, 5
0040	22.283	85.320	July 1976	O, 5
0050	13.010	79.212	May 1977	O, 5
0060	13.148	79.815	May 1977	O, 5
0070	12.422	81.260	May 1977	O, 5
0080	14.482	88.917	June 1977	O, 5
0090	15.118	90.668	June 1977	O, 5
0200	12.753	77.066	June 1977	O, 5
0210	13.376	83.117	Oct. 1981	O, 5
0220	16.702	80.901	Oct. 1981	O, 5
0230	16.089	79.613	Oct. 1981	O, 5
0240	13.822	84.003	Oct. 1981	O, 5
0250	15.588	85.840	Oct 1981	O, 5
0260	20.381	92.862	Oct. 1984	O, 5
Sandmúli	20.362	94.620	Oct. 1984	L, 9

*) Stations of bench marks in star-like pattern are marked "O", and those with markers on two lines more or less perpendicular to each other are marked "L", the number of marker in each station is indicated.

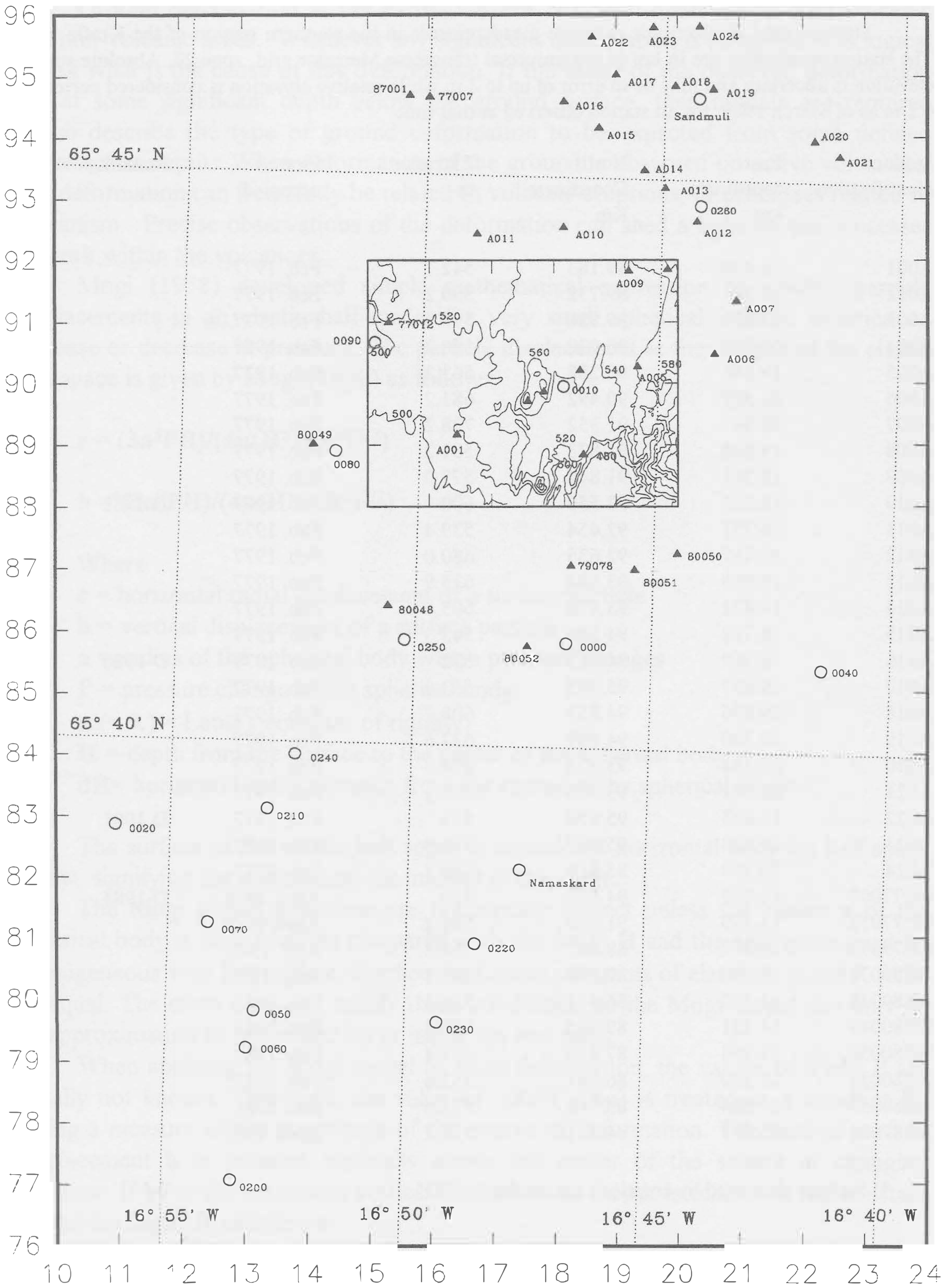

Fig. I,1. Location of optical levelling tilt stations (open circles) and stations for electronic distance measurements (solid triangles) in the Krafla area. A rectangle with contour lines inside is the area of several maps later in this report. Numbers outside the frame are coordinates in kilometers in transverse Mercator projection.

Table I,2

Stations used in electronic distance measurements in the southern section of the Krafla area. The station coordinates are in km in the universal transverse Mercator grid, zone 27. Absolute station elevation is uncertain and may be in error of up to 3 m while relative elevation is considered correct to 0.1 m as of March 1989, for all station observed at that time.

Station identification	East coordinate km	North Coordinate Km	Elevation m	First occupied	Remarks
A001	16.439	89.183	542.7	Feb. 1977	
A002	17.581	89.732	590.1	Feb. 1977	
A003	17.834	89.880	593.5	Feb. 1977	
A004	18.419	90.230	550.2	Feb. 1977	
A005	19.346	90.288	563.3	Feb. 1977	
A006	20.597	90.492	681.2	Feb. 1977	
A007	20.943	91.352	728.2	Feb. 1977	
A008	19.838	91.873	581.2	Feb. 1977	
A009	19.201	91.844	577.0	Feb. 1977	
A010	18.155	92.550	600	Feb. 1977	D 1981
A011	16.771	92.454	539.4	Feb. 1977	
A012	20.317	92.635	680.0	Feb. 1977	
A013	19.809	93.184	625.9	Feb. 1977	
A014	19.471	93.470	605.6	Feb. 1977	
A015	18.732	94.180	543.3	Feb. 1977	
A016	18.169	94.613	522	Feb. 1977	D 1980
A017	19.007	95.045	553.4	Feb. 1977	
A018	19.976	94.853	608.7	Feb. 1977	
A019	20.590	94.802	637.6	Feb. 1977	
A020	22.194	93.935	674.3	Feb. 1977	
A021	22.601	93.675	713.1	Feb. 1977	
A022	18.623	95.659	523	Feb. 1977	D 1981
A023	19.623	95.807	575.9	Feb. 1977	
A024	20.369	95.815	645.7	Feb. 1977	
NE77007	16.017	94.691	513	April 1978	D 1984
NE77012	15.339	91.016	546.2	April 1978	
NE79077	18.477	88.862	558.3	Aug. 1979	
NE79078	18.276	87.056	494.4	Aug. 1979	
NE80048	15.328	86.411	536.6	Feb. 1981	
NE80049	14.131	89.045	572.4	Feb. 1981	
NE80050	19.994	87.250	621.4	Feb. 1981	
NE80051	19.300	86.987	552.6	Feb. 1981	
NE80052	17.564	85.748	515.6	Feb. 1981	
NE87001	15.697	94.721	517.1	April 1988	

*) Stations destroyed by eruptions are marked by "D"

THE MOGI MODEL

Ground deformation at the earth's surface has been observed in both volcanic and non-volcanic areas. Whenever any significant deformation is observed, it is logical to ask what is the cause of this deformation. If the cause of the observed deformation lies at some significant depth below the ground surface, then models are required which describe the type of ground deformation to be expected from some defined processes at depth. When deformation of the ground is observed on active volcanoes, this deformation can frequently be related to volcanic eruptions, or processes related to volcanism. Precise observations of the deformation can shed a light on the processes at work within the volcanoes.

Mogi (1958) developed simple mathematical expression to predict particle displacements in an elastic half-space if a very small spherical volume experienced increase or decrease in pressure. The particle displacement at the surface of the elastic half space is given by Mogi (1958) as follows:

$$\mathbf{r = (3a^3PR)/(4\mu(H^2 + R^2)^{3/2})}$$

$$\mathbf{h = (3a^3PH)/(4\mu(H^2 + R^2)^{3/2})}$$

Where
r = horizontal radial displacement of a surface particle
h = vertical displacement of a surface particle
a = radius of the spherical body where pressure changes
P = pressure change in the spherical body
μ ($= \lambda$) = Lame's constant of rigidity
H = depth from the surface to the center of the spherical body
dR= horizontal radial distance from the center of the spherical body

The surface of the elastic half space is considered horizontal with the half space below, signifying the surface and the interior of the earth.

The Mogi model equations are not strictly correct unless the radius **a** of the spherical body is very small as compared with the depth **H** and the half space must be homogeneous with flat surface. Further the Lame's constants of elasticity **μ** and **λ** must be equal. The earth does not satisfy these conditions, so the Mogi model can only be an approximation to processed on or inside the real earth.

When applying the Mogi model to earth deformation, the values of **a** and **P** are usually not known. Therefore, the value of **$(3a^3P)/(4\mu)$** is treated as a constant **K**, giving a measure of the magnitude of the source of deformation. The vertical surface displacement **h** is greatest vertically above the center of the sphere of changing pressure. If **h0** is the maximum vertical displacement, then it is related to the constant **K** and the depth **H** as follows:

$$\mathbf{h0 = K/H^2}$$

This equation tells us that if we have pressure source of given magnitude (**K**), the maximum vertical ground displacement is inversely proportional to the source depth squared.

It has frequently been observed that ground deformation at active volcanoes are similar to those predicted by the Mogi model when a pressure changes in a small spherical volume at depth. In those cases the observations can be compared with components of deformation as predicted by this model (Figs II,1, II,2, II,3), and if good fit is obtained, then the source magnitude and source location is inferred. However, it must always be kept in mind that the conditions at depth below an active volcano do not agree with the strict requirements of the Mogi model. Therefore, any comparison of observed ground deformation can at best give a suggestion as to the magnitude and depth of the source of the deformation.

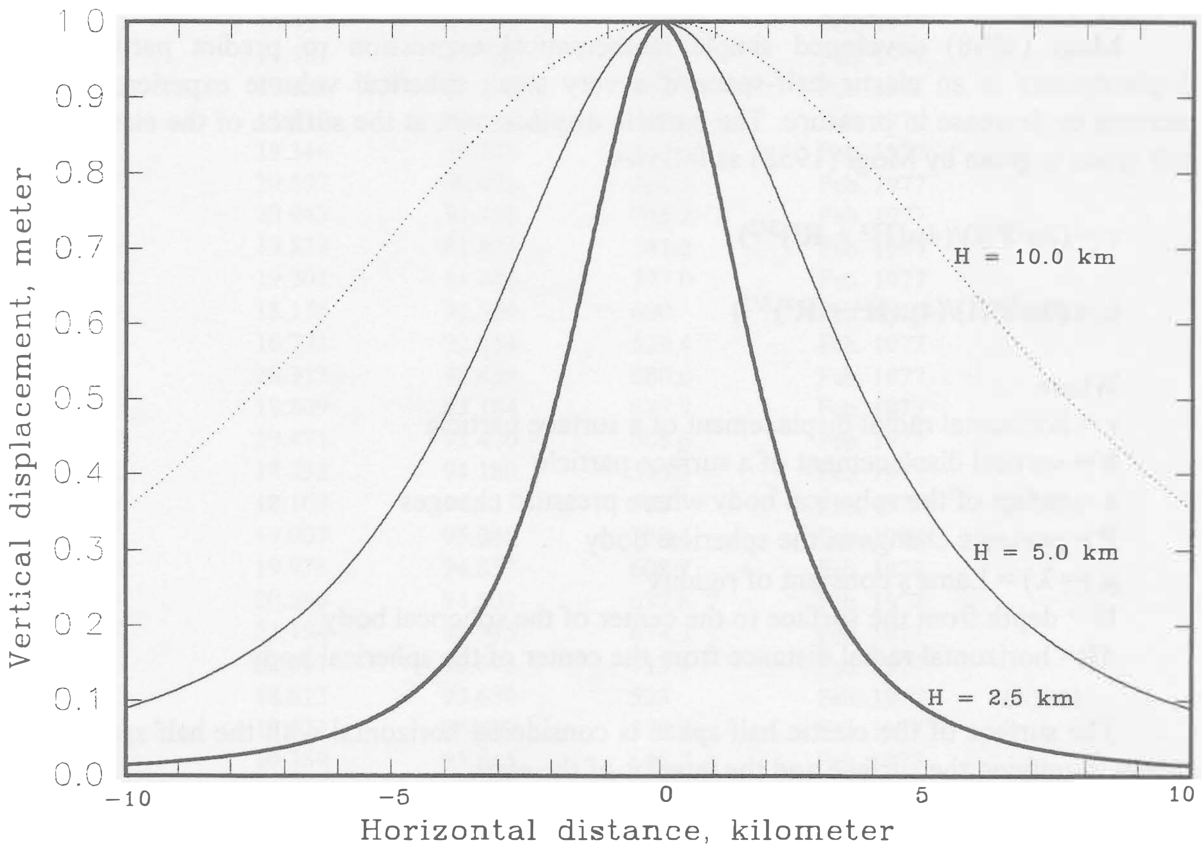

Fig. II,1. Vertical displacement (ground uplift) if a point source of increased pressure lies at 2.5 km, 5.0 km, or 10.0 km depth as predicted by the Mogi model. The maximum uplift is taken as 1.0 m, and the diagrams show predicted ground uplift along a 20 km profile centred at point zero, vertically above the point source.

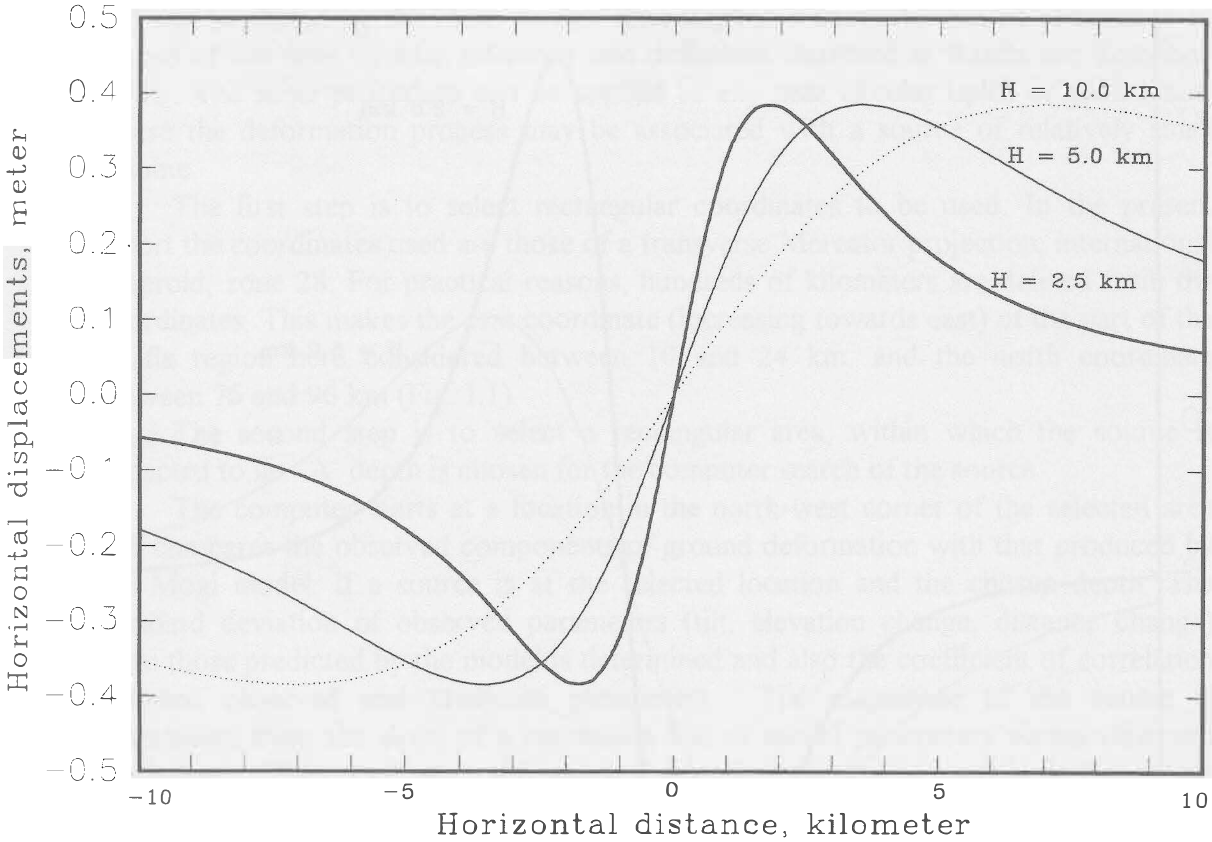

Fig. II,2. Horizontal displacement of the earth's surface as predicted by the Mogi model along a 20 km profile, centred vertically above the point source. The magnitude of the point source is so selected that it causes maximum predicted uplift of 1.0 m.

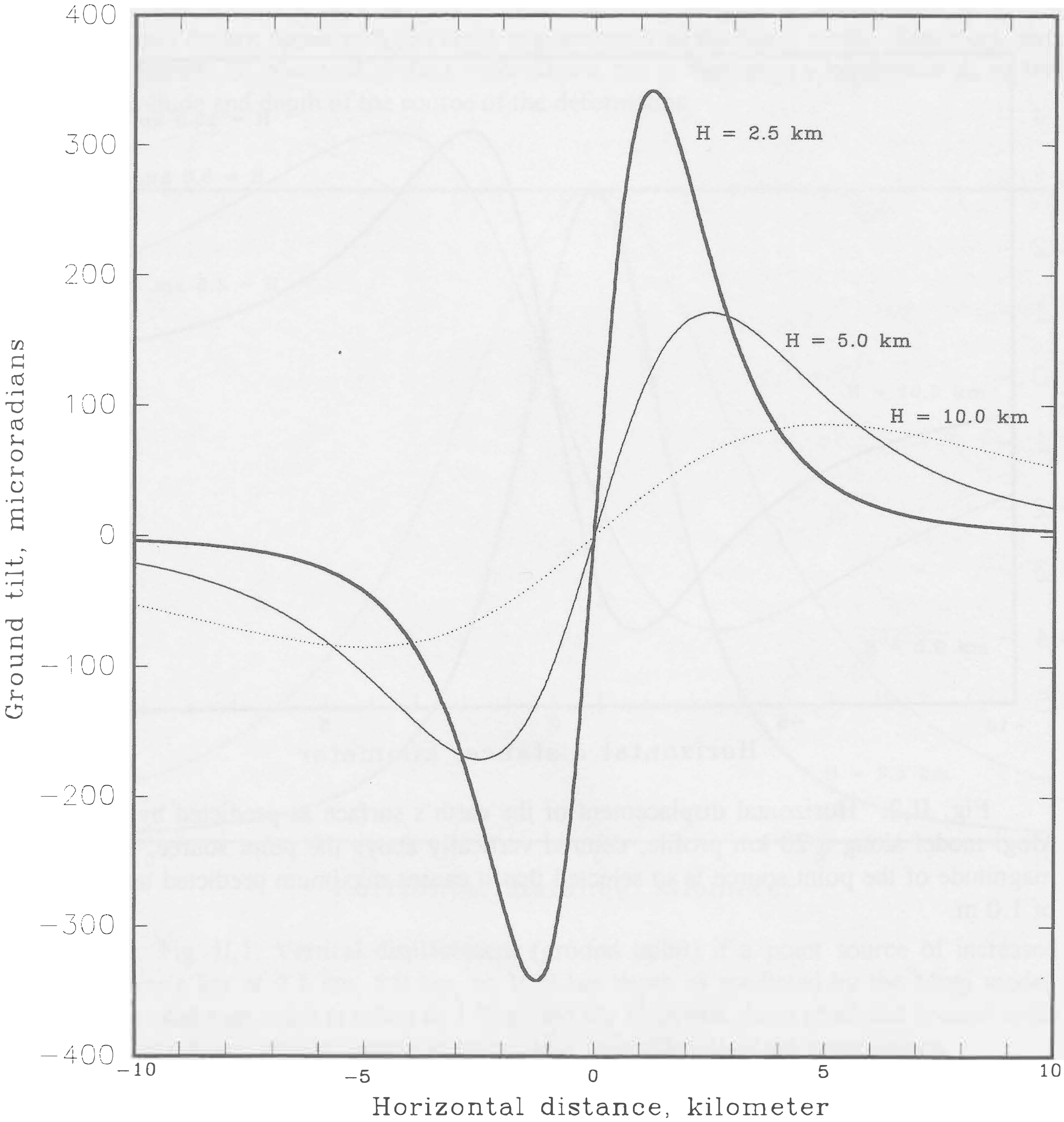

Fig. II,3. Mogi model prediction of ground tilt along a 20 km profile, centred vertically above a point source at 2.5 km, 5.0 km, and 10.0 km depth below ground surface. The magnitude of the source is so selected that the maximum predicted uplift is 1.0 m.

COMPUTER PROGRAMS AND COMPUTING PROCEDURE

The problem is to produce a point source Mogi model, which predicted deformation field is as close to the observed deformation as is possible. This requires that a location is found which minimises the difference between observed deformation and that predicted by the Mogi model. The steps in a computer search of location of source of the near circular inflations and deflations observed at Krafla are described below. The same procedure can be applied to any near circular uplift or subsidence, where the deformation process may be associated with a source of relatively small volume.

The first step is to select rectangular coordinates to be used. In the present report the coordinates used are those of a transverse Mercator projection, international spheroid, zone 28. For practical reasons, hundreds of kilometers are deleted from the coordinates. This makes the east coordinate (increasing towards east) of the part of the Krafla region here considered between 10 and 24 km, and the north coordinate between 76 and 96 km (Fig. I,1).

The second step is to select a rectangular area, within which the source is expected to lie. A depth is chosen for the computer search of the source .

The computer starts at a location in the north-west corner of the selected area and compares the observed components of ground deformation with that produced by the Mogi model, if a source is at the selected location and the chosen depth. The standard deviation of observed parameters (tilt, elevation change, distance change) from those predicted by the model is determined and also the coefficient of correlation between observed and predicted parameters. The magnitude of the source is determined from the slope of a regression line of model parameters versus observed parameters. The coordinates, the standard deviation, the source magnitude (maximum vertical ground displacement), and the correlation are stored as possible source parameters in the computer memory.

A new location is selected, moving towards east a fixed distance, and the standard deviation, correlation and source magnitude are again determined. If the standard deviation is smaller than that found earlier, the new location, the new standard deviation, the new source magnitude and the new correlation are stored as possible source in stead of those parameters previously stored. This procedure is repeated, moving the selected location eastward until the east edge of the selected rectangle is reached. Then a location is selected at the west edge of the selected rectangular, a fixed distance south of the beginning location, and the same procedure is repeated for a second line towards east. This repetition is continued until all grid points of the selected rectangle have been occupied.

The coordinates of the grid point with the smallest standard deviation of observations from model, are now stored as most probable location of a point source of deformation, provided the chosen source depth is correct.

A new depth of the source is selected, and the same procedure carried out. If the smallest standard deviation of observations from model is smaller than that of the earlier search, the second source depth is considered as more probable than the first one. By selecting several trial depths, the most probable source depth is found as the depth which gives best agreement between observations and model.

In most of the solutions presented in this report, the smallest standard deviation between observed ground parameters, and those predicted by the Mogi model is accepted as indication of best agreement between model and observations. Sometimes, if tilt observations are compared with models, highest correlation between radial component of observed tilt, and model tilt is considered to indicate best agreement between observations and model.

The type of observations which have been used to search for probable point source of deformation include repeated tilt observations at several optical levelling tilt stations, and repeated distance measurements of several lines between permanent bench marks. Other measurements which are not included in this study of the Krafla volcano, but which can be used in similar way, include repeated precision levelling along extended profiles with a number of permanent bench marks, tilt observations with recording tiltmeters, and repeated precise location determinations using navigational satellites (GPS measurements).

Tilt measurements.

The Mogi equation which defines vertical displacements on horizontal surface of homogeneous half space, because of pressure change at a point within the half space, can be written as follows:

$$\mathbf{h = (K^*H)/(D^3)} \qquad (1)$$

Here, **h** is the vertical component of particle displacement at the horizontal surface of the homogeneous half space, at slant distance **D** from the point source of pressure change. **K** is a constant which defines the intensity or magnitude of the point source, and can be expressed in terms of the radius of the spherical source volume (**a**), the pressure change (**P**), and the modulus of rigidity (**μ**) of the half space (**K=(3a^3*P)/(4μ)**).

The constant **K** can also be expressed by the maximum vertical displacement **h0** at zero horizontal distance from the source (**R = 0**), and the depth **H** from the horizontal surface of the half space to the point source of changing pressure. Equation (1) gives **h0 = K/H^2** or **K = h0*H^2**. **D** is the slant distance from the point source to a point on the horizontal surface of the half space (**D=(R^2+H^2)$^{1/2}$**). The symbol * means multiplication.

The Mogi-model tilt **t** of the horizontal surface of the half space, because of point source of changing pressure, is found by determining the first derivative of the vertical surface displacement with respect to horizontal distance from the source:

$$\mathbf{t = (dh/dR) = -\ (3K^*H^*R)/((H^2+R^2)^{5/2})} \qquad (2)$$

By introducing a new variable **B = R/H**, the equation (2) becomes:

$$\mathbf{t = -\ 3K^*B/(H^{3*}(1+B^2)^{5/2})} \qquad (3)$$

Distance measurements.

The Mogi model defines the horizontal displacement **r** of a point on the horizontal surface as follows:

$$\mathbf{r = (K*R)/D^3} \tag{4}$$

This horizontal displacement is radial with respect to the point source of changing pressure. The change of distance between two arbitrary points on the horizontal surface of the homogeneous half space can be obtained from equation (4) as follows:

A coordinate system is placed on the surface with origin vertically above the point source of changing pressure. The X-axis is towards east, the Y-axis towards north.

The coordinates of the two points before changes occur are **X1**, **Y1** and **X2**, **Y2**.
After the change in pressure at the point source, the coordinates will be:

X11 = X1 + (K*X1)/(D1)³ = X1+x1
Y11 = Y1 + (K*Y1)/(D1)³ = Y1+y1.
X22 = X2 + (K*X2)/(D2)³ = X2+x2
Y22 = Y2 + (K*Y2)/(D2)³ = Y2+y2.

The distance between these two points before the change is found as **S1**, where:

$$S1^2 = (X1-X2)^2 + (Y1-Y2)^2 \tag{5}$$

And after the change the distance is **S2**, given by:

$$S2^2 = (X1+x1-X2-x2)^2 + (Y1+y1-Y2-y2)^2 \tag{6}$$

As the distance change **s** can be regarded very small as compared with the total distance between the two points, we can write:

$$s = S2 - S1 \sim (S2^2 - S1^2)/(2*S1) \quad \text{or}$$
$$s \sim ((X1-X2)(x1-x2) + (Y1-Y2)(y1-y2))/S1 \tag{7}$$

Equation (7) can be developed as follows:

$$S1^2 = X1^2 - 2X1*X2 + X2^2 + Y1^2 - 2Y1*Y2 + Y2^2 \tag{8}$$

$$S2^2 = X1^2 + 2X1*x1 - 2X1*X2 - 2X1*x2 + x1^2 - 2x1*X2 - 2x1*x2 + X2^2 + 2X2*x2 + x2^2 + Y1^2 + 2Y1*y1 - 2Y1*Y2 - 2Y1*y2 + y1^2 - 2y1*Y2 - 2y1*y2 + Y2^2 - 2Y2*y2 + y2^2. \tag{9}$$

In the present case, the Mogi model is to be used on actual cases of deformation of the earth's crust. Measurements of crustal deformation in Iceland suggest that change in length between points on the earth's surface never exceeds about 300 parts per million of the length between the points, if the deformation is purely elastic. Non-elastic deformation is not considered in the Mogi model. This means that **s/S** (and similarly **x1/X1**, **x2/X2**, **y1/Y1**, and **y2/Y2**) is generally smaller than 0.0003.

As **x1**, **x2**, **y1**, and **y2** are very much smaller than **X1**, **X2**, **Y1**, and **Y2** respectively, the product of any two of the lower case terms is negligible as compared with products of one upper case term and one lower case term, and therefore all products of two lower case terms can be deleted from the above equation without introducing any significant error and the difference of $S1^2$ and $S2^2$ is very close to:

$$S2^2 - S1^2 = 2*X1*x1 - 2*X1*x2 - 2*x1*X2 + 2*X2*x2 + 2*Y1*y1 - 2*Y1*y2 - 2*y1*Y2 - 2*Y2*y2, \text{ or} \qquad (10)$$

$$S2^2 - S1^2 = 2*(X1 - X2)*(x1 - x2) + 2*(Y1 - Y2)*(y1 - y2). \qquad (11)$$

As $S2 = S1 + s$, then $S2^2 - S1^2 = 2*S1*s + s^2$ almost equal $2*S1*s$ as **s** is quite insignificant compared to S1. Therefore, the following expression is almost correct:

$$s = (S2^2 - S1^2)/(2*S1) = ((X1-X2)*(x1-x2) + (Y1-Y2)*(y1-y2))/S1 \qquad (12)$$

as stated in equation (7).

Computing procedure

A. A file is prepared with the data used in the computation If tilt observations are used, this file contains one row for each tilt station, and four columns, containing east- and north- coordinates of the tilt stations and east and north component of tilt at each station. The tilt is in μrad and the coordinates in kilometers, although any measure of tilt and coordinates can be used.

If distance changes are used, the file contains one row for each pair of stations between which distance and distance change is used for the solution, and six columns, two for coordinates of each station, one for the distance between the stations and one for the change of distance between the stations over the period for which the solution is sought.

B. A grid is defined by coordinates of a central point, and distance between grid points. The grid consists of 31 rows and 51 column and distance between grid points is so defined that a print-out of the grid with one digit in each grid point, is in a selected map scale. The number of rows and columns can be changed, but the above numbers will print out a undistorted square map area. The center of the grid area is placed where maximum vertical ground displacement is expected, and the size of the grid area is usually so selected that a print-out produces a map of scale 1:50000, 1:20000, or 1:10000. The source depth is selected, and also a multiplication constant with which the standard deviation is multiplied to obtain proper numerical values for the print-out.

The following discussion applies to search for point source, using tilt observations.

C. The computer starts at the upper left corner of the grid, and computes predicted tilt at each tilt station used (File of **A** above), assuming a point source of changing pressure lying vertically below the selected grid point at the chosen depth. The constant **K** (equation 1) is to be determined, but provisionally taken as unity.

D. The computer determines the radial component of observed tilt at each tilt station, with respect to the selected grid point, and determines the regression line and correlation of model tilt and observed radial component of tilt. From the regression line the apparent value of the constant **K** is found, and thereby the suggested maximum vertical ground displacement, provided a single point source of changing pressure lies vertically below the grid point. The coefficient of correlation and the suggested maximum vertical ground displacement is put in temporary memory, and also the coordinates of the grid point.

E. The computed model tilt for each tilt station is modified to agree with the suggested value of maximum vertical ground displacement, and the vector difference between such modified model tilt and actual observed tilt is found for each tilt station. The scalar standard deviation of the difference of the model tilt and observed tilt is determined, and its value is placed in temporary memory.

F. The obtained standard deviation is multiplied by a selected constant, and the obtained numerical value is placed as one digit integer or symbol in a file representing the selected grid. If the numerical value deviates less than 0.25 from a whole number, the whole number is placed in the grid file. If the numerical value deviates more than 0.25 from a whole number, no symbol is placed in the appropriate place in the grid file. If the numerical value exceeds 9.75, a star (*) is placed in the grid file.

G. The computer selects a next grid point, first row, second column, and carries out the same computations as above, now with respect to coordinates of this second grid point. The obtained standard deviation of observed tilt from model tilt is compared with previous value in the temporary memory. If the new standard deviation is smaller than that of the temporary memory, then the value in the temporary memory are replaced by the new value, together with the grid point coordinates, the suggested maximum vertical ground displacement, and the coefficient of correlation between model tilt and radial component of observed tilt. If the obtained standard deviation of observed tilt from model tilt is greater than that in the temporary memory, no change is made in the temporary memory.

H. The computer selects following grid points in a similar manner as reading a text, first finishing the top row from left to right, then the second row from left to right, and so on until the last row is finished. Then the values of the temporary memories are placed at the bottom of the grid file.

I. With minor modifications of the computer program, the coefficient of correlation between model tilt and radial component of observed tilt, can be used in stead of standard deviation to define most probable source location. Also, quantities other than standard deviation (maximum suggested vertical ground displacement, or coefficient of correlation) can be placed in the grid file.

J. If distance measurements are used to search for location of the hypothetical point source of pressure change, which can explain the observed ground deformation, the procedure is basically the same as described above, with the exception that a different equation (7) is used to obtain the distance changes predicted by the Mogi model.

Computing programs

To carry out the computations required to compare ground deformation measurements with a deformation model, the single point source Mogi model, several FORTRAN programs were written. These programs were modified several times. The final version of two programs are shown below, one program to compare single point source Mogi model with repeated distance measurements, and one program to compare single point source Mogi model with tilt measurements.

FORTRAN program to compare Mogi model with distance measurements.

```
c       program model.for
c       program to compute location og point source of
c       deformation from repeated distance measurtements
c       and draw a map of standard deviation of difference of
c       observations and model.
        dimension x1(50),x2(50),y1(50),y2(50),dist(50),dd(50),ddc(50)
        character*1 er(51),tab(12)
        character*40 iname
        tab(1)='
        tab(2)='0'
        tab(3)='1'
        tab(4)='2'
        tab(5)='3'
        tab(6)='4'
        tab(7)='5'
        tab(8)='6'
        tab(9)='7'
        tab(10)='8'
        tab(11)='9'
        tab(12)='*'
        write(*,500)
500     format(' write name of the data file')
        read(*,510)iname
510     format(a20)
        open(3,file=iname,status='old')
        write(*,520)
520     format(' center of grid, xo, yo, ho, i km')
        read(*,530)xo,yo,ho
530     format(3f10.3)
        write(*,535)
535     format(' scale of x and y, km/mm')
        read(*,536)step
        step=step*1000.
536     format(f10.3)
        write(*,550)
550     format(' constant of multiplication')
        read(*,555)cc
555     format(f8.3)
```

```
      if(cc.eq.0.)cc=1.
      open(4,file='temp',status='new')
      write(4,561)iname
      write(4,562)xo,yo,ho
      write(4,563)step,cc
      write(*,561)iname
      write(*,562)xo,yo,ho
      write(*,563)step,cc
      write(4,564)
      write(4,564)
561   format(' distance measurements ',a20)
562   format(' xo=',f8.3,' km, yo=',f8.3,' km, ho=',f8.3,' km')
563   format(' scale', f8.3,' m/mm, multiplication=',f8.3)
564   format('   ')
      rewind 3
      n=0
100   n=n+1
      read(3,540,end=120)x1(n),y1(n),x2(n),y2(n),dist(n),dd(n)
540   format(5f10.3,f8.3)
      if(n.gt.50)go to 120
      go to 100
120   n=n-1
c     all data have been read

      xo=xo*1000.
      yo=yo*1000.
      ho=ho*1000.
      do 110 i=1,n
      xa=x1(i)
      xb=x2(i)
      ya=y1(i)
      yb=y2(i)
      write(*,901)x1(i),y1(i),x2(i),y2(i)
      x1(i)=17834.+0.9921*xa+0.12535*ya
      x2(i)=17834.+0.9921*xb+0.12535*yb
      y1(i)=89880.-0.12535*xa+0.9921*ya
      y2(i)=89880.-0.12535*xb+0.9921*yb
      write(*,901)x1(i),y1(i),x2(i),y2(i)
110   write(*,564)
901   format(4f12.0)
      serr=1000.
      dx=step*2.54
      dy=step*25.4/6.
      xoo=xo-dx*26.
      yoo=yo+dy*16.
      write(*,900)xoo,yoo,dx,dy,n
      write(4,900)xoo,yoo,dx,dy,n
900   format(' beginning',2f8.0,' step',2f6.1,' lines',i4)
      do 310 ii=1,31
```

```
      yo=yoo-dy*ii
      do 300 jj=1,51
      xo=xoo+dx*jj
            do 130 i=1,n
            r1=sqrt((x1(i)-xo)**2+(y1(i)-yo)**2)
            r2=sqrt((x2(i)-xo)**2+(y2(i)-yo)**2)
            if(r1.eq.0.)go to 126
            if(r2.eq.0.)go to 127
            dr1=(ho**2)*r1/((ho**2+r1**2)**1.5)
            dr2=(ho**2)*r2/((ho**2+r2**2)**1.5)
            dx1=(x1(i)-xo)*dr1/r1
            dy1=(y1(i)-yo)*dr1/r1
            dx2=(x2(i)-xo)*dr2/r2
            dy2=(y2(i)-yo)*dr2/r2
            go to 128
126         dx1=0.
            dy1=0.
            go to 128
127         dx2=0.
            dy2=0.
            go to 128
128         continue
            xxx=(x1(i)-x2(i))*(dx1-dx2)
            yyy=(y1(i)-y2(i))*(dy1-dy2)
130         ddc(i)=(xxx+yyy)/dist(i)
      sdo=0.
      sdc=0.
      sumo=0.
      sumc=0.
      do 140 i=1,n
      sumo=sumo+dd(i)**2
      sumc=sumc+ddc(i)**2
      sdo=sdo+dd(i)
140   sdc=sdc+ddc(i)
      dom=sdo/n
      dcm=sdc/n
      ssdo=0.
      ssdc=0.
      ssdoc=0.
            do 150 i=1,n
            fdd=(dd(i)-dom)**2
            fddc=(ddc(i)-dcm)**2
            fddoc=(ddc(i)-dcm)*(dd(i)-dom)
            ssdo=ssdo+fdd
            ssdc=ssdc+fddc
150         ssdoc=ssdoc+fddoc
      rr=ssdoc**2/(ssdo*ssdc)
      dhc=sqrt(sumo/sumc)
      if(ssdoc.lt.0.)dhc=dhc*(-1.)
```

```
      sdel=0.
      do 160 i=1,n
      ddc(i)=ddc(i)*dhc
      del=ddc(i)-dd(i)
160   sdel=sdel+del**2
      stdev=(sqrt(sdel/(n-1)))*cc
      if(stdev.ge.9.8)go to 710
      istd=stdev
      astd=istd
      d=stdev-astd
      if(d.le.0.2)go to 720
      if(d.ge.0.8)go to 730
      nn=1
      go to 740
710   nn=12
      go to 740
720   nn=istd+2
      go to 740
730   nn=istd+3
740   continue
      er(jj)=tab(nn)
      sterr=stdev/cc
      if(sterr.gt.serr)go to 300
      xtemp=xo/1000.
      ytemp=yo/1000.
      htemp=ho/1000.
      dhtemp=dhc
      serr=sterr
      rrr=rr
300   continue
      write(*,580)(er(k),k=1,51)
      write(4,580)(er(k),k=1,51)
580   format(51a)
310   continue
      write(*,570)xtemp,ytemp,htemp,dhtemp,serr,rrr
      write(4,564)
      write(4,564)
      write(4,570)xtemp,ytemp,htemp,dhtemp,serr,rrr
570   format(4f8.2,2f8.4)
999   end
```

```
 Distance measurements d89.94
 xo =  18.000 km, yo =  89.000 km, ho =   2.500 km
 Scale   50.000 m/mm, multification =   1.000


 beginning  14698.  92387. step 127.0 211.7 lines  40
****     8888          *********************       9
***    8888             **********************
**   8888         7777   **********************
   8888       777777777777**********************
  888       77777       7777*********************
 88       77777            77**********************
88      7777      6666666    77********************
88    77777     666       66   77******************
8    7777     66     5555    66  77****************
8    777     66   55       555  66  77**************
8    777    66  55   44444   55   6  77 ***********
8   777    66  55  44      44   5  66  7   ********
    77    66  55  4   3333   44  55  6  77   88****
   777   66   5  44  33   333  44  5  6   7   88
   777   66   5   4  33     33  4  55  6   7   888
  777    66   55   4   333333   4  55  66  77   888
  777    666    55   44         44  55  66   77   88
  777     666     55    444444    55   66   77   88
  7777      6666     5555      555    66    77    8
  77777        66666                666    777    8
   777777          66666666666666666       777    8
    77777777                               77    88
      77777777777777                      777    88
          777777777777777777777777    77777    888
                          77777777777777777     88
8                                             888
88888                                       8888
8888888888888        888888888888888888888888
     8888888888888888888888                     999
             88888888                      9999999
999                          99999999999999999


   18.00    89.21    2.50  -28.24  2.6342    .7553
```

Fig. III,1. An example of the output of computer program to locate possible point source of deformation, source depth constrained at 2.5 km.

Table III,1

Observational data of distance changes that go into computation of most probable center of a point source of deformation, giving solutions shown in Figs. III,1, III,2, and III,3. Two first column (X1 and Y1) are approximate coordinates of geodimeter stations in a rectangular system originating at the station A003 near the expected center of inflations and deflations. Column 3 and 4 give the coordinates of the reflector stations in the same coordinate system. Fifth column gives the measured distance between the stations and column 6 gives the observed change in distances between observations of March 1989 and March 1994.

X1 M	Y1 m	X2 m	Y2 M	Distance m	Dist, change cm
1451.703	586.153	-236.578	-177.879	185.945	-11.40
1451.703	586.153	0.000	0.000	1567.432	-9.50
1451.703	586.153	537.862	417.030	929.638	-3.90
1451.703	586.153	2669.831	938.205	1273.505	0.50
1451.703	586.153	2910.760	1834.120	1927.284	2.00
1451.703	586.153	1750.092	2218.427	1659.831	-0.20
1451.703	586.153	1121.022	2114.614	1564.206	-2.30
1451.703	586.153	2134.743	3033.139	2543.802	3.20
1451.703	586.153	1564.718	3517.590	2934.919	1.60
1451.703	586.153	760.000	-934.500	1671.089	-12.70
760.000	-934.500	-1298.964	-859.148	2063.734	-8.80
760.000	-934.500	-232.578	-177.879	1249.506	-6.00
760.000	-934.500	0.000	0.000	1205.530	-9.10
760.000	-934.500	2669.831	938.205	2678.504	-13.10
760.000	-934.500	2134.743	3033.139	4201.829	-13.00
760.000	-934.500	778.000	-2754.000	1819.589	-7.90
760.000	-934.500	226.000	-4137.000	3247.734	-6.20
760.000	-934.500	2460.000	-2354.400	2215.885	-7.10
760.000	-934.000	1802.000	-2698.500	2048.719	-7.30
2134.743	3033.139	537.862	417.030	3068.380	1.00
2134.743	3033.139	2669.831	938.205	2162.717	-0.50
2134.743	3033.139	2910.760	1834.120	1429.269	0.10
2134.743	3033.139	1750.092	2218.427	906.483	2.90
2134.743	3033.139	1121.022	2114.614	1371.894	2.40
2134.743	3033.139	1564.718	3517.590	750.068	1.20
2134.743	3033.139	1195.041	3761.903	1191.562	0.70
-2611.058	829.723	-1298.964	-859.148	2139.428	-7.60
-2611.058	829.723	-232.578	-177.879	2585.896	-6.40
-2611.058	829.723	0.000	0.000	2743.253	-5.20
-2611.058	829.723	1121.022	2114.614	3952.145	-11.20
-2611.058	829.723	-1363.697	2428.887	2028.381	-3.40
-2611.058	829.723	2134.743	3033.139	5238.859	-8.90
-2611.058	729.723	-2074.600	-3746.600	4608.053	-12.30
-2611.058	829.723	-3578.300	-1272.400	2313.886	-6.70
226.000	-4137.000	-1298.964	-859.148	3616.687	-8.10
226.000	-4137.000	-2074.600	-3746.600	2333.864	-5.30
226.000	-4137.000	-3578.300	-1272.400	4762.908	-9.20
226.000	-4137.000	2460.000	-2354.400	2860.823	-7.80
226.000	-4137.000	1802.000	-2698.500	2134.726	-2.90
226.000	-4137.000	778.000	-2754.000	1490.308	1.50

```
 Distance measurements d89.94
 xo=  18.000 km, yo=  89.000 km, ho=   3.000 km
 scale  50.000 m/mm, multiplication=   1.000

 beginning  14698.  92387. step 127.0 211.7 lines  40

*   8888               *************************
   888          777777  *************************
 888        7777777777777**************************
88       777777        7777************************
      777777               7***********************
   777777        6666666     7*********************
  7777        66666    6666    7*******************
  777      6666            666   7*****************
 777     6666     555555555   66   7***************
 777    666    555          55   6   7*************
 77    666    55   44444444   55   6   77**********
 77    66   55   44         44   5   6   7  *******
777   666   5   44  33    33   4  55  66  77   8***
77    66   55  44  33        3  44  5  66   7    88
77    66   55   4  33   222   3  44  5  66   77   8
77    66    5   44  33        3   4  55  66   77
77    666   55    4    3333333   44  55  66   77
77     666    55    44          44   55   66   77
77      666     555     4444444     55   666   77
777      6666       5555         5555    666   77
7777       666666         5555555       666    77
 7777          66666666               66666    77
  777777             66666666666666666666      77
   777777777                                  777
      777777777777                           777
          7777777777777777777777777777 77777777
                 77777777777777777777777777       8
88                                              888
8888888                                  88888888
  88888888888          88888888888888888888
        8888888888888888888                       9


   18.00   89.21    3.00  -27.21  2.1202   .8337
```

Fig. III,2. Same as Fig. III,1 except the depth is constrained at 3.0 km.

```
 Distance measurements d89.94
 xo=  18.000 km, yo=  89.000 km, ho=   3.500 km
 scale  50.000 m/mm, multiplication=   1.000

 beginning  14698.  92387. step 127.0 211.7 lines  40

888         77777777777 ***************************
8       77777777777777777**************************
     77777777          777*************************
  777777                  77***********************
7777             6666        **********************
77         666666666666666     ********************
7       666666            666    ******************
7     6666         5555       666   ****************
     666       55555     5555    66   **************
    666     555             555   66   7***********
    66    555    4444   4444   55   66   77********
   666    55   444           44  55   66   77 *****
   666   55   44   3333  333   44  55  66   77   **
   66   55   44  33          3   4   5   66   77
   66   55   44  33           33  4   5   66   77
   666   55   44   33          33   4   5   66   77
   666    55   44   333     333   4   55  66    77
    666    555   444     3333     44   55   66   77
    6666     555    4444        444    55   66    7
     6666      5555      444444      555   666    7
7      6666       55555            55555    666   7
77       66666         5555555555555      666     7
777         6666666                      6666     7
77777           66666666666           666666      7
 777777                66666666666666666666      77
   77777777                                     777
     77777777777                          77777
         77777777777777777777777777777777777777
              77777777777777777
8888                                            888
88888888                          8888888888888888


   18.00    89.21    3.50  -26.35  2.2123   .8549
```

Fig. III,3. Same as Fig. III,1 except the depth is constrained at 3.0 km.

Figures III,1, III,2, and III,3 show examples of output of the FORTRAN program "model.for" to compare the Mogi model with repeated distance measurements in the Krafla region. The data file used for the comparison (Table III,1) gives the coordinates of the EDM stations in meters, measured toward east (X1, X2) and north (Y1, Y2) from station A003, near the center of the Krafla volcano, measured distances between the stations in March 1994 and change in the measured distances since May, 1989. Included in the computer program is conversion to universal transverse Mercator projection coordinates. A total of 40 measured lines were used in the present analysis. The print-out of the output of the FORTRAN program shown here is for constrained source depth of 2.5 km (Fig. III,1) 3.0 km (Fig. III,2) and 3.5 km (Fig. III,3). The top lines gives the name of the source file, the selected east (xo) and north (yo) coordinates in km in the universal transverse Mercator projection, zone 28,, of the center of the 1581 point computed grid and the chosen source depth (ho). The third line gives map scale and multiplication factor needed in the computation. The forth line gives the coordinates of the first computed grid point, in the upper left corner of the grid, and also horizontal distances (steps) in meters between the grid points, and number of lines used in the computation. Lines 5 to 36 present the standard deviation of observed distance changes from the point source model changes for point source at depth ho below each grid point. As the multiplication factor is one (1), the standard deviation is presented in centimeters, stars meaning more than 9.75 cm. The last line gives the coordinates in km of the grid point of lowest standard deviation between observations and model, The constrained source depth in km, the maximum vertical ground displacement in cm for this "best" solution, the smallest standard deviation in cm between observations and model, and finally the coefficient of correlation squared of observed distance changed versus model distance changes.

FORTRAN program to compare Mogi model with tilt measurements

```
c       program mogite.for
c       program to compute location of a point source of deformation
c       from tilt observations and to draw lines of equal
c       standard deviation of measurements from the Mogi-model
        character*20 iname
        dimension xa(15), ya(15), tx(15), ty(15), to(15), tc(15)
        dimension tto(15), ttc(15), er(15)
        character*1 eer(51),tab(12)
        tab(1)='
        tab(2)='0'
        tab(3)='1'
        tab(4)='2'
        tab(5)='3'
        tab(6)='4'
        tab(7)='5'
        tab(8)='6'
        tab(9)='7'
        tab(10)='8'
        tab(11)='9'
        tab(12)='*'
```

```
      write(*,500)
500   format(' write the name of the data file')
      read(*,510) iname
510   format(a20)
      open(3,file=iname,status='old')
      rewind 3
      write(*,550)
550   format(' center of grid, xo, yo, ho')
      read(*,560) xo,yo,ho
560   format(3f10.2)
      write(*,551)
551   format(' scale in x og y, km/mm')
      read(*,536)step
536   format(f10.3)
      write(*,552)
552   format(' constant of multiplication')
      read(*,553)cc
553   format(f10.5)
      open(4,file='temp',status='new')
      n=0
100   n=n+1
      read(3,520,end=120)xa(n),ya(n),tx(n),ty(n)
520   format(4f10.3)
      go to 100
120           n=n-1
      write(4,561)iname
      write(4,562)xo,yo,ho
      write(4,563)step,cc
      write(4,564)
      write(4,564)
      write(*,561)iname
      write(*,562)xo,yo,ho
      write(*,563)step,cc
      write(*,565)n
      write(4,565)n
565   format(' number of tilt stations',i4)
561   format(' tilt measurements ',a20)
562   format( 'xo=',f8.3,' km, yo=',f8.3,' km, ho=',f8.3,'km')
563   format( 'scale',f8.3,' km/mm, multiplication=',f10.5)
564   format('   ')
      dx=step*2.54
      dy=step*25.4/6.
      xxo=xo-dx*26.
      yyo=yo+dy*16.
      serm=1000.
      write(*,566)dx,dy,xxo,yyo
      write(4,566)dx,dy,xxo,yyo
566   format(' step =',2f10.4,' beginning =',2f10.3)
320   do 300 ii=1,31
```

```
      yo=yyo-dy*ii
      do 310 jj=1,51
      xo=xxo+dx*jj
      do 130 i=1,n
      call torad(xa(i),ya(i),tx(i),ty(i),xo,yo,tor)
130   to(i)=tor
      do 140 i=1,n
      call tcrad(xa(i),ya(i),xo,yo,ho,tcr)
140   tc(i)=tcr
      so=0.
      sc=0.
      do 150 i=1,n
      so=so+to(i)
150   sc=sc+tc(i)
      an=n
      tom=so/an
      tcm=sc/an
      sso=0.
      ssc=0.
      soc=0.
      do 160 i=1,n
      tto(i)=to(i)-tom
      ttc(i)=tc(i)-tcm
      ttto=tto(i)**2
      tttc=ttc(i)**2
      ttoc=ttc(i)*tto(i)
      sso=sso+ttto
      ssc=ssc+tttc
160   soc=soc+ttoc
      rr=(soc*soc)/(sso*ssc)
      dho=sqrt(sso/ssc)
      if(tom.lt.0.)dho=-dho
      do 170 i=1,n
      tc(i)=tc(i)*dho
      call cerr(tx(i),ty(i),tc(i),xa(i),ya(i),xo,yo,err)
170   er(i)=err
      sse=0.
      do 180 i=1,n
180   sse=sse+(er(i)**2)
      ser=sqrt(sse/(n-1))
      stdev=ser*cc
      if(stdev.ge.9.8)go to 710
      if(stdev.le.0.)go to 710
      istd=stdev
      astd=istd
      d=stdev-astd
      if(d.le.0.2)go to 720
      if(d.ge.0.8)go to 730
      nn=1
```

```
      go to 740
710   nn=12
      go to 740
720   nn=istd+2
      go to 740
730   nn=istd+3
740   continue
      eer(jj)=tab(nn)
      if(ser.lt.serm)go to 350
      go to 310
350   serm=ser
      dhho=dho
      xtemp=xo
      ytemp=yo
      rro=rr
310   continue
      write(*,580)(eer(k),k=1,51)
      write(4,580)(eer(k),k=1,51)
580   format(51a)
300   continue
      write(*,570)xtemp,ytemp,ho,dhho,serm,rro
      write(4,564)
      write(4,564)
      write(4,570)xtemp,ytemp,ho,dhho,serm,rro
570   format(4f10.2,2f10.4)
      end

      subroutine torad(x,y,tx,ty,xo,yo,tor)
c     computes radial component af observed tilt
      phi=3.141593
      tilt=atan(tx/ty)
      if(ty.lt.0.)tilt=tilt+phi
      ddy=yo-y
      if(ddy.eq.0.)ddy=0.001
      dir=atan((xo-x)/ddy)
      if(y.gt.yo)dir=dir+phi
      angl=dir-tilt
      tobs=sqrt(tx**2+ty**2)
      tor=(cos(angl))*tobs
      return
      end

      subroutine tcrad(x,y,xo,yo,ho,tcr)
c     commputes model tilt
      r=sqrt((x-xo)**2+(y-yo)**2)
      rr=(ho**2+r**2)**2.5
      tcr=3.*r*(ho**3)/rr
      return
      end
```

```
      subroutine cerr(tx,ty,tc,xa,ya,xo,yo,err)
c     computes difference of observed tilt and model tilt
      ss=sqrt((xo-xa)**2+(yo-ya)**2)
      xxo=((xo-xa)*tc)/ss
      yyo=((yo-ya)*tc)/ss
      err=sqrt((tx-xxo)**2+(ty-yyo)**2)
      return
      end
```

Table III,2

Observational data on ground tilt between observations of June 1989 and July 1994 in the form required by the FORTRAN computer program above. First two columns are east and north coordinates of the tilt stations in kilometers. Next two column show the east component and north component of observed ground tilt. Last column is not used by the computer program, but it shows identification numbers of the stations. Bold letters identify stations used to obtain the result presented in fig. III,5.

East coord. km	North coord. km	East tilt μrad	North tilt μrad	Tilt stations
17.434	**82.091**	**5.842**	**-0.542**	**Námaskarð**
18.188	**85.767**	**14.381**	**-25.250**	**0000**
18.153	89.948	-3.155	42.645	0010
10.963	**82.863**	**-2.823**	**-3.773**	**0020**
22.283	**85.320**	**9.650**	**0.983**	**0040**
14.482	**88.917**	**-31.902**	**-3.474**	**0080**
15.118	**90.668**	**-46.085**	**31.134**	**0090**
13.376	83.117	-7.535	-7.408	0210
13.822	84.003	-10.172	2.358	0240
15.588	**85.840**	**-15.575**	**-20.550**	**0250**
20.381	**92.862**	**11.641**	**3.412**	**0260**

```
tilt measurements t896.947
xo=  17.000 km, yo=  89.000 km, ho=   2.500km
scale   .050 km/mm, multiplication=    .30000


 number of tilt stations  11
 step =     .1270     .2117 beginning =    13.698    92.387
  *************************************************
  *************************************************
  *************************************************
  **************     ******************************
 *************         ****************************
************  9999999   ***************************
*********** 9        99  **************************
***********9   8888    99  ************************
******** 9   88     88   99  **********************
******    88    77    888   99  *********
***** 9  88  777777777    88888888     999999
***  9  88  77        77777777 6 5 56  88    999999
*** 9   8  77                6 5   45  7  88      9
*** 9  8   7    666666666666  5  444  6 7   88
*** 9 88  77   666           55     5 6  7    888
****  8  77   666         5555     55  6  77   888
****  8  77   666     555555       55  6   77    88
*** 9 8  77    66    5555         55   66  777   88
**  9 88  77    66   555         555   66   77   88
*  9   8   77   66    555       555   66   777   88
*  9   88   77   66    5555  55555   66   777   88
   9    88   77   66     555555     66   77    88
   99   888   77   666            66   777   88
   99    88    77    66666    6666    77   88    99
   99    888   777      66666666    77   88    9999
   999    888   777                77   88   999
    999    88    7777777          77   8   99
*     999   88    777777777777777777  8  99     ***
**      999  88               77777  8 99   *******
*****      9  888                  8 9  ***********
************      88888888888888888  **************


     18.14     89.64      2.50    -339.50   11.4079     .8165
```

Fig. III,4. An example of the output of computer program "mogite" to locate possible point source of deformation from tilt measurements. Used are all tilt obtained for the period June 1989 to July 1994, presented in Table III,2

```
tilt measurements tj896.947
xo=  17.000 km, yo=  89.000 km, ho=   2.500km
scale    .050 km/mm, multiplication=    .30000

 number of tilt stations   8
 step =     .1270     .2117 beginning =    13.698    92.387

**************  99     888888888888            9999
*************  99    8888       8888          9999
************  99   8888           888        9999
************ 9    88      7777     888      99999
*********** 9  888     7777777777   888     9999
**********   88    7777         77   888    9999
*********  88  777      6666666   77   88    999
********* 8 77    6666          6   7  88    999
*******  8   6        555555555   6  7  88    999
***** 9 8 7   55555             5  6  7  88   999
**** 9 8 7 6 55     4444444 444  5  6  7  88   99
*** 9  8 7 6 5   444           44 5  6 7   8   999
** 9  8  7 6 5   4    333   333 4    6 77  8   999
** 9  8 7  6 5   4   33       3 4    6 77  8   99
** 9 8  7 6  55  4   3        3 4 5  6 7  88  99
**   8 7  6  55  44  33      3  4 5 6  7  88  99
*** 8  7  66  55  44  333333  44 5  6  7  8   9   *
***988 7   66  55  44        4  5  6  77  8   9   *
** 9 8  77  66   5   4444444  55  6   7  88  99   *
** 9  8  77   6   55        55   6   7   8   99   *
*  9  88   77  66    5555555   66  77   8   99   **
*  9   88   77   66          66   77   88  99    **
*  99   88   77    6666 66666    77   88   99   ***
   99    88   77      6666      77   88   99   ****
   999    88   77              77   88   9    *****
    999   888   777        777777   8   9   *******
*    999   88   7777777777777777   88  9   ********
**     99   88    77               8  9  **********
****     99  8                    8  9 ************
*********  9  88   88888888888888    **************
*************                     9 ***************


     17.13      89.21      2.50   -258.16     7.5012      .9209
```

Fig. III,5. Same as Fig. III,4 except that observations at only 8 of the tilt stations, those presented in bold letters, of Table III,2. are included in the computation.

Figures III,4 and III,5 show the computer output of search for center of deformation, based on observed ground tilt between June 1989 and July 1994, about the same time as covered by similar treatment of distance measurements, presented in Figs. III,1, III,2, and III,3. The figures are constructed in the same way as those based on distance changes by printing values of computed standard deviation (multiplied by a constant) in rectangular grid on map of scale 1:50000. The distance between the grid points in the field is selected to fit the printer on which the result is printed. The maximum computed vertical ground displacement is presented in mm (-339.50 mm in Fig. III,4 and -258.16 mm in Fig. III,5), while in solutions based on distance measurements (Figs III.1, III.2, III.3) these maximum displacements are given in cm. Negative values of ground displacements represent subsidence.

When the station 0010 (Leirhnjúkur) is included in the computer treatment, irregular pattern in distribution of standard deviation is usually observed, as can be seen on Fig. III,4. The reason for this is that this station (0010) is usually observed with large tilt, relative to other stations in the Krafla area, and the tilt azimuth deviates considerably from that suggested by observations at other stations. This suggests irregular tilt field in the area of greatest uplift or subsidence. The different location of the suggested point source of solutions in Figs III,4 and III,5 is caused by the large tilt at station 0010. The significant difference in computed maximum vertical ground displacement, -339.50 mm in Fig. III,4 and -258.16 mm in Fig. III,5, is partly because of large tilt at station 0010, and partly because the maximum ground displacement is computed for two different locations about 1.1 km apart.

ANALYSIS OF 1976-1979 TILT OBSERVATIONS

Numerous tilt measurements at Krafla during the years 1976-1979, were studied to determine the average tilt variation at the optical levelling tilt stations, relative to the north component of tilt at the Krafla power station (Tryggvason 1979). It was observed that near linear relation existed between observed ground tilt at several optical levelling tilt stations, and the tilt measured by the water tube tiltmeter at the Krafla power station. However, if non-elastic ground deformation (fissure opening, fault displacement) did occur in the vicinity of the tilt stations, this linear relation was disturbed. Therefore, periods of known rifting in the near vicinity of the tilt stations were excluded from the study.

High correlation was observed between tilt components at optical levelling tilt stations and the north component of tilt at the power station, if the stations were within 10 km of Leirhnjúkur, but stations farther away showed poor or no correlation (Table IV,1).

The water tube tiltmeter at the Krafla power station is oriented in azimuth 13 degrees east of north. The average azimuth of tilt at the Krafla power station has been obtained from a bore hole tiltmeter close to the power station. This allows true north and east components of tilt at the power station to be estimated from the observed N13°E tilt component.

Table IV,1

Relative components of tilt at tilt stations in the Krafla region as obtained in 1979 (Tryggvason, 1979) The tilt as read by the water tube tiltmeter at the Krafla power station is taken as unity, and all other tilt components are computed by obtaining the average ratios of these tilt components to that of the water tube tiltmeter. The water tube tiltmeter at the power station is oriented about N13°E, and the average azimuth of tilt at the power station appear to be about 352° according to a bore hole tiltmeter installed at the site.

Station	North component	East component	Azimuth	N (1)
A	0.08±0.02 (2)	0.01±0.03	13±20	6
0000	0.42±0.05	-0.04±0.04	354±6	14
0010	-0.62±0.16	-0.58±0.14	223±10	13
0020	0.01±0.06	0.04±0.05	(3)	8
0040	0.08±0.11	0.12±0.06	301±38	6
0050	0.02±0.06	0.00±0.06	(3)	9
0060	-0.01±0.09	-0.01±0.09	(3)	10
0070	0.01±0.06	0.04±0.05	(3)	11
0080	0.14±0.06	0.67±0.07	79±6	9
0090	-0.65±0.09	0.70±0.09	133±5	9
0200	0.05±0.09	-0.04±0.05	(3)	6
Krafla (4)	1.06	-0.15(±0.07)	352(±4)	n.a.

(1) Number of observations used to determine relative tilt

(2) This tilt values have been corrected from that of Tryggvason (1979)

(3) No tilt azimuth is obtained as standard error of relative tilt is greater than computed relative tilt.

(4) Water tube tiltmeter at the Krafla power station with tilt azimuth obtained from a bore hole tiltmeter.

The average relative tilt at the optical levelling tilt stations (Table IV,1) was compared with point source Mogi model, both by using all 12 tilt stations that had been established in the Krafla area before 1979, including the water tube tiltmeter at the power station, and also by using fewer stations, either near to the center of Krafla volcano, where observed tilt correlated well with the observations of the water tube tiltmeter, or farther away from the center of Krafla volcano. The result of this comparison is presented in Table IV,2.

Comments on Table IV,1: There is a good correlation between observed tilt at the different tilt stations near Krafla during inflations and deflations of Krafla volcano. This is especially clear for the optical levelling tilt stations 0000, 0010, 0080, 0090, and the water tube tiltmeter at the Krafla power station. Several other optical levelling tilt stations also observe tilt during large inflations or deflations which definitely correlate with the tilt at the Krafla power station, although in most cases, the tilt at these stations is too small to be clearly observed as observational errors are similar or larger than the ground tilt which is caused by ground uplift or subsidence at Krafla. The numerical values presented in Table IV,1 are obtained by comparing observed tilt between observations of the optical levelling tilt stations and the north (N13°E) component of tilt at the Krafla power station for the same period. Only those periods when either inflation or deflation dominates are considered, and periods of deflations with ground rifting near the center of deformation are omitted. The subsidence event of early September 1977 is omitted, partly because of observed rifting of the ground at Leirhnjúkur, partly because the ratio between tilt at different stations was quite anomalous during this event. The subsidence event of late April 1977 is omitted because no optical levelling tilt station was observed shortly before this event, and the tilt observed between measurements of May 1977 and previous observation which was made in November 1976 included two large subsidence events and two extensive inflation periods.

Table IV,2

Solutions for most probable location of point source based on the relative tilt (Table IV,1). Depth is constrained as 3.0 km. X0 and Y0 are horizontal coordinates of the accepted point source. DH0 is the maximum vertical ground displacement (vertically above the source) corresponding to tilt of 1 μrad measured by the water tube tiltmeter at the Krafla power station. St. dev. is the standard deviation of relative tilt from the tilt predicted by the Mogi model. R^2 is the coefficient of correlation squared, between relative tilt and Mogi model tilt.

X0 km	Y0 km	DH0 mm	St. dev. μrad	R^2	Number of stations
17.51	89.42	4.14	0.194	0.942	12 (all stations)
18.27	87.73	1.96	0.035	0.856	7 (A, 0020, 0040, 0050. 0060. 0070. 0200)
17.44	89.42	3.61	0.330	0.650	5 (0000, 0010, 0080, 0090, power station)
17.51	90.27	5.26	0.025	0.999	4 (A, 0000, 0020, 0040)

Comments on Table IV,2: This table compares the computed point source parameters for various selection of tilt stations used in the computation. The station tilt, relative to north component of tilt at the Krafla power station is used (Table IV,1), and source depth is constrained at 3.0 km. The value of DH0, the maximum vertical ground displacement, is given for tilt values which correspond to 1 µrad tilt, up toward north, as observed by the water tube tiltmeter at the Krafla power station. If all 12 optical levelling tilt stations are used (1st row), and also if 4 nearest tilt stations and the power station tiltmeter are used (3rd row), then the computed location of the point source of deformation is very similar to the average location as given in Table IV,6. If the western stations 0080 and 0090 are excluded, and only more distant stations are used, the computed source location tends to be displaced towards south-east (2nd row), and correlation between relative tilt and computed model tilt is low. If the western stations are excluded and only stations relatively near to the source are used (4th row), the computed source location is 0.6 to 0.8 km farther north than the average locations of Table IV,6 and maximum vertical ground displacement is calculated as greater than for most other models, while the correlation between observed and model tilt is near perfect. The computed maximum ground displacement and the computed point source locations depend greatly on the stations used. This suggests that the individual tilt stations observe ground tilt which is only partly controlled by the location and magnitude of a single point source of increased or decreased pressure, but partly controlled by some unknown causes which may be related to ground topography, deviation from homogeneous and perfect elastic behaviour of the geologic formations, and the source may deviate greatly from the single point source used in the model study.

Table IV,3

Variation of computed source parameters if constrained source depth is varied, based on 7 stations (A, 0000, 0010, 0020, 0040, 0080, 0090) and tilt relative to 1 µrad tilt at the Krafla power station. See Table IV,2 for explanation of column headings. H is the constrained source depth.

X0 km	Y0 km	H km	DH0 mm	St.dev. µrad	R^2
17.70	89.74	2.00	6.84	0.213	0.972
17.51	89.53	2.50	4.66	0.174	0.963
17.13	89.21	3.00	3.85	0.137	0.945
16.87	89.11	3.50	4.04	0.160	0.932
16.68	89.11	4.00	4.48	0.214	0.902
16.68	89.21	4.50	5.26	0.279	0.853

Table IV,4

Same as IV,3, except that 6 stations (A, 0000, 0020, 0040, 0080, 0090) are used in the computation, deleting station 0010 which is located very near the center of uplift/subsidence, and is generally observed with large relative tilt, and thus influences computed source solutions greatly.

X0 km	Y0 km	H km	DH0 mm	St. dev. μrad	R^3
16.93	89.16	2.00	4.89	0.108	0.976
16.76	89.21	2.50	3.70	0.106	0.970
16.54	89.28	3.00	3.38	0.108	0.962
16.39	89.35	3.50	3.61	0.125	0.950

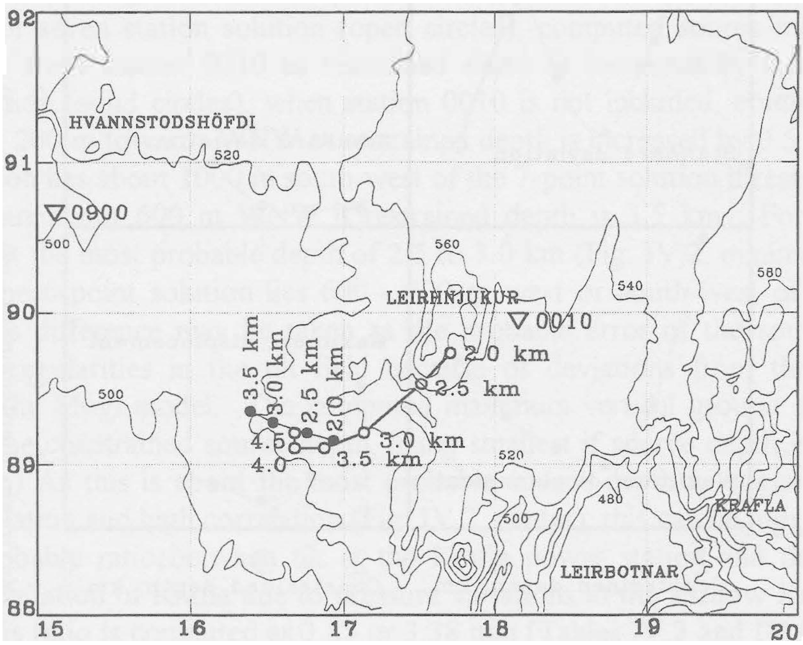

Fig. IV,1. Computed location of a single point source at Krafla as computed from relative tilt at 7 optical levelling tilt stations at less than 10 km distance from Leirhnjúkur (open circles, Table IV,3) and from tilt at six stations, leaving out the station 0010, which lies very close to the computed center of deformation (solid circles, Table IV,4). The apparent source location is computed for several values of constrained source depth, showing migration of the computed center as constrained depth changes.

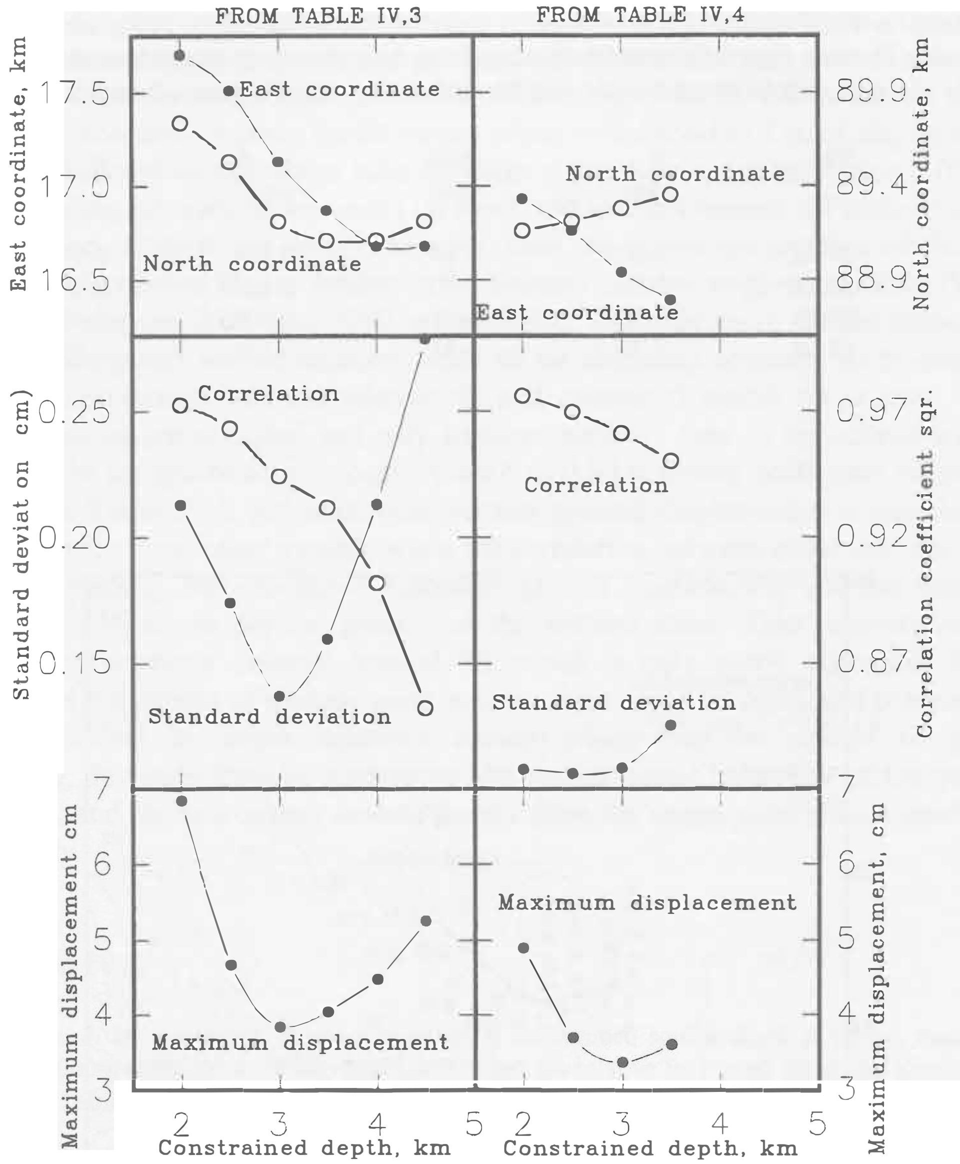

Fig. IV,2. Variation of various components of the computed point source of deformation of Krafla as constrained source depth is varied. Left part presents data of Table IV,3 and right part presents data of Table IV,4. The standard deviation of observed tilt from model tilt is smallest if source depth is constrained at about 3.0 km, while correlation between radial component of observed tilt from model tilt is highest for the shallowest source depth (2.0 km) for which source components are computed. The computed maximum vertical ground displacement (bottom) is given in mm for 1 μrad tilt at Krafla power station.

Comments on Figures IV,1 and IV,2 and Tables IV,3 and IV,4. Seven optical levelling tilt stations are used to obtain the solutions here discussed. These are all the optical levelling tilt stations of 1977 - 1979 within about 10 km distance from the indicated center of deformation at Krafla. All observations made before 1980 at these stations were compared with observed north component of tilt at the Krafla power station, and relative tilt at these stations was obtained from this comparison (Table IV,1). Relative tilt component at each station was accepted as the average ratio of this tilt component to the north component of tilt at the Krafla power station as observed by the water tube tiltmeter. In obtaining this relative tilt, certain observations were excluded, as they were considered not representative for the average relative tilt. These included tilt observations over periods covering the subsidence events of April 1977 and September 1977, but during these events, rifting occurred in the vicinity of the tilt stations, and also near the Krafla power station. Also are excluded certain observations which cover periods of both inflation and deflation, with small net tilt, as inflation tilt and deflation tilt cancel each other to large extend. Fig. IV,1 shows definite westward migration of computed source location as constrained depth is increased. For seven station solution (open circles), computed source moves 200 to 500 m away from station 0010 as restrained depth is increased by 0.5 km. For 6 stations solution (solid circles), when station 0010 is not included, computed source moves about 200 m towards WNW as restrained depth is increased by 0.5 km. The 6-station solution lies about 1000 m south-west of the 7-point solution if restrained depth is 2.0 km, but about 600 m WNW if restrained depth is 3.5 km. For the source constrained at the most probable depth of 2.5 to 3.0 km (Fig. IV,2, minimum standard deviation), the 6-point solution lies 600 - 800 m west or south-west of the 7-point solution. This difference may be taken as the probable error of the source location caused by irregularities in the tilt field because of deviations from the conditions required by the Mogi model. The computed maximum vertical ground displacement varies with the constrained source depth, being smallest if source depth is 3 km (Fig. IV,2, bottom) As this is about the most probable source depth as suggested by low standard deviation and high correlation (Fig. IV,2, center), this can be judged as giving the most probable ratio between tilt at the Krafla power station and the maximum inflation or deflation of Krafla due to pressure variations in the shallow Krafla magma chamber. This ratio is computed as 3.85 or 3.38 mm (Tables IV,3 and IV,4) maximum vertical ground displacement for each μrad of tilt at the Krafla power station, if 7 or 6 tilt stations are accepted as giving correct picture of the inflation bulge or deflation bowl at Krafla during the period 1976-1979.

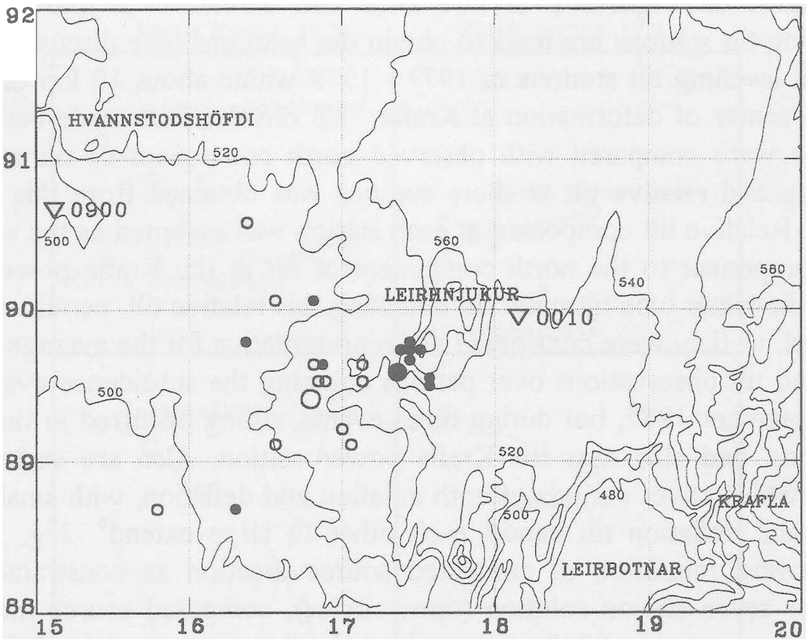

Fig. IV,3 Computed point source locations for periods 1976 to 1978 (See table IV,5). Tilt at 4 stations, 0000, 0010, 0080, and 0090, is used in these computations and source depth is constrained at 2.5 km (solid circles) and 3.0 km (open circles). Weighted average locations are shown as large circles, and tilt stations as triangles.

Comments on Table IV,5 and Fig. IV,3: It is clear from Fig. IV,3 that the solutions for constrained depth of 2.5 km (solid circles) are more tightly packed than solutions for constrained source depth of 3.0 km This dense group of computed source locations for 2.5 km depth of the source is at the south end of the small hill Leirhnjúkur. Most of the solutions for constrained depth of 3.0 km lie about 0.5 km to the west of the south end of Leirhnjúkur.

There are 4 solutions for constrained depth of 2.5 km which lie outside the dense group at the south end of Leirhnjúkur, all to the west of 17 km E coordinate. One of these is solution for the period of August 16 to September 11, 1977, which includes the subsidence and rifting event of September 8, 1977. Another is a solution for the period May 19 to June 28, a period of relatively small inflation but relatively large standard deviation of observed tilt from model tilt.

The standard deviation reported in Table IV,5 is usually much higher than the expected error limit of the tilt measurements of about 5 μrad (Tryggvason 1980). This shows that the observed tilt can only partly be explained as caused by a point source of the Mogi model.

Table IV,5

Computed most probable center and maximum vertical displacement for a point source (Mogi model) for periods between tilt observations 1977 through 1979. Four tilt stations are used, 0000, 0010, 0080, 0090. Maximum correlation between observed and computed tilt is used as criteria of best solution.

First date	Last date	X0 km	Y0 km	H km	DH0 mm	St. dev. μrad	R^3
77 06 14	77 07 18	17.44	89.74	2.5	278.9	10.88	0.726
		16.87	89.53	3.0	199.7	10.67	0.889
77 07 18	77 08 16	17.38	89.74	2.5	241.6	7.14	0.860
		16.81	89.64	3.0	183.6	10.11	0.608
77 08 16	77 09 11	16.81	90.06	2.5	-724.3	78.39	0.864
		16.38	90.58	3.0	-738.9	114.09	0.738
77 09 11	77 12 02	17.44	89.74	2.5	908.7	9.91	0.993
		16.86	89.53	3.0	609.8	18.13	0.923
78 05 19	78 06 28	16.87	89.64	2.5	161.3	15.34	0.986
		16.56	90.06	3.0	174.2	25.03	0.968
78 09 30	78 11 12	17.57	89.53	2.5	-797.4	15.15	0.973
		17.06	89.11	3.0	-586.7	33.96	0.999
78 11 12	79 02 16	17.57	89.53	2.5	889.0	13.34	0.992
		17.00	89.21	3.0	643.6	25.82	0.895
79 08 02	79 08 19	17.44	89.74	2.5	63.8	4.93	0.958
		17.13	89.64	3.0	55.6	4.67	0.736
79 08 19	79 10 03	16.30	88.68	2.5	108.1	8.11	0.864
		15.79	88.68	3.0	114.8	9.31	0.495
79 10 03	79 11 22	17.51	89.74	2.5	119.1	7.60	0.822
		17.13	89.53	3.0	90.8	8.17	0.617
79 08 02	79 11 22	16.36	89.79	2.5	181.9	12.14	0.876
		16.56	89.11	3.0	223.9	9.31	0.912
Weighted average		17.36	89.59	2.5			
		16.79	89.41	3.0			

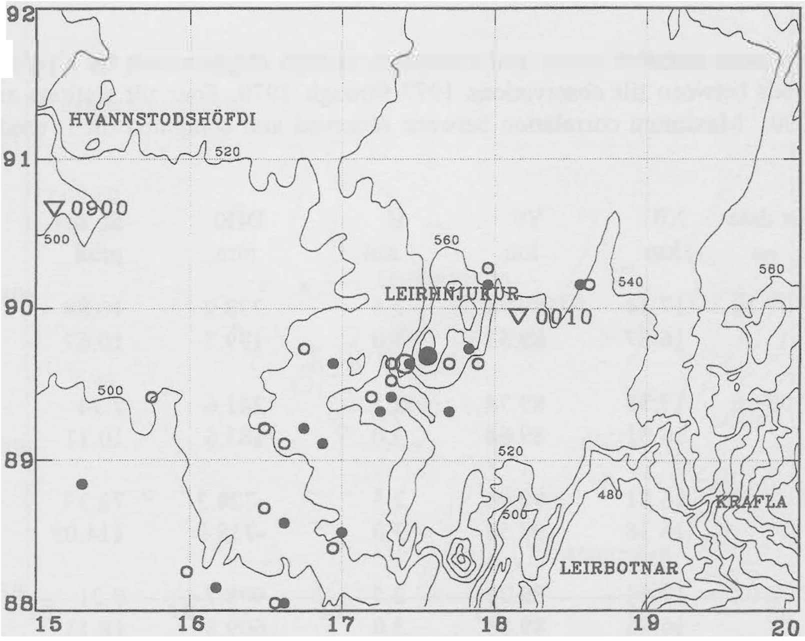

Fig. IV,4. Computed point source location for deformation at Krafla for periods between tilt observations from June 1977 to November 1979 (see Table IV,6). Three tilt stations are used, 0000, 0080, and 0090. Solid circles are solutions for source depth constrained at 2.5 km, and open circles are for depth of 3.0 km. Larger symbols are average locations, and tilt stations are shown as triangles.

Comments of Fig. IV,4 and Table IV,6: The data used to obtain the solutions presented in Table IV,6 and Fig. IV,4 are basically the same as used for Table IV,5 and Fig. IV,3 above. The difference lies in the number of tilt stations used to compute the source parameters. Four stations were used to obtain the values of Table IV,5 and Fig. IV,3 while only three of these tilt stations were used to obtain the solutions of Table IV,6 and Fig. IV,4.

The scatter of computed source locations is greater on Fig. IV,4 than on Fig. IV,3, and there are more solutions shown in this latter figure. This is because on several occasions, station 0010 was not observed at the same time as the other tilt stations. Most of the locations which are computed to lie far away from the average location are based on observations over periods of small deformation, where observational errors are expected to be large relative to actual ground tilt. This is true for the periods 78 05 19 - 78 06 28, 79 08 02 - 79 08 19, 79 08 19 - 79 10 03, and 79 10 03 - 79 11 22.

One solution, for a period of very large deformation, has very low standard deviation of observed from model tilt, and the computed source location is anomalous, being farther north than any other computed location in this data set. This is the solution for the period 78 01 11 - 78 06 28, during inflation following the second greatest deflation of the Krafla volcano during the whole 1975-1989 period of high tectono-volcanic activity. This strongly suggests that the center of deformation during the inflation following the deflation of January 1978, lay about 0.5 km to the north-east of the average source location for other inflations of the period 1977-1979.

Table IV,6

Computed most probable point source and source magnitude for periods between observations from 1977 to 1979. Three tilt stations are used, (0000, 0080, 0090). Maximum correlation between radial component of observed tilt and computed tilt is used as criterion on best solution. As only 3 stations are used, perfect correlation is always obtained.

First date	Last date	X0 km	Y0 km	H km	DH0 mm	St. dev. μrad
77 06 14	77 07 18	16.94	89.64	2.5	260.6	13.13
		16.75	89.74	3.0	221.7	15.21
77 07 18	77 08 16	17.70	89.32	2.5	227.3	9.24
		17.89	89.64	3.0	227.1	9.43
77 09 11	77 12 02	17.32	89.42	2.5	770.9	4.45
		17.19	89.42	3.0	624.7	6.98
77 12 02	78 01 11	17.25	89.32	2.5	-891.7	7.67
		17.32	89.53	3.0	-861.5	5.83
78 01 11	78 05 19	17.95	90.16	2.5	1412.9	2.53
		17.95	90.27	3.0	1134.5	3.25
78 05 19	78 06 28	15.30	88.84	2.5	103.4	14.27
		15.75	89.42	3.0	108.9	20.61
78 06 28	78 08 05	16.75	89.21	2.5	-326.8	14.46
		16.49	89.21	3.0	-293.0	17.59
78 08 05	78 09 30	16.87	89.11	2.5	336.5	8.65
		16.62	89.11	3.0	288.0	10.82
78 09 30	78 11 12	17.44	89.64	2.5	-779.6	4.76
		17.32	89.64	3.0	-614.6	7.12
78 11 12	79 02 16	17.83	89.74	2.5	1063.2	10.91
		17.70	89.64	3.0	789.8	8.42
79 08 02*	79 08 19	16.62	88.05	2.5	40,0	4.58
		16.56	88.05	3.0	36.1	4.53
79 08 02*	79 08 19	17.00	88.52	2.5	42.7	5.14
		16.94	88.41	3.0	42.3	4.96
79 08 19	79 10 03	16.17	88.15	2.5	85.0	8.38
		15.98	88.26	3.0	85.9	7.72
79 10 03	79 11 22	18.59	90.16	2.5	244.4	6.72
		18.59	90.16	3.0	208.3	7.51
79 08 02	79 11 22	16.62	88.58	2.5	202.8	2.00
		16.49	88.68	3.0	186.6	1.05
Average		17.56	89.69	2.5		
weighted		17.41	89.64	3.0		

*) Two different solutions of perfect correlation

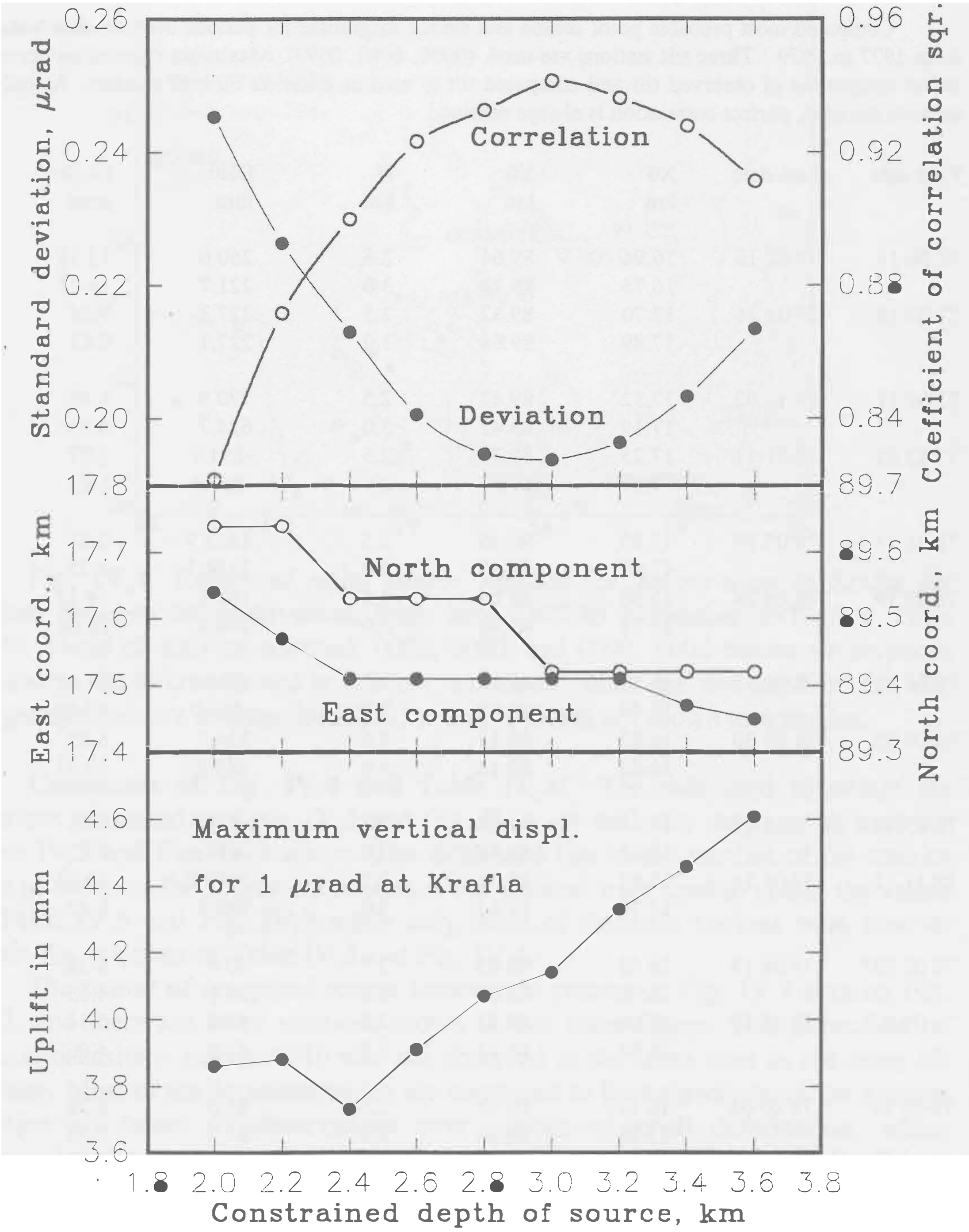

Fig. IV,5. Variation of single point source parameters with restrained source depth, as computed from relative tilt at all tilt stations in the Krafla region during the period 1976 to 1979. The optical levelling stations are eleven: A, 0000, 0010, 0020, 0040, 0050, 0060, 0070, 0080, 0090, and 0200, and the twelfth station used is the Krafla power station water tube tiltmeter. Data used are presented in Table IV,7. The minimum standard deviation of observed tilt from model tilt is found for restrained depth of about 3.0 km. The same depth gives maximum correlation between observed radial tilt and model tilt, suggesting this to be most probable source depth.

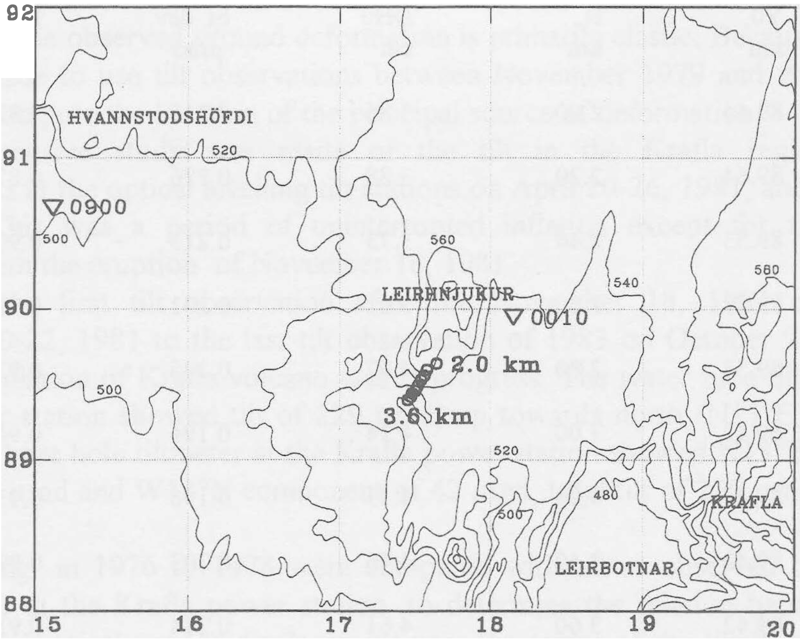

Fig. IV,6. Computed source location for inflations and deflations of Krafla volcano 1976-1979, using relative tilt at 11 optical levelling stations and the water tube tiltmeter at the Krafla power station. Location is computed for restrained depth of 2.0 to 3.6 km at 0.2 km depth intervals. The data are presented in Table IV,7 and Fig. IV,5.

Comments on Figures IV,5 and IV,6 and Table IV,7. The data for these figures and table is relative tilt at all tilt stations near Krafla which were available before 1980. The present table and figures use the calculated relative tilt, even though this is not significantly different from zero at 5 or even more stations of the 12 stations used. Therefore the reliability of these results may be disputed. The source location changes less with changing restrained depth, than that computed by using only tilt station with relative tilt which differ significantly from zero (comparison of Fig. IV,1 and Fig. IV,6). Lowest standard deviation and also highest correlation is found if source depth is restrained at 3.0 km (Fig. IV,5), suggesting this depth to be most probably for the true source depth.

TABLE IV,7

Computed point source parameters from and their variation if restrained point source depth is varied from 2.0 km to 3.6 km. Used are relative tilt data from all 12 optical levelling tilt stations in the vicinity of Krafla, and also the water tube tiltmeter at the Krafla power station. The relative tilt at each station is found by correlation the station tilt with the north component of tilt at the Krafla power station as observed by a water tube tiltmeter. Values of DH0 (maximum vertical ground displacement) and st. dev. (standard deviation of relative observed tilt from computed model tilt) are based on a value of 10 μrad tilt at the Krafla power station.

X0, km	Y0, km	H, km	DH0 cm	St. dev. μrad	R^2
17.64	89.64	2.00	3.86	0.245	0.822
17.57	89.64	2.20	3.88	0.226	0.872
17.51	89.53	2.40	3.73	0.213	0.900
17.51	89.53	2.60	3.91	0.201	0.923
17.51	89.53	2.80	4.07	0.195	0.933
17.51	89.42	3.00	4.14	0.194	0.941
17.51	89.42	3.20	4.33	0.196	0.936
17.47	89.42	3.40	4.46	0.203	0.928
17.45	89.42	3.60	4.61	0.214	0.911

ANALYSIS OF 1981-1983 TILT OBSERVATIONS

The period between the tilt observations on November 22, 1979 and April 22, 1981 was characterised by frequent eruptions and extensive ground rifting in the Krafla volcano, making determination of center of deformation unreliable. This activity started with an eruption on March 16, 1980, followed by eruptions in July and October 1980 and January 1981. During two of these eruptions, those of March and October 1980, ground fissures with horizontal and vertical fault displacements extended across the central area of the Krafla volcano, causing very significant non-elastic ground deformation, but a criteria for determining the center of deformation, using the Mogi model, is that the observed ground deformation is primarily elastic. Because of this, no effort was made to use tilt observations between November 1979 and April 1981 to estimate or compute the location of the principal source of deformation.

An extensive study was made of the tilt in the Krafla region between measurements at the optical levelling tilt stations on April 20-26, 1981, and October 7-9, 1983. This was a period of uninterrupted inflation except for the deflation associated with the eruption of November 18, 1981.

From the first tilt observation after the November 18, 1981 eruption, on November 20-22, 1981 to the last tilt observation of 1983 on October 7 to 9. 1983, continuous inflation of Krafla volcano was in progress. The water tube tiltmeter at the Krafla power station showed tilt of 229 µrad, up towards north (N13°E) during this period. The bore hole tiltmeter at the Krafla power station showed N13°E component of tilt of 225 µrad and W13°N component of 42 µrad, total tilt of 229 µrad in azimuth N2°E

Levelling in 1976 to 1978 were compared with tilt as observed by the water tube tiltmeter at the Krafla power station, to determine the relation between this tilt and maximum vertical ground displacement near the center of the Krafla volcano, and it was found that one µrad of tilt corresponded to about 3.4 mm maximum vertical ground displacement (Björnsson et al 1979). This suggests that ground uplift at the center of Krafla volcano between November 21 1981 and October 8, 1982 amounted to 78 cm, equivalent to 3.41 mm uplift per 1.0 µrad of tilt at the Krafla power station as observed by the water tube tiltmeter.

At 14 different times from April 1981 to October 1983, two or more optical levelling tilt stations in the Krafla area were observed (Table V,1). Only tilt stations at distances less than 10 km from the suggested center of deformation were considered in the present analysis.

If 5 or more stations were occupied at two successive tilt measurements, the observed tilt between these times of measurements was used to calculate the most probable single point source which might be responsible for the observed tilt. An exception to this is that the observations of October 3-9, 1981 were not used. That would have meant that the period from August 29 1981 to November 8, 1981 would have been treated as two periods, both with small observed tilt and expected low precision of solutions.

The period between observations of November 6-8 1981 and November 20-22 1981 includes the deflation of November 18 1981. This deflation was associated with considerable lava eruption and ground rifting near to and north of Leirhnjúkur. Because of this ground rifting, and associated vertical and horizontal fault displacement in the immediate vicinity of the suggested center of deformation, the calculated location of a point source may be unreliable, but comparison of observed tilt and Mogi model shows that tilt agrees reasonable well with the model, and the computed center of deformation is as reliable as those computed for period of no known non-elastic deformation.

The periods for which solutions of point source locations were sought were the following:

22 April 1981 to 29 August, 1981
29 August 1981 to 8 November 1981
8 November 1981 to 21 November 1981
21 November 1981 to 21 February 1982
21 February 1982 to 15 May 1982
15 May 1982 to 2 September 1982
2 September 1982 to 22 June 1983
22 June 1983 to 8 October 1983

Further three longer periods were treated the same way:

21 November 1981 to 15 May 1982
15 May 1982 to 8 October 1983
21 November 1981 to 8 October 1983

Table V,1

Observations of the optical levelling tilt stations in the Krafla region April 1981 through October 1983.

Date of observations	Year	Number of stations 1 to 10 km from Leirhnjúkur	Date of observations used in comparisons
20 - 26 April	1981	6	22 April
19 - 21 June	1981	4	
22 July	1981	2	
27- 31 August	1981	7	29 August
3 - 7 October	1981	9	
6 - 8 November	1981	9	8 November
20 - 22 November	1981	7	21 November
21 - 22 February	1982	7	21 February
14 - 16 May	1982	9	15 May
24 August	1982	2	
1 - 3 September	1982	8	2 September
19 - 20 October	1982	4	
21 - 24 June	1983	9	22 June
7 - 9 October	1983	9	8 October

The rate of inflation at Krafla has been observed to vary more or less regularly with time since previous subsidence event, but between 1975 and 1981 had the time between subsidence events never exceeded one year (Tryggvason 1995). The frequency of extensive tilt observations did not allow a study of any possible systematic variation of the location and behaviour of the inflation source as inflation rate decreased at this high rate of deflation events. The almost three years between successive deflations of November 1981 and September 1984 made it possible to determine if the technique and frequency of tilt observations did show any significant change in either location or other characteristics of the inflation source from the rapid inflation of late 1981 to the slow inflation of 1982 and 1983.

Table V,2

Locations of Mogi model point source and maximum vertical ground displacement which gives smallest standard deviation of observed tilt from computed model tilt. Used are measurements at all optical levelling tilt station at less than 10 km distance from Leirhnjúkur.

First y m d	Last y m d	X0 km	Y0 km	H km	DH0 mm	Krafla tilt µrad	Krafla DH0 mm
81 04 22	81 08 29	16.63	89.58	2.5	115.5	43.2	146.9
81 08 29	81 11 08	17.53	89.85	1.9	118.2	8.3	28.2
81 11 08	81 11 21	16.78	88.90	2.3	-509.9	-109.0	-370.6
81 11 21	82 02 21	17.19	89.29	2.8	481.8	139.1	472.9
82 02 21	82 05 15	no solution				3.1	10.5
82 05 15	82 09 02	16.78	89.21	2.2	42.1	11.0	37.4
82 09 02	83 06 22	17.21	89.74	2.2	252.5	50.8	172.7
83 06 22	83 10 08	17.05	89.62	1.9	75.8	25.0	85.0
81 11 21	83 10 08	16.76	89.32	2.5	696.5	229.0	778.6
Average (Weighted)		16.83	89.43	2.42			

The two first column in Table V,2 are dates of first and last tilt observations used in the model calculation, X0 is the east coordinate of the computed point source in kilometers, increasing eastward, Y0 is The north component of the computed point source in kilometers increasing northward. H is the apparent depth of the computed point source in km from the earth's surface and DH0 is the computed vertical ground displacement, vertically above the computed source. The last two columns present the north component of tilt at the Krafla power station, observed with a water tube tiltmeter, and calculated maximum vertical ground displacement in mm, assuming the average relation of maximum vertical ground displacement to water tube tiltmeter readings of 3.4 mm per one µrad, found for the period 1976-1978 (Björnsson et al. 1979).

Comments on Tables V,2 and V,3: The weight factor used to obtain the average values at the bottom of these tables, (and also at Tables V,4, V,5, V,6, and V,7) is |DH0|/(st. dev.). The computed most probable source depth in Table V,2 (H) is somewhat smaller than that found from observations of 1976 to 1979 (Tables IV,2 and IV,4), but this difference is probably not significant, because the procedure and observational data used cannot give precise source depth, and also because several new tilt stations were constructed in late 1981. Therefore, the observations of 1976 to 1979 and those of 1981-1983 are not of the same quality.

It is of interest to compare the maximum vertical ground displacement as obtained from observations at the optical levelling tilt stations, using the Mogi model, and the measurements of the water tube tiltmeter at the Krafla power station. The correlation between these two estimates of maximum vertical ground displacement (column 6 and 8 of Table V,2) is actually very poor. The greatest relative difference is found for the period 29 August to 8 November 1981, when the Mogi model, using 7 tilt stations, determined maximum vertical displacement of 118.2 mm (Table V,2) while water tube tiltmeter readings gave an estimate of 28.2 mm. The reason for this difference lies in anomalous tilt observations at several optical levelling tilt stations. It should be noted that observational error at the optical levelling tilt stations is usually less than 3 μrad, but unexplained ground surface strain may cause errors of more than 5 μrad of tilt. Such errors will occasionally cause significant errors in the calculated maximum vertical ground displacement, and also in the calculated most probable location of the hypothetical point source.

Table V,3

Coordinates of point source giving best agreement (least standard deviation) with observations if source depth is restrained at 2.5 km. Calculated from measurements at all tilt stations at less than 10 km from Leirhnjúkur (A, 0000, 0010, 0020, 0040, 0080, 0090, 0210, 0240, 0250)

First y m d	Last y m d	X0 km	Y0 km	DH0 mm	St. dev. μrad	R^2	N
81 04 22	81 08 29	16.68	89.64	166.3	11.30	0.935	6
81 08 29	81 11 08	16.87	90.06	80.6	11.01	0.542	7
81 11 08	81 11 21	16.94	89.00	-535.5	25.31	0.927	8
81 11 21	82 02 21	17.51	89.53	590.7	14.25	0.992	8
82 02 21	82 05 15	16.05	89.64	58.8	7.74	0.838	8
82 05 15	82 09 02	16.81	89.21	45.8	6.02	0.620	10
82 09 02	83 06 22	16.94	89.64	237.2	12.26	0.912	10
83 06 22	83 10 08	16.94	89.53	94.8	9.05	0.666	10
81 11 21	82 05 15	16.68	89.11	424.7	18.48	0.938	8
82 05 15	83 10 08	16.94	89.64	327.5	18.85	0.855	10
81 11 21	83 10 08	16.75	89.32	694.6	21.71	0.975	8
Weighted average		16.93	89.43				

The standard deviation of observed tilt from model tilt (St. dev.) is presented in the sixth column of the Tables V,3 to V,7. The coefficient of correlation squared between the radial component (with respect to the point source) of observed tilt and the tilt predicted by the Mogi model is presented in column 7 of Table V,3 to V,7. The last column of Table V,3 gives the number of tilt stations used in the model calculation presented in each line of the table. The same stations were used to obtain the data of Tables V,4 to V,7.

The estimated maximum vertical ground displacement during the eruption and subsidence event of 18 November 1981 is -509.9 mm based on 8 optical levelling tilt stations, and -370.6 mm according to the water tube tiltmeter (Table V,2). This difference is greater than can be explained by observational errors. The eruption and associated ground rifting occurred near several of the tilt stations, which certainly caused ground deformation, other than that which can be explained by a point source of decreased pressure.

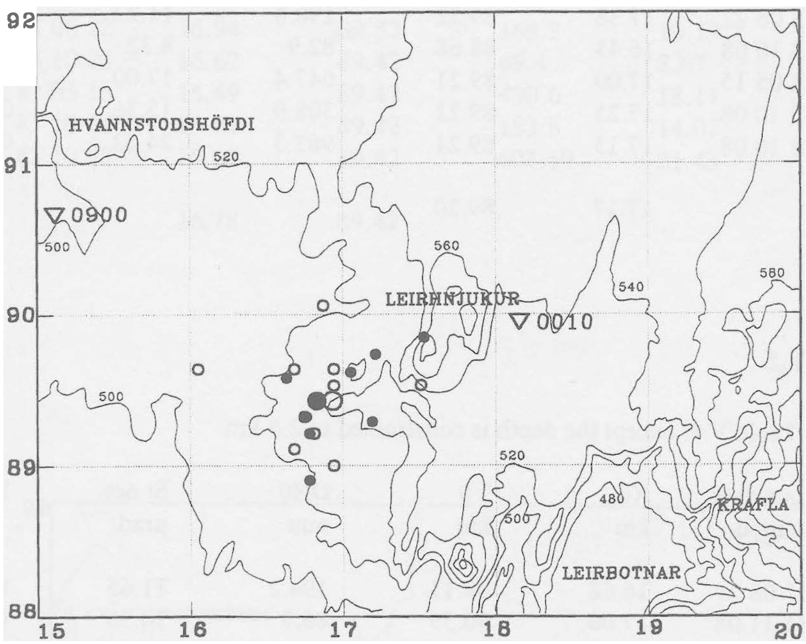

Fig. V,1. Computed point source locations for ground deformation at Krafla 1981-1983. Filled circles are data from Table V,2 where source depth is not constrained and all stations at less than 10 km distance from Leirhnjúkur are used in model calculation. Open circles are computed point source locations of Table V,3, where source depth is constrained at 2.5 km and all stations at less than 10 km distance are used in the model calculation. Small circles are individual solutions and large circles are weighted mean locations.

Table V,4

Most probable parameters of point source if depth is constrained at 2.0 km, using all optical levelling tilt stations at less than 10 km distance from Leirhnjúkur, except station 0010, Leirhnjúkur.

First date y m d	Last date y m d	X0 km	Y0 km	DH0 mm	St. dev µrad	R^2
81 04 22	81 08 29	16.75	89.00	242.5	11.63	0.950
81 11 08	81 11 21	16.62	89.11	-547.2	23.52	0.901
81 11 21	82 02 21	17.19	89.21	653.3	11.93	0.977
82 05 15	82 09 02	16.87	89.00	50.1	6.33	0.244
82 09 02	83 06 22	17.38	89,32	290.8	11.22	0.971
83 06 22	83 10 08	16.43	88.68	82.9	8.32	0.364
81 11 21	82 05 15	17.00	89.21	647.4	17.00	0.971
82 05 15	83 10 08	17.25	89.21	308.0	15.36	0.961
81 11 21	83 10 08	17.13	89.21	983.3	24.62	0.975
Average		17.17	89.20			

Table V,5

Same as Table V,4, except the depth is constrained to 2.5 km

First date y m d	Last date y m d	X0 km	Y0 km	DH0 mm	St dev µrad	R^2
81 04 22	81 08 29	16.68	89.11	194.2	11.65	0.951
81 08 29	81 11 08	17.00	90.59	86.9	10.35	0.380
81 11 08	81 11 21	16.30	89.11	-432.5	23.95	0.860
81 11 21	82 02 21	17.06	89.32	483.4	11.69	0.977
82 02 21	82 05 15	15.41	89.53	48.3	6.30	0.839
82 05 15	82 09 02	16.56	89.11	35.6	6.25	0.201
82 09 02	83 06 22	17.25	89.42	209.5	10.79	0.971
83 06 22	83 10 08	16.56	89.00	73.3	8.53	0.343
81 11 21	82 05 15	16.75	89.32	464.1	17.08	0.961
82 05 15	83 10 08	17.06	89.21	219.2	14.85	0.953
81 11 21	83 10 08	16.87	89.21	700.2	23.04	0.954
Average		16.75	89.34			

When Table V,5 and Table V,3 are compared, the effect of station 0010 (Leirhnjúkur) can be seen. This station is included in the results presented in Table V,3, but not in Table V,5, (nor Tables V,4, V,6, and V,7), otherwise same data is used to obtain the results of both tables, Table V,3 and Table V,5.

Table V,6

Same as Table V,4, except the depth is constrained at 3.0 km.

First date y m d	Last date y m d	X0 km	Y0 km	DH0 mm	St. dev. μrad	R^2
81 04 22	81 08 29	16.49	89.32	175.6	11.70	0.933
81 11 08	81 11 21	16.17	89.32	-442.3	27.09	0.869
81 11 21	82 02 21	16.81	89.42	414.9	12.38	0.964
82 05 15	82 09 02	15.60	89.32	31.2	6.06	0.117
82 09 02	83 06 22	16.94	89.53	168.3	10.19	0.969
83 06 22	83 10 08	16.62	89.42	69.4	8.67	0.328
81 11 21	82 05 15	16.49	89.42	430.6	18.11	0.941
82 05 15	83 10 08	16.81	89.42	183.8	14.07	0.944
81 11 21	83 10 08	16.62	89.42	607.19	21.43	0.950
Average		16.78	89.42			

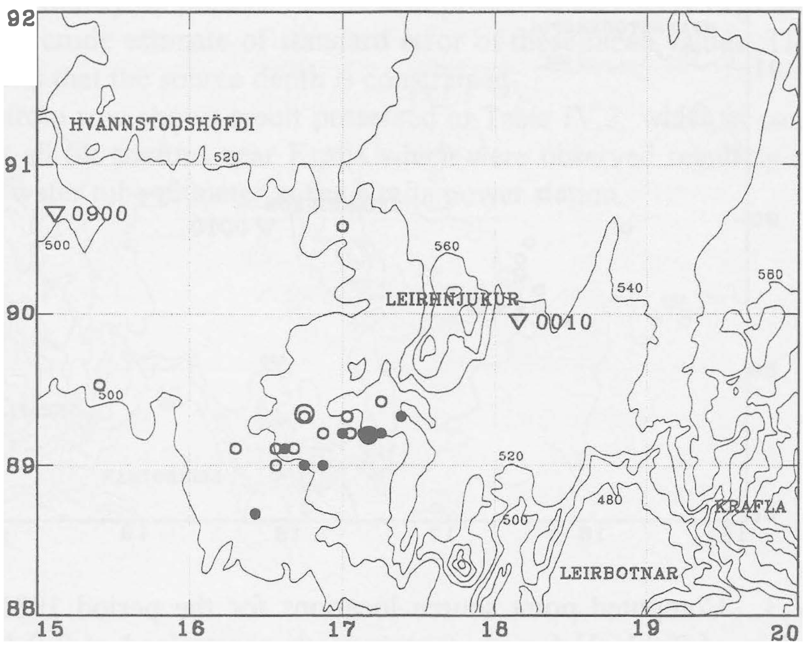

Fig. V,2. Computed point source locations for ground deformation at Krafla in the period 1981-1983. Solid circles are data of Table V,4 where source depth is constrained at 2.0 km and all stations at less than 10 km distance from Leirhnjukur are used, except for the station 0010 (Leirhnjúkur). Open circles are data of Table V,5 where source depth is constrained at 2.5 km. Two solutions at X=17.00, Y=90.59 and X=15.41, Y=89.53 are computed for periods of unreliable solutions because of small ground deformation. Those periods are not included in Table V,4.

Table V,7

Same as Table V,4, except the depth is constrained at 3.5 km.

First date y m d	Last date y m d	X0 km	Y0 km	DH0 mm	St. dev. µrad	R^2
81 04 22	81 08 29	15.79	89.95	217.5	11.75	0.888
81 11 08	81 11 21	16.36	89.42	-522.5	34.43	0.871
81 11 21	82 02 21	16.75	89.53	441.4	15.63	0.946
82 05 15	82 09 02	15.41	89.32	40.5	5.77	0.103
82 09 02	83 06 22	16.49	89.74	161.4	9.34	0.967
83 06 22	83 10 08	16.43	89.85	69.6	8.74	0.324
81 11 21	82 05 15	16.49	89.64	478.9	22.77	0.932
82 05 15	83 10 08	16.36	89.53	179.6	12.83	0.935
81 11 21	83 10 08	16.36	89.53	652.6	22.49	0.924
Average		16.57	89.62			

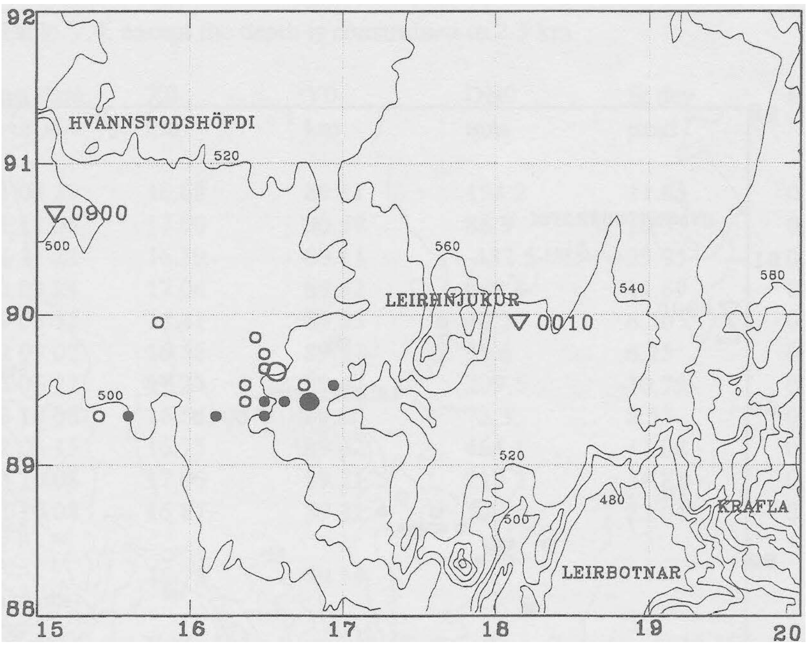

Fig V,3. Computed point source locations for the period 1981-1983. Solid circles are data of Table V,6 with source depth constrained at 3.0 km, using all stations at less than 10 km distance from Leirhnjúkur, except the station 0010 (Leirhnjúkur). Open circles are similar data from Table V,7 with source depth constrained at 3.5 km. Small symbols are individual solutions and large symbols are weighted average locations, with weight factor equal to maximum vertical ground displacement divided by standard deviation of observed tilt from model tilt.

TABLE V,8

Most probable location of Mogi model point source as derived from observations at optical levelling tilt stations.

Method, explanations, periods	E-coord Km	N-coord km	Depth km
Minimum standard deviation, 1981-1983	16.83	89.43	2.42
Minimum standard deviation, 1976-1979	17.13	89.21	3.0
1977-1979, 4 station average	17.36±0.34	89.59±0.28	2.5(R)
1977-1979, 4 station average	16.79±0.33	89.41±0.37	3.0(R)
1977-1979, 3 station average	17.56±0.50	89.69±0.51	2.5(R)
1977-1979, 3 station average	17.41±0.59	89.64±0.57	3.0(R)
1977-1979, 12 stations	17.51	89.42	3.0(R)

Comments on Table V,8: This table compares several average values of computed (or estimated) coordinates of a hypothetical point source of deformation as obtained from study of tilt observations 1976 to 1983 at optical levelling tilt stations in the vicinity of Krafla volcano. The first row gives the average result presented in Table V,2 which is based on observations at all observed stations at distances less than 10 km from the suggested source location, not including the water tube tiltmeter at the Krafla power station.

Second row presents result from Table IV,3 which is based on relative tilt at 7 optical levelling tilt stations at distances less than 10 km from the suggested source.

The next four rows present results also presented in Tables IV,5 and IV,6. The error limits are crude estimate of standard error of these mean values. The (R) in last column signifies that the source depth is constrained.

The bottom row shows result presented in Table IV,2, which is computed from relative tilt at all tilt stations near Krafla which were observed regularly before 1980, including the water tube tiltmeter at the Krafla power station.

ANALYSIS OF 1984-1997 TILT OBSERVATIONS

The period from 1984 to 1997 is characterised by a rather large eruption of Krafla in September 1984, and associated deflation of the volcano. Otherwise, inflation of Krafla volcano was persistent until 1989, but later, slow deflation of the volcano has been observed. For a period of about 18 month in 1985 and 1986, practically no deformation was observed although several measurements suggest deflation at similar scale as after 1989. Some of the tables and figures presented hereafter include data from 1982 and 1983.

Table VI,1

Computed most probable location of a point source of deformation at Krafla volcano for various periods from 1982 to 1997. The computations use tilt observations at all observed optical levelling tilt stations at less than 10 km distance from Leirhnjúkur, usually 9 to 11 stations (in 1995 only 5 stations were observed). Source depth is constrained at 2.5 km below ground surface. The "most probable point source" is defined as the point where source of a Mogi model will produce the smallest possible standard deviation between observed tilt and model tilt.

First date	Last date	X0 km	Y0 km	DH0 mm	St. dev. µrad	R^2
82 02 15	83 06 23	17.25	89.85	256.0	13.12	0.923
83 06 23	84 06 09	17.25	89.85	185.3	11.12	0.887
84 06 09	84 10 03	17.25	88.79	-555.4	29.48	0.836
84 10 03	85 06 01	17.51	89.42	325.4	10.03	0.994
85 06 01	86 10 22	15.58	89.39	-30.4	5.04	0.469
86 10 22	87 04 29	16.75	89.21	211.7	7.23	0.965
87 04 29	88 06 24	16.49	89.64	69.6	7.98	0.784
88 06 24	89 06 23	17.25	90.06	136.8	10.58	0.699
89 06 23	90 06 25	16.36	89.00	-42.2	3.98	0.742
90 06 25	91 07 08	18.27	89.64	-106.2	5.93	0.578
91 07 08	92 06 19	17.76	88.79	-43.8	4.65	0.754
92 06 19	93 06 29	17.22	86.46	-48.1	6.17	0.342
93 06 29	94 07 06	19.03	87.52	-38.6	4.01	0.604
94 07 06	95 07 24	17.89	89.21	-31.0	4.43	0.310
95 07 24	96 07 26	18.65	86.04	-56.1	5.16	0.771
96 07 26	97 07 08	15.22	88.79	-22.4	3.56	0.374
89 06 23	94 07 06	18.14	89.64	-339.5	11.40	0.816
94 07 06	97 07 08	18.14	89.64	-115.5	7.19	0.866
89 06 23	97 07 08	18.14	89.64	-461.0	18.68	0.829

Comments on Table VI,1: The observed tilt between dates of first two columns is used to compute the source parameters presented in Table VI,1. It is clear that solutions for periods of small ground displacements have relatively small standard deviation (6th column), frequently about 5 µrad if maximum ground displacement is less than 100 mm, but the standard deviation usually exceeds 10 µrad if maximum ground displacement exceeds 100 to 200 mm. Standard deviation of about 30 µrad was computed in the solution which includes the large deflation of September 1984. This very large standard deviation suggests considerable non-elastic deformation, caused by fault displacement near the center of deformation.

It has been estimated that average levelling error causes about 3.0 μrad error in tilt at the optical levelling tilt stations (Tryggvason 1983). Therefore, any standard deviation of observed tilt from model tilt which greatly exceeds this value suggests significant deviation of ground deformation from the Mogi-model deformation. The fact that the standard deviation is positively correlated with maximum ground displacement also suggest that the actual ground deformation differs significantly from the Mogi model deformation.

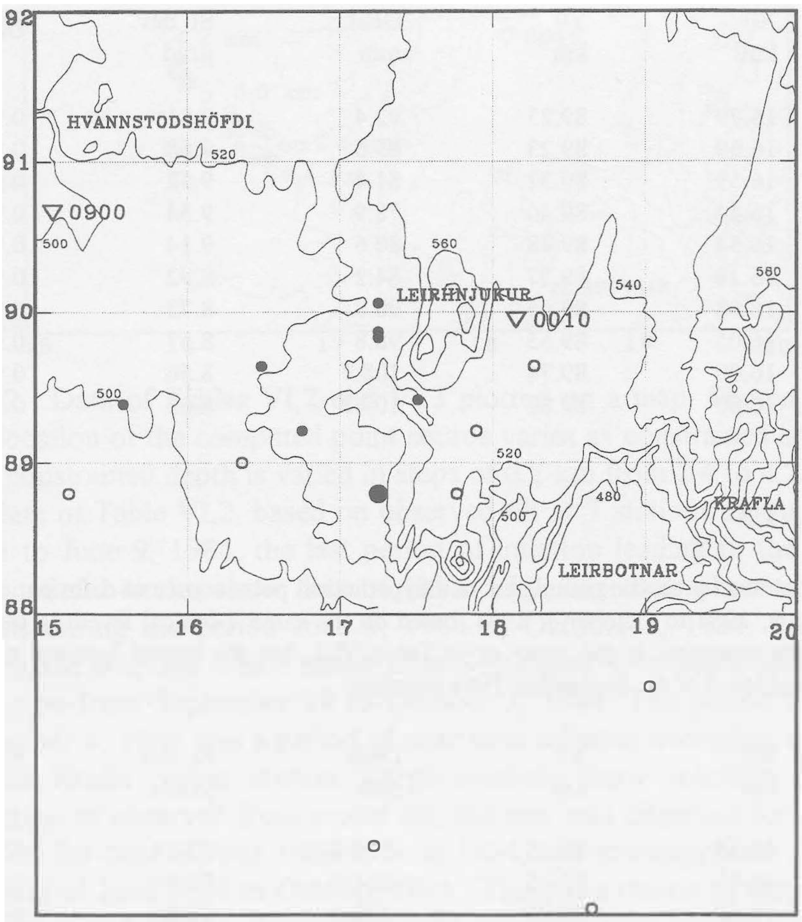

Fig. VI,1. Map of the central area of Krafla volcano showing locations of the best "point source" of deformation for each periods between tilt observations from 1982 to 1997 (Table VI,1). The source depth is constrained at 2.5 km below the ground surface. Solid circles are solutions for periods before June 1989, most of them periods of inflation. Solution for the period of deflation during the September 1984 eruption is shown by a large solid circle. Open circles are solutions for periods after June 1989, when continuous slow deflation was in progress. Three solutions of Table VI,1 lie to the south of the area usually covered by maps of source locations in this report. Therefore the map is extended 2 km southward without topographic contours. The great scatter of computed source location during the slow deflation after 1989 is the result of observational errors as tilt associated with small deformation is small as compared to observational errors The computed most probable point source for the period of deflation during the eruption of September 1984 (large solid circle) is not reliable because of non-elastic deformation caused by the ground rifting.

Table VI,2

Computed most probable parameters of a hypothetical point source of deformation at Krafla for the period June 23, 1983 to June 9, 1984, based on 7 optical levelling tilt stations (A, 0000, 0080, 0090, 0210, 0240, 0250). Shown are parameters of the Mogi model which best agrees with observations as constrained source depth is varied from 2.4 km to 4.2 km in increments of 0.2 km. The period June 1983 to June 1984 is the last period of observation at these tilt station before the eruption of September 1984.

H km	X0 km	Y0 km	DH0 mm	St. dev. µrad	R^2
2.4	16.79	89.23	92.4	9.81	0.959
2.6	16.69	89.23	85.6	9.68	0.953
2.8	16.59	89.32	81.4	9.52	0.940
3.0	16.44	89.40	78.9	9.34	0.922
3.2	16.34	89.48	80.6	9.14	0.916
3.4	16.18	89.57	84.2	8.92	0.905
3.6	16.08	89.65	90.8	8.73	0.905
3.8	16.05	89.65	98.8	8.57	0.921
4.0	16.00	89.74	108.7	8.56	0.924
4.2	16.00	89.82	109.2	8.65	0.926

Table VI,3

Computed most probable parameters of a hypothetical point source of deformation at Krafla for the period June 9, 1984 to October 3, 1984. based on the same 7 optical levelling tilt stations as in Table VI,2. Data treatment is the same as in Table VI,2, but the period between tilt observations includes the subsidence of the September 1984 eruption.

H km	X0 km	Y0 km	DH0 mm	St. dev. µrad	R^2
2.4	16.59	89.15	-535.4	23.24	0.901
2.6	16.49	89.15	-504.6	23.95	0.888
2.8	16.39	89.23	-489.4	24.86	0.887
3.0	16.34	89.32	-494.1	26.40	0.886
3.2	16.34	89.32	-520.2	28.4	0.879
3.4	16.39	89.40	-546.7	31.01	0.881
3.6	16.49	89.48	-576.6	34.03	0.887

Comments on Tables VI,2 and VI,3: These tables are based on identical treatment of tilt data for two different periods, the last observational period before the September 1984 eruption, and the observational period which includes the same eruption. It is worth noting that the standard deviation (5th column) is about three times larger in Table VI,3 than in Table VI,2. Also that the coefficient of correlation is higher in Table VI,2 than in Table VI,3, although the ratio of standard deviation to maximum displacement is higher in Table VI,2 than in Table VI,3. Usually, a low ratio (St.dev./DH0) corresponds to high correlation.

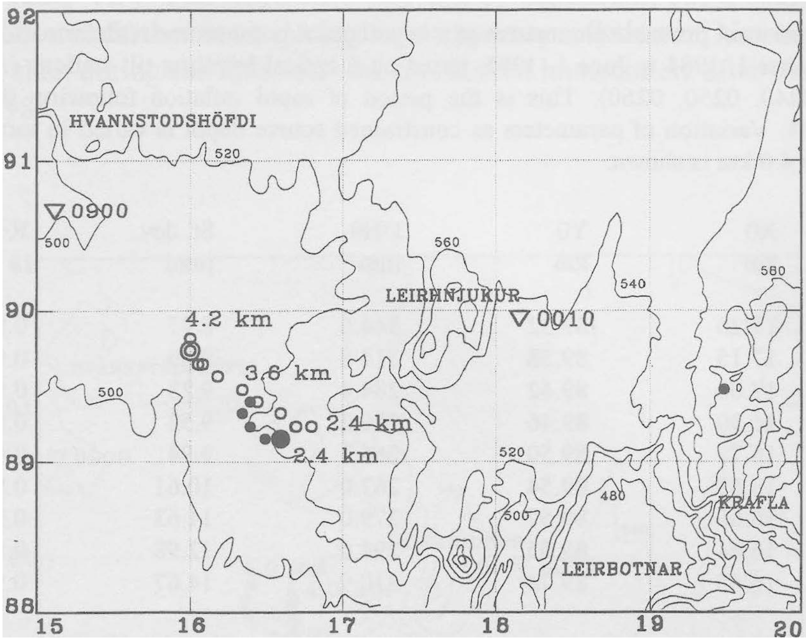

Fig. VI,2. Data of Tables VI,2 and VI,3 plotted on a map. Shown is how the geographical location of the computed point source varies as constrained source depth is varied. The constrained depth is varied in steps of 0.2 km from 2.4 to 4.2 km. Open circles show data of Table VI,2, based on observed tilt at 7 stations during the period June 23, 1983 to June 9, 1984, the last period of inflation leading to the September 1984 eruption. Solid circles show data of Table VI,3, based on observed tilt at the same 7 stations during the period June 9, 1984 to October 3, 1984, the period of deflation during the eruption which lasted from September 4 to September 18, 1984, and rapid inflation from September 18 to October 3, 1984. The period from June 9 1984 to September 4, 1984 was a period of near zero inflation according to recording tiltmeter at the Krafla power station. Large symbols show solutions of smallest standard deviation of observed from model tilt, but this was observed for constrained depth of 4.0 km for data of June 1983 to June 1984, and at constrained depth of 2.4 km for the period of June 1984 to October 1984. There is a reason to assume that the solution for the period of the September 1984 eruption is anomalous because the north-south eruption fissure was opened across Leirhnjúkur, and significant non-elastic deformation must have resulted from this eruption in the vicinity of Leirhnjúkur. Still, the suggested center of deformation is almost the same for these two periods, one before the eruption, another during the eruption of September 1984.

Table VI,4

Computed most probable parameters of a hypothetical point source of deformation at Krafla for the period October 3, 1984 to June 1, 1985, based on 8 optical levelling tilt stations (A, 0000, 0080, 0090, 0210, 0240, 0250, 0260). This is the period of rapid inflation following the eruption of September 1984. Variation of parameters as constrained source depth is varied in increments of 0.2 km from 2.4 to 4.0 km is shown.

H km	X0 km	Y0 km	DH0 mm	St. dev. µrad	R^2
2.40	17.20	89.32	344.6	8.97	0.978
2.60	17.15	89.38	314.5	9.06	0.981
2.80	17.00	89.42	284.4	9.23	0.974
3.00	16.90	89.46	270.2	9.52	0.973
3.20	16.79	89.50	266.7	9.94	0.963
3.40	16.69	89.54	267.0	10.61	0.957
3.60	16.66	89.57	279.0	11.63	0.943
3.80	16.64	89.65	294.0	12.98	0.933
4.00	16.65	89.74	310.9	14.67	0.919

Table VI,5

Computed most probable parameters of a hypothetical point source of deformation at Krafla for the period October 22, 1986 to April 4, 1987. based on 8 optical levelling tilt stations (A, 0000, 0080, 0090, 0210, 0240, 0250, 0260). Shown are source parameters as constrained source depth is varied from 2.4 km to 4.0 km in increments of 0.2 km..

H km	X0 km	Y0 km	DH0 mm	St. dev. µrad	R^2
2.40	16.90	89.40	231.6	7.24	0.967
2.60	16.79	89.42	214.0	7.13	0.962
2.80	16.64	89.45	168.3	7.08	0.960
3.00	16.54	89.48	169.8	7.14	0.952
3.20	16.39	89.57	197.5	7.40	0.944
3.40	16.35	89.63	208.1	8.02	0.933
3.60	16.33	89.67	223.2	9.04	0.917
3.80	16.35	89.74	239.8	10.48	0.897
4.00	16.39	89.82	257.5	12.24	0.873

Comments on Tables VI,4 and VI,5: The period covered by the computations presented in Table VI,4 is that of relatively rapid inflation of Krafla volcano immediately following the eruption of September 1984. At some time before June 1, 1985, the inflation ceased temporarily, and was resumed in the beginning of November 1986. Table VI,5 covers the period of this resumed inflation, which lasted until the spring of 1987. Same tilt stations are used in both cases, the same stations which were used to obtain the results presented in Tables VI,2 and VI,3 with addition of one new station, 0260 (Hreindýrahóll) which was first observed on October 3, 1984. As both tables are based on observations at the same tilt stations, and the magnitude of deformation measured in maximum ground uplift is not very different, and the standard deviation is similar in both cases, the computed source parameters are expected to be comparable. The source locations of Table VI,5 are for all constrained source depths

0.3 to 0.4 km farther west and 0.0 to 0.1 km farther north than corresponding source locations of Table VI,4. This difference may not be significant, but it suggests that the center of uplift was farther west during the temporary inflation of November 1986 to March 1987, than during the inflation which followed immediately after the eruption of September 1984.

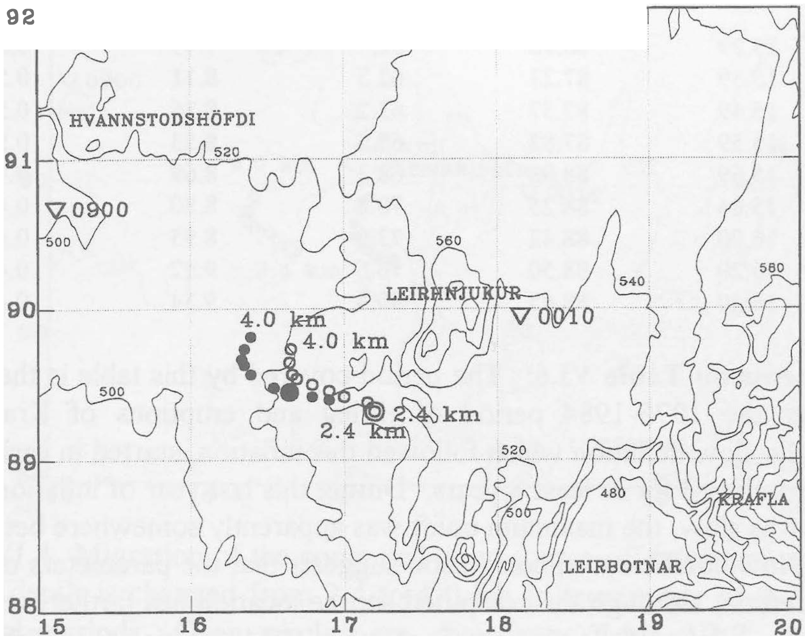

Fig. VI,3. Illustration of the source locations of Tables VI,4 and VI,5, showing how the computed source location migrates as the constrained source depth varies from 2.4 km to 4.0 km, in increments of 0.2 km. The single point source location is computed from tilt observations at 8 tilt stations. Open circles present computed source location during the period October 3, 1984 to June 1, 1985, a period of rather rapid inflation following the deflation associated with the September 1984 eruption. The inflation ceased temporarily in the spring of 1985, so the data here presented is for the last (and major) part of the continuous inflation following the deflation during the eruption. Closed circles present data for the period October 22, 1986 to April 4, 1987, a period of resumed inflation after about 18 month period of practically no inflation nor deflation of Krafla volcano. The large symbols present the solution of smallest standard deviation of observed from model tilt. This is found at source depth of 2.4 km for the period October 1984 to June 1985, and at source depth of 2.8 km for the period October 1986 to April 1987. The migrating path of both periods appear very similar, but the source is computed as about 0.3 km farther west in the later period, than in the first period. This difference may not be significant. The migrating pattern of the computed point source is believed to be controlled entirely by the locations of the tilt stations used in the computation.

Table VI,6

Computed most probable parameters of a hypothetical point source of deformation at Krafla and their variation as constrained source dept is varied. Used are tilt observations for the period June 24, 1988 to June 23, 1989. at 8 optical levelling tilt stations (A, 0000, 0080, 0090, 0210, 0240, 0250, 0260).

H km	X0 km	Y0 km	DH0 mm	St. dev. µrad	R^2
2.40	15.29	86.98	61.7	7.43	0.637
2.60	15.39	87.23	62.3	8.11	0.577
2.80	15.49	87.57	63.2	8.36	0.526
3.00	15.59	87.82	65.5	8.53	0.500
3.20	15.69	88.08	68.3	8.69	0.478
3.40	15.84	88.25	70.8	8.80	0.473
3.60	16.00	88.42	73.9	8.95	0.468
3.80	16.20	88.50	76.6	9.12	0.479
4.00	16.40	88.65	80.4	9.34	0.479

Comments on Table VI,6: The period covered by this table is the last year of inflation after the 1975-1984 period of rifting and eruptions of Krafla volcano. Apparently, the slow deflation which followed this inflation, started in early summer of 1989 and it continued for at least 8 years. During this last year of inflation, the rate of deformation was slow, the maximum uplift was apparently somewhere between 60 and 80 mm. The low coefficient of correlation suggests that the parameters of Table VI,6 are quite uncertain, although the computed source location lies farther west and south than that of the inflation following the September 1984 eruption (see Tables VI,4 and VI,5).

Table VI,7

Computed most probable parameters of a hypothetical point source of deformation at Krafla for the period June 23, 1989 to June 25, 1990. based on 8 optical levelling tilt stations (A, 0000, 0080, 0090, 0210, 0240, 0250, 0260). Variation with varied constrained source depth.

H km	X0 km	Y0 km	DH0 mm	St. dev. µrad	R^2
2.40	16.59	89.57	-53.1	2.00	0.907
2.60	16.49	89.63	-50.4	2.04	0.906
2.80	16.44	89.67	-51.1	2.11	0.899
3.00	16.34	89.71	-51.9	2.26	0.891
3.20	16.30	89.74	-54.6	2.49	0.876
3.40	16.28	89.78	-58.5	2.83	0.858
3.60	16.30	89.82	-63.1	3.25	0.835
3.80	16.34	89.91	-68.0	3.76	0.807
4.00	16.44	89.99	-72.8	4.32	0.774

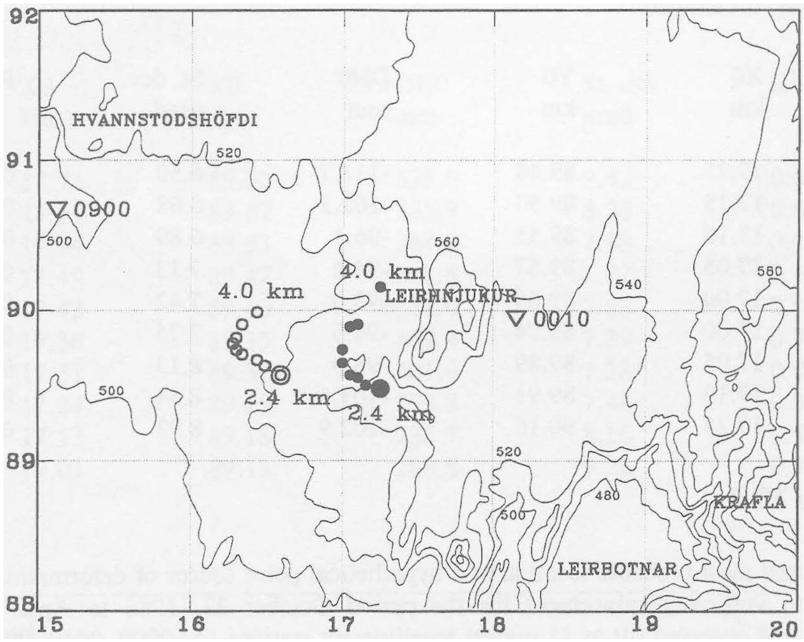

Fig. VI,4. Migration of the computed point source of deformation at Krafla as constrained depth is changed from 2.4 to 4.0 km in increments of 0.2 km for two observational periods. Open circles are data from Table VI,7, based on tilt observations at 8 stations for the period June 23, 1989 to June 25, 1990, the beginning of slow deflation of Krafla volcano. Solid circles show data of Table VI,8, based on observations at the same 8 stations for the period June 25, 1990 to June 19, 1992, a period of continuing slow deflation of Krafla volcano. The migrating path of the computed point source as constrained depth is varied is similar for these two periods, and also similar to that of previous periods presented in Fig. VI,3, as is expected because same stations are used in all cases. However, computed source for the period June 1989 to June 1990 lies approximately 0.7 km farther west than that of the period June 1990 to June 1992. It is not known if this shift of computed point source from one period to another is significant, but there is an indication that it is, as several solutions for later periods (see Table VI,17) can be interpreted as eastward migration of the source.

Table VI,8

Computed most probable parameters of a hypothetical point source of deformation at Krafla for the period June 25, 1990 to June 19, 1992. based on 8 optical levelling tilt stations (A, 0000, 0080, 0090, 0210, 0240, 0250, 0260). shown are variation of computed source location as constrained source depth (H) is changed.

H km	X0 km	Y0 km	DH0 mm	St. dev. µrad	R^2
2.40	17.25	89.48	-113.7	6.50	0.697
2.60	17.15	89.50	-102.3	6.68	0.676
2.80	17.10	89.55	-96.4	6.89	0.661
3.00	17.05	89.57	-94.2	7.13	0.646
3.20	17.00	89.65	-93.0	7.42	0.628
3.40	17.00	89.74	-94.6	7.75	0.613
3.60	17.05	89.89	-98.0	8.13	0.599
3.80	17.10	89.91	-101.5	8.54	0.580
4.00	17.25	90.16	-102.9	8.93	0.537

Table VI,9

Computed most probable location of a hypothetical point source of deformation at Krafla, and also maximum vertical displacement for the period October 22, 1986 to April 29, 1987. The computation used observed tilt at 11 optical levelling tilt stations (A, 0000, 0010, 0020, 0040, 0080, 0090, 0210, 0240, 0250, 0260)

H km	X0 km	Y0 km	DH0 mm	St. dev. µrad	R^2
2.5	16.81	89.32	205.2	7.39	0.974
2.6	16.87	89.32	215.5	7.04	0.972
2.7	16.87	89.32	222.0	6.97	0.967
2.75	16.87	89.32	225.2	7.04	0.963
3.0	16.81	89.32	236.4	8.16	0.933

Comments on Table VI,9: This table shows how the search for most probable source depth is made. First constrained depth was 2.5 km, then 3.0 km, and as 3.0 km depth gave worse fit than 2.5 km, the most probable depth is less than 3.0 km. Next the depth is selected 2.75 km, and that gave better fit (smaller standard deviation) than either of the previous tests, showing that the most probable depth is between 2.5 and 3.0 km, and probably between 2.5 and 2.75 km. The depth was next selected as 2.6 km, which gave equal fit as 2.75 km, and a slightly better fit was found for constrained depth of 2.7 km, which concluded the search for the most probable source depth based on the 11 tilt stations for the period October 22, 1986 to April 29, 1987. The corresponding maximum vertical ground displacement was 222 mm, and geographic coordinates 16.87 km east, 89.32 km north.

Table VI,10

Search for parameters of a hypothetical point source of deformation at Krafla, using measurements of optical levelling tilt stations on September 29 1984 and June 1, 1985. Used are all 18 tilt stations within about 15 km of Krafla. Asterisk marks lowest standard deviation and best correlation.

H km	X0 km	Y0 km	DH0 mm	St. dev. μrad	R^2
2.00	17.71	89.72	528.0	9.42	0.946
2.40	17.59	89.57	385.7	8.26	0.960
2.50	17.54	89.53	364.9	7.98	0.962
2.60	17.49	89.47	341.5	7.72	0.963*
2.70	17.42	89.40	321.0	7.52	0.962
2.80	17.36	89.35	309.4	7.39	0.960
2.90	17.31	89.30	301.9	7.38*	0.956
3.00	17.24	89.25	293.8	7.48	0.951
3.25	17.13	89.18	288.7	8.16	0.931
3.50	17.01	89.13	288.8	9.22	0.906

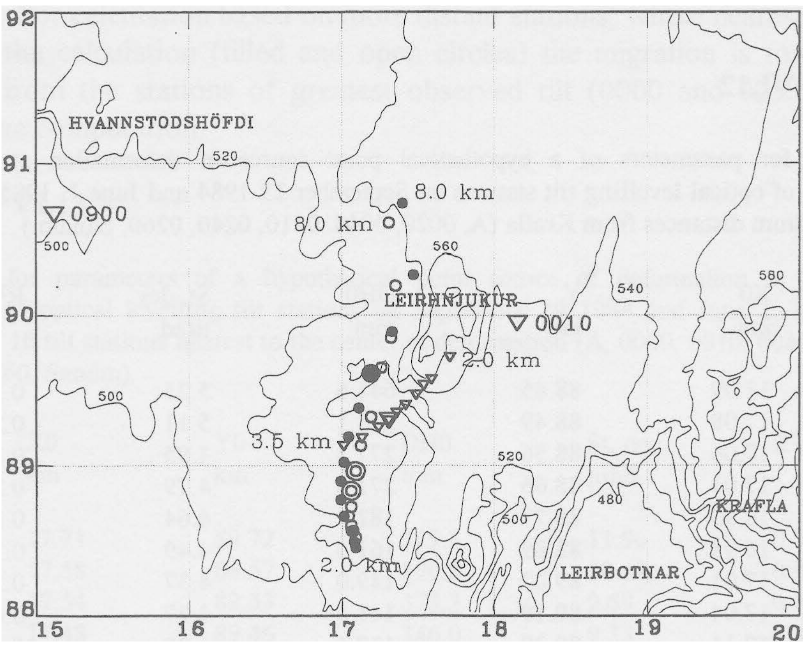

Fig. VI,5 Migration of computed point source of deformation at Krafla volcano as constrained source depth is changed in increments of 0.5 km (or less) from 2.0 km to 8.0 or 3.5 km. Data of Tables VI,10 (open triangles), VI,11 (open circles), and VI,12 (solid circles) for the period September 29, 1984 to June 1, 1985 are plotted. Large symbols show the solutions of smallest standard deviation of observed from model tilt. This is at depth of 4.5 or 5.0 km for data of 13 most distant stations, at depth of 6.5 km for data of 7 medium distance stations, and at depth of 2.9 km for all stations, where nearest stations weigh most heavily.

Table VI,11

Search for parameters of a hypothetical point source of deformation at Krafla, using measurements of optical levelling tilt stations on September 29 1984 and June 1, 1985 using the 13 most distant tilt stations (A, 0020, 0040, 0050, 0060, 0070, 0200, 0210, 0220, 0230, 0240, 0260, Sandm).

H km	X0 km	Y0 km	DH0 mm	St. dev. µrad	R^2
2.00	17.09	88.52	701.1	4.72	0.575
2.50	17.07	88.56	425.8	4.62	0.579
3.00	17.06	88.60	299.1	4.52	0.584
3.50	17.04	88.66	233.3	4.42	0.588
4.00	17.06	88.72	195.1	4.35	0.594
4.50	17.06	88.83	172.6	4.30*	0.596*
5.00	17.09	88.96	158.8	4.30*	0.594
5.50	17.12	89.13	150.4	4.34	0.584
6.00	17.19	89.32	145.6	4.43	0.568
6.50	17.26	89.65	144.0	4.55	0.542
7.00	17.32	89.85	145.4	4.71	0.507
7.50	17.35	90.20	149.7	4.92	0.466
8.00	17.31	90.61	156.7	5.17	0.423

Table VI,12

Search for parameters of a hypothetical point source of deformation at Krafla, using measurements of optical levelling tilt stations on September 29 1984 and June 1, 1985. Using 7 tilt stations at medium distances from Krafla (A, 0020, 0040, 0210, 0240, 0260, Sandm.)

H km	X0 km	Y km	DH0 mm	St. dev. µrad	R^2
2.00	17.09	88.45	644.6	5.25	0.238
2.50	17.08	88.49	393.1	5.11	0.252
3.00	17.06	88.56	277.4	4.95	0.272
3.50	17.01	88.66	271.5	4.79	0.295
4.00	16.99	88.77	182.5	4.64	0.326
4.50	16.99	88.89	161.5	4.49	0.360
5.00	17.01	89.02	149.0	4.37	0.393
5.50	17.04	89.19	141.5	4.27	0.426
6.00	17.11	89.38	137.6	4.20	0.457
6.50	17.19	89.61	137.5	4.17*	0.478
7.00	17.33	89.89	140.6	4.21	0.487*
7.50	17.47	90.27	148.7	4.37	0.478
8.00	17.40	90.74	161.8	4.74	0.453

Comments on Tables VI,11, VI,12, VI,13, and Fig. VI,5: Shown are the most probable point sources of deformation for the period September 29, 1984 to June 1, 1985, the period of inflation first after the eruption of September 1984. Different selection of tilt stations is used for the solutions presented in each table.

Table VI,11 and open circles on Fig. VI,5 show solutions from observations at the 13 optical levelling tilt stations at distances 4 to 13 km from the center of deformation which were observed at the above times. Table VI,12 and solid circles on

Fig. VI,5 show solutions from observations at 7 stations at distances between about 4 km and 9 km from the center of inflation. Table VI,13 and open triangles in Fig. VI,5 show solutions based on observations at the 10 nearest tilt stations, at distances of about 0.8 to 7.5 km from the center of inflation.

Solutions based on observations at the more distant stations (Tables VI,11 and VI,12) are presented for constrained depths from 2.0 km to 8.0 km in increments of 0.5 km while solutions based on the nearest stations are for constrained depths of 2.0 to 3.5 km in variable increments. It is of interest to note that data of the 10 nearest stations give smallest standard deviation of observed tilt from model tilt if constrained depth is 2.8 km while the more distant stations give smallest standard deviation if constrained depth is 4.5 to 5.0 km (Table VI,11) or 6.5 km (Table VI,12). Thus the most probable source depth appear shallower if only near stations are used for analysis of tilt data, than if observations at more distant stations are used. This suggest a systematic deviation between observed ground tilt and the Mogi model, in such a way, that tilt at distant stations is greater than that predicted from the Mogi model and tilt observations at near stations. Also, tilt at near stations is generally greater than that predicted from the Mogi model and observed tilt at the distant stations.

One aspect of Fig VI,5 is that computed source migrates as constrained source depth is increased. For calculations based on the nearest tilt stations (triangles) this migration is towards south-west, away from the nearest tilt station (0010) used in the computation. For calculation based on more distant stations, where nearest stations are not used in the calculation (filled and open circles) the migration is towards north, again away from the stations of greatest observed tilt (0000 and 0250) which are included in the computation.

Table VI,13

Search for parameters of a hypothetical point source of deformation at Krafla, using measurements of optical levelling tilt stations on September 29 1984 and June 1, 1985 based on observed tilt at 10 tilt stations nearest to the center of deformation (A, 0000, 0010, 0040, 0080, 0090, 0240, 0250, 0260, Sandm).

H km	X0 km	Y0 km	DH0 mm	St. dev. μrad	R^2
2.00	17.71	89.72	529.3	11.96	0.938
2.40	17.58	89.57	390.8	10.11	0.960
2.50	17.54	89.53	373.3	9.69	0.963*
2.60	17.48	89.46	346.0	9.33	0.963*
2.70	17.41	89.40	329.3	9.08	0.961
2.80	17.35	89.34	317.4	9.00*	0.958
2.90	17.28	89.30	311.5	9.14	0.954
3.00	17.20	89.25	304.5	9.54	0.948
3.25	17.04	89.19	301.6	11.35	0.924
3.50	16.87	89.21	303.5	13.70	0.904

Table VI,14

Search for center of inflation between observations of June 1, 1985 and June 22, 1989 using measurements at optical levelling tilt stations in the vicinity of Krafla. Stations south of highway 1 (0050, 0060, 0070, 0200, 0220, 0230) were omitted, as the tilt at these stations appeared not to be affected by inflation of Krafla volcano. Station Sandmúli was not included in the calculation. A total of 11 stations were used, and the effect of sequential deletion of nearest station is studied.

I. Constrained source depth 2.5 km

X0 km	Y0 km	DH0 mm	St. dev. µrad	R^2	N	station deleted
16.93	89.61	374.2	22.03	0.921	11	
16.99	89.18	308.8	21.27	0.953	10	0010
17.24	89.50	347.0	22.16	0.896	9	0090
14.35	89.85	930.8	14.72	0.945	8	0080
14.11	89.64	867.5	8.76	0.940	7	0000
16.91	88.36	390.7	8.46	0.638	6	0250

II. Constrained source depth 3.0 km

X0 km	Y0 km	DH0 mm	St. dev. µrad	R^2	N	station deleted
16.55	89.50	383.4	24.69	0.808	11	
16.55	89.29	253.7	20.07	0.926	10	0010
15.21	88.97	252.6	18.69	0.830	9	0090
14.49	89.64	619.6	15.17	0.929	8	0080
14.24	89.21	524.9	9.18	0.918	7	0000
16.91	88.36	280.9	8.19	0.632	6	0250

III. Constrained source depth 4.0 km

X0 km	Y0 km	DH0 mm	St. dev. µrad	R^2	N	station deleted
15.97	89.50	331.4	17.58	0.904	10	0010
15.24	89.21	370.9	16.60	0.915	9	0090
14.87	89.42	444.1	17.54	0.878	8	0080
14.49	89.00	423.4	12.61	0.866	7	0000
16.76	88.36	196.7	7.63	0.567	6	0250

Comments on Table VI,14: This table is intended to show if different groups of tilt stations give similar or dissimilar solution for the most probable parameters of a hypothetical point source of deformation at Krafla. The period of observations is from June 1985 to June 1989, the last period of inflation of the volcano Krafla, before deflation commenced in 1989. The tilt stations used were 11 optical levelling tilt stations, nearest to the center of deformation at Krafla (except the station Sandmúli, which was not included in this study, because it was not observed in June 1989). Source depth was constrained at either 2.5 km, 3.0 km, or 4.0 km.

A solution using data of all 11 station gave the most probable parameters as shown in first row of Table VI,14, part I and II, for constrained depth of 2.5 and 3.0 km. The second row gives similar parameters when data of 10 stations are used, leaving out data of station 0010, the station nearest to the center of deformation, Similarly the third row gives solution for data of 9 stations, leaving two nearest stations out, and 4th, 5th, and 6th lines give solution using data of 8, 7, and 6 stations respectively, deleting the nearest station used to obtain the solution of the preceding row. Section III of the table shows the same, except that no solution is given by using all 11 stations, and the source depth is constrained at 4.0 km.

There are several items in Table VI,14 which are worth noticing:

A. The standard deviation of observed tilt from model tilt is significantly greater if 9, 10, or 11 stations are used, than if fewer stations are used. The reason for this is that the observed tilt at the nearest stations is greater than at the more distant stations, and deviation of observed tilt from model tilt is more or less proportional to the observed tilt.

B. The coefficient of correlation is similar for any number of stations greater than 6, used to obtain the solution. This suggest also that the deviation of station tilt from the corresponding model tilt is approximately proportional to observed tilt. The solution of the last line of each section of Table VI,14 has significantly lower correlation between radial component of observed tilt and model tilt. This solution is based on observations of the six stations which are farthest away from the center of deformation, of the 11 stations of this study. The observed tilt at these six stations is smaller than at the nearer stations, and observational errors are larger relative to the ground tilt. The low correlation in the last line is believed to be the result of large error to signal ratio of the observational data.

C. The calculated most probable maximum vertical ground displacement (3rd column) is similar for solutions using 11, 10, or 9 stations (250 to 370 mm), but the solution using 8 or 7 station gives much greater maximum vertical ground displacement, although quite different for different constrained source depth. This is caused by tilt anomaly at the station 0250 (Syðri Bjarghóll). This anomaly causes the computed source location to be about 3 km farther west than given by solutions using 9 to 11 stations. The anomaly at station 0250 is primarily in the azimuth of tilt, which pulls the source solution westward when tilt at this station is large relative to tilt at other stations used for the solution. In fact, the stations with greatest ground tilt, of the stations used for solution of source parameters, will weigh heavily in the solutions.

Table VI,15

Computed most probable parameters of a hypothetical point source of deformation at Krafla, and how they vary as constrained depths is varied. Used are observations at 10 stations (A, 0000, 0020, 0040, 0080, 0090, 0210, 0240, 0250, 0260) on June 1, 1985 and June 22, 1989.

X0 km	Y0 km	H km	DH0 mm	St. dev. µrad	R^2
16.99	89.18	2.50	308.8	21.27	0.953
16.55	89.29	3.00	253.7	20.07	0.926
16.10	89.39	3.50	270.4	18.32	0.908
15.37	89.50	4.00	331.4	17.58*	0.904
16.16	89.61	4.50	393.4	19.75	0.877
16.61	89.92	5.00	426.2	23.76	0.809

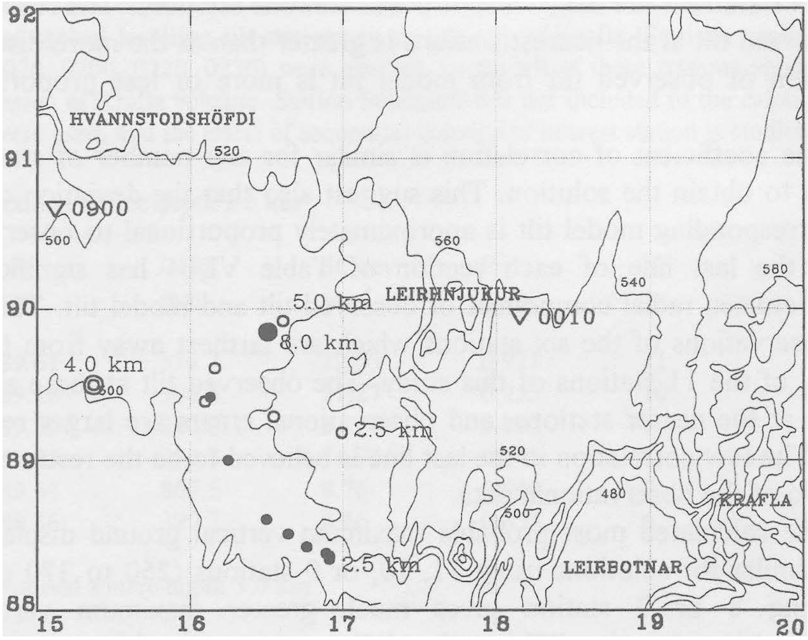

Fig. VI,6. Data of Tables VI,15 and VI,16 are plotted to illustrate the migration of the computed center of most probable point source as constrained source depth is varied. The observational data is ground tilt from June 1, 1985 to June 22, 1989, and the source location is computed from observations at 10 stations at about 2.7 to 9.3 km distance from the computed source (open circles) and at 6 stations at about 4.3 to 9.3 km from the computed source (closed circles). Depth increments are 0.5 km, from 2.5 to 5.0 km for the ten-station solutions (open circles), and from 2.5 km to 8 km for the six-station solutions (solid circles). Large symbols are the solution of smallest standard deviation of observed tilt from model tilt, found at 4.0 km depth in the ten-station solution and at 8.0 km depth for the six-station solution.

Table VI,16

Same as Table VI,15 except observations at 6 stations (A, 0020, 0040, 0210, 0240, 0260) are used, leaving out stations at less than about 5 km distance from the computed center of deformation.

X0 km	Y0 km	H km	DH0 mm	St. dev. μrad	R^2
16.91	88.36	2.5	390.7	8.85	0.638
16.91	88.36	3.00	280.9	8.19	0.632
16.89	88.36	3.5	225.3	7.90	0.620
16.76	88.36	4.00	196.7	7.63	0.567
16.64	88.58	4.50	175.3	7.33	0.700
16.64	88.58	5.00	170.5	7.06	0.693
16.25	89.00	6.00	161.9	6.62	0.842
16.13	89.42	7.00	161.8	6.43	0.932
16.51	89.85	8.00	165.4	6.37	0.928

Comments on Tables VI,15 and VI,16 and Fig VI,6: The observational data for these tables and illustration are observed tilt from June 1, 1855 to June 22, 1989, the slow last inflation of Krafla before continuous deflation started in 1989. The solutions of Table VI,15 show peculiar migration of the computed source (open circles on Fig. VI,6), the computed source being far to the west for constrained depth of 4.0 km. The reason for this apparently anomalous observed tilt at one or two stations, which dominate the solution if constrained depth is 4.0 km. These stations of suggested anomalous tilt (0080 and 0250) are not included in the computation of Table VI,16, making its migration more continuos (Solid circles on Fig. VI,6)

It is worth noticing that lowest standard deviation of observed tilt from model tilt is found for constrained depth of 4.0 km for the 10 station solutions, but at 8.0 km for the six station solutions, suggesting that the computed most probable source depth depends on which stations are used for the computation, and if stations are more distant, the computed most probable source is deeper.

There is a reason to point out that after 1984, when rifting of the Krafla fissure zone had ceased, the fissure zone has subsided at a relatively constant rate. This subsidence causes the ground to tilt down towards the center of the fissure zone (Tryggvason 1995). During periods of slow inflation or deflation of Krafla, the tilt caused by subsidence of the fissure zone will affect the observed tilt direction greatly at most tilt stations in the Krafla area. When a point source of deformation at Krafla is searched for, then the tilt caused by subsidence of the linear fissure zone is a disturbing factor. No effort has been made to remove the effect of the fissure zone subsidence from the tilt observations.

Table VI,17

Computed most probable parameters of a point source of deformation at Krafla, for various periods between observations between June 1989 and July 1996, if depth is constrained as 2.5 km. Used are data from 8 optical levelling tilt stations (A, 0000, 0020, 0040, 0080, 0090, 0250, 0260)

First date	Last date	X0 km	Y0 km	DH0 mm	St. dev. μrad	R^2
89 06 22	90 06 26	16.52	89.61	-49.9	3.24	0.847
89 06 22	91 07 09	17.15	89.82	-133.6	6.25	0.863
89 06 22	92 06 17	16.90	89.50	-144.0	5.84	0.908
89 06 22	93 06 29	16.96	89.29	-208.6	9.41	0.907
89 06 22	94 07 06	17.09	89.18	-253.3	7.53	0.916
89 06 22	96 07 26	17.37	89.40	-337.0	11.27	0.928
90 06 26	91 07 09	17.41	90.14	-92.2	6.71	0.638
91 07 09	92 06 17	15.31	89.71	-31.7	4.14	0.605
92 06 17	93 06 29	16.71	88.55	-59.2	6.25	0.704
93 06 29	94 07 06	18.49	88.12	-46.0	4.40	0.623
94 07 06	96 07 26	17.50	89.93	-88.19	7.34	0.897

Table VI,18

Same as Table VI,17 except that data from 11 stations are used (A, 0000, 0010, 0020, 0040, 0080, 0090, 0210, 0240, 0250, 0260)

First date	Last date	X0 km	Y0 km	DH0 mm	St. dev. μrad	R^2
89 06 22	90 06 26	16.36	89.00	-42.2	3.98	0.742
89 06 22	91 07 09	18.14	89.64	-187.8	7.39	0.619
89 06 22	92 06 17	17.76	89.42	-195.4	6.94	0.820
89 06 22	93 06 29	18.14	89.64	-313.4	12.95	0.756
89 06 22	94 07 06	18.13	89.53	-338.9	16.13	0.672
89 06 22	96 07 26	18.12	89.65	-444.2	13.98	0.860
90 06 26	91 07 09	18.27	89.64	-106.2	5.93	0.578
91 07 09	92 06 17	17.76	88.79	-43.8	4.65	0.754
92 06 17	93 06 29	17.22	86.46	-48.1	6.17	0.342
93 06 29	94 07 06	19.03	87.52	-38.6	4.01	0.604
94 07 06	96 07 26	18.18	89.65	-118.2	6.63	0.879

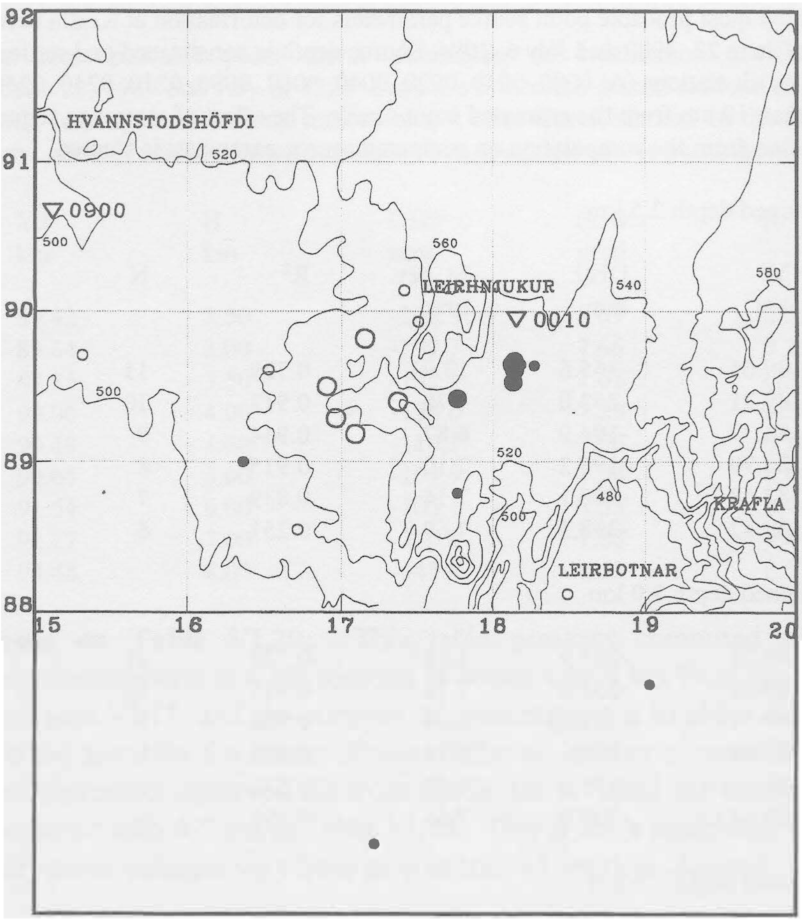

Fig. VI,7. Computed source locations for periods of deflations between June 1989 and July 1994. Data of Table VI,17, computed from tilt observations at 8 optical levelling tilt stations, are plotted as open circles. Data of Table VI,18, computed from tilt observations at 11 stations. are plotted as solid circles. Small symbols are solutions based on one (or two) year's periods (top row and bottom 5 rows), large symbols are solutions based on 2 to 7 year's periods beginning in June 1989.

Comments on Tables VI,17 and VI,18 and Fig VI,7: The scatter of computed most probable source location is great for solutions based on one-year tilt. Two solutions lay outside the map area most commonly used in this report. Therefore the map area was extended without topographic contours 2 km to the south. The difference in computed source locations based on observations at 8 tilt stations (Table VI,17, open circles) and observations at 11 tilt stations (Table VI,18 and solid circles) is rather large. The computed locations based on observed tilt over extended periods (large symbols) are rather closely packed together, especially those based on observations at 11 stations. The 11 station computations are usually about one km farther east than similar solutions using observations at 8 station.

Table VI,19

Computed most probable point source parameters for deformation at Krafla between observations of June 22, 1989 and July 6, 1994. Source depth is constrained and stations used are 11 optical levelling tilt stations (A, 0000, 0010, 0020, 0040, 0080, 0090, 0210, 0240, 0250, 0260) at distance less than 10 km from the estimated point source. The effect of removing sequentially the nearest tilt station from the computation on computed source parameter is studied.

X0 km	Y0 km	DH0 mm	St. dev. µrad	R^2	N	Station removed
Constrained depth 2.5 km						
18.14	89.64	-365.6	13.01	0.729	11	
17.13	89.21	-253.0	7.78	0.913	10	0010
17.25	88.79	-194.9	6.87	0.944	9	0090
17.13	88.79	-198.2	7.10	0.915	8	0080
17.51	88.58	-205.1	7.14	0.839	7	0000
16.62	89.42	-298.3	7.69	0.251	6	0250
Constrained depth 3.0 km						
18.02	89.21	-265.9	12.87	0.720	11	
17.13	89.21	-253.0	7.78	0.913	10	0010
17.13	89.79	-169.01	6.64	0.938	9	0090
17.13	87.94	-118.6	6.74	0.896	8	0080
17.38	88.36	-155.0	7.02	0.830	7	0000
16.62	89.64	-200.0	7.66	0.291	6	0250
Constrained depth 3.5 km						
17.76	89.00	-255.8	13.68	0.761	11	
16.75	89.42	-214.5	8.98	0.879	10	0010
17.00	88.79	-164.5	6.73	0.928	9	0090
17.13	87.94	-129.1	6.59	0.885	8	0080
17.25	88.15	-139.0	7.05	0.808	7	0000
16.62	89.85	-152.1	7.63	0.321	6	0250

Comments on TableVI,19: This table is similar to Table VI,14 and is intended to show how the computed source parameters vary as the observations at the near tilt stations are removed from the data used for the computation. The standard deviation decreases very much as observations at station 0010 (Leirhnjúkur) are deleted, suggesting that the large tilt at this station deviates greatly from that predicted by the Mogi model. It is of interest to note that the standard deviation is smallest for 3.0 km constrained source depth if solution is based on observation at 9, 10, or 11 stations, while it is smallest for 3.5 km constrained depth if observations at 6, 7, or 8 more distant stations are used to obtain solutions. This shows that observations at near stations favour shallow source while observations at more distant stations favour deeper source.

Table VI,20

Computed most probable point source parameters of deformation at Krafla between observations of June 22, 1989 and July 6, 1994. Used are 6 medium distant stations (A, 0020, 0040, 0210, 0240, 0260), leaving out 5 nearest stations and 7 most distant stations in the Krafla-Mývatn area. Studied is the effect of varied constrained depth H on computed source parameters.

X0 km	Y0 km	H km	DH0 mm	St. dev. µrad	R^2
16.62	89.42	2.50	-298.3	7.69	0.251
16.62	89.64	3.00	-199.7	7.66	0.290
16.62	89.85	3.50	-152.1	7.63	0.321
16.62	90.06	4.00	-128.0	7.59	0.346
16.49	90.48	4.50	-116,1	7.56	0.385
16.62	90.65	5.00	-107.9	7.54	0.405
17.00	91.54	6.00	-105.1	7.55	0.449
17.00	92.27	7.00	-130.0	7.88	0.442
16.49	93.48	8.00	-145.3	8.53	0.379

Comments on Table VI,20: This table presents computed source point solutions, using observations at 6 tilt stations at about 4 to 9 km from the source. It is comparable to Table VI,12, and the purpose of presenting it is to show if the apparent source depth is the same for the center of slow deflation, as that of rapid inflation. The lowest standard deviation observed tilt from model tilt is found for constrained depth of 5.0 km, compared with 6.5 km in Table VI,12. This is not a significant difference as the standard deviation changes very little as constrained depth is changed.

ANALYSIS OF DISTANCE MEASUREMENTS 1977-1995

The electronic distance measurements (EDM) were initiated in the Krafla area in February 1977 and were repeated frequently during the following years. Repetition of these measurements on a limited number of lines in July, August, and October 1977 (Tryggvason 1978) did show very significant deformation of the ground. Efforts were made to repeat the EDM observations soon after major deflation events, to determine the extend of rifting. The station network was originally constructed to determine the amount of widening of the Krafla fissure zone in the region where ground rifting had been observed during deflation events in October 1976 and January 1977, that is from Krafla in the south to Hrútafjöll in the north, a distance of about 12 km. Irregular lines of stations were laid across the fissure zone at one to two km intervals with some stations of each line outside the zone of active rifting.

The first EDM observations were made with instruments of about 2 km maximum range, which limited the station to station distance of 1 to 2 km. When EDM instruments of greater range ("Geodimeter 6BL" and later "Geodimeter A14") were acquired, the plan of observations were changed in March 1978 from the station to station measurements along crooked lines to measurements from a few selected Geodimeter stations to many reflector stations.

Addition of new stations in 1978 extended the area covered by the dense EDM station network towards west and north, to improve the observations of rifting of the Krafla fissure zone.

It became soon evident that the EDM results gave important data for studying volcanic processes at depth, and in 1981 the EDM network was extended southward to improve the possibility of using EDM observations to study processes at depth below the Krafla volcano. Prior to 1981, the dense EDM station network covered only the north flanks of the Krafla volcano, and the Krafla fissure zone to the north of the volcano.

During the years of frequent deflation and rifting events, 1976 to 1981, many periods between EDM observations included both inflation and deflation of Krafla volcano. If the period between two EDM observations was characterised by continuous inflation as shown by daily tilt observations at the Krafla power station, then the observations were used to search for the most probable point source (Table VII,1, Table VII,3). In Table VII,1 the first line is based on average length changes of 17 lines, relative to the tilt observed at the Krafla power station. The relative length change is found by comparing all observed length changes of these lines with readings of the water tube tiltmeter at the Krafla power station and to determine the average ratio between observed tilt and observed length changes.

Comments on Table VII,1: This table is based on a computer search which used the highest correlation between observed distance changes and predicted distance changes, using the single point source Mogi model. The table is presented here to demonstrate the different result obtained by searching for best correlation as done here, and searching for smallest standard deviation for observations from model, as is done in Table VII,3. The observational data for these two tables is the same, but the selection of lines used in the computer search, is not the same and table VII,3 covers observations after 1984, which are not included in Table VII,1.

It is worth pointing out that the columns heading "DH0" and "Kr" both show estimate of maximum vertical ground displacement, and should have identical numerical values, if the observations are perfectly correct, and if the Mogi model is a correct representation of the elastic behaviour of the earth's crust in the Krafla area. It is obvious that the values in these two columns are sometimes greatly different, especially if the estimated maximum vertical ground displacement is small, and if the correlation between observed length changes and model length changes is low. In these cases, observational errors of distances are suggested as primary cause of disagreement between vertical displacements as estimated from tilt and distance measurements. In other cases, numerical differences of these two columns suggest that the ground deformation deviates greatly from that predicted by the single point source Mogi model. It is demonstrated in Table VII,8 that the selection of lines used in the computer search for a point source will greatly affect the computed source parameters. This suggests that the selection of lines used to obtain the source parameters of Table VII,1 is causing some of this difference, but this selection is largely controlled by the lines which were measured during each observational period.

Table VII,1

Computed most probable source of deformation and maximum vertical ground displacement for a point source at Krafla, for various periods between distance measurements from 1977 to 1984 based on EDM-measurements. Source depth is constrained at 2.5 km. Criteria for the most probable point source is maximum correlation between observed distance changes and the Mogi model distance changes.

First date	Last date	X0 km	Y0 km	DH0 mm	Kr mm	R^2	N
1977	1980	17.81	89.67	3.58*	3.50*	0.8788	17
78 03 12	78 06 25	17.81	89.56	569.33	591.7	0.8292	21
78 06 25	78 07 21	17.68	89.77	-557.2	-513.2	0.8933	16
78 07 21	78 08 10	17.56	90.19	262.6	179.9	0.8635	7
78 08 10	78 08 29	17.81	89.35	185.3	137.1	0.6966	10
78 07 21	78 08 29	17.88	89.67	440.8	317.0	0.8970	14
79 08 04	79 11 21	17.94	89.35	229.3	247.9	0.9235	19
79 08 04	79 08 24	17.62	89.88	80.3	35.6	0.4248	21
79 08 24	79 10 06	18.00	89.45	139.7	149.3	0.6305	15
79 10 06	79 11 21	18.45	88.71	81.0	65.5	0.5842	13
80 03 17	80 04 15	17.81	89.67	338.4	361.1	0.7609	18
81 02 08	81 04 05	17.49	89.45	480.2	294.8	0.9794	12
81 04 05	81 07 05	17.68	89.56	186.5	128.6	0.6866	37
82 02 22	82 04 16	17.05	90.62	69.9	12.7	0.4105	8
82 04 16	83 03 20	18.07	89.56	195.9	192.3	0.8035	28
83 03 20	84 03 15	18.32	89.35	186.7	151.8	0.7348	21
1978-1983	average	17.77	89.61				

*) The first row is based on average length changes relative to observed tilt at the Krafla power station, the DH0 value is based on length changes per 1 μrad tilt as observed by the water tube tiltmeter at Krafla, north (N13°E) component.

Headings of columns are as in Table A1, except "Kr mm" for column 6 which presents an estimate of maximum vertical ground displacement, based on water tube tiltmeter observation of tilt at the Krafla power station and the last column which gives the number of measured lines used in the calculation.

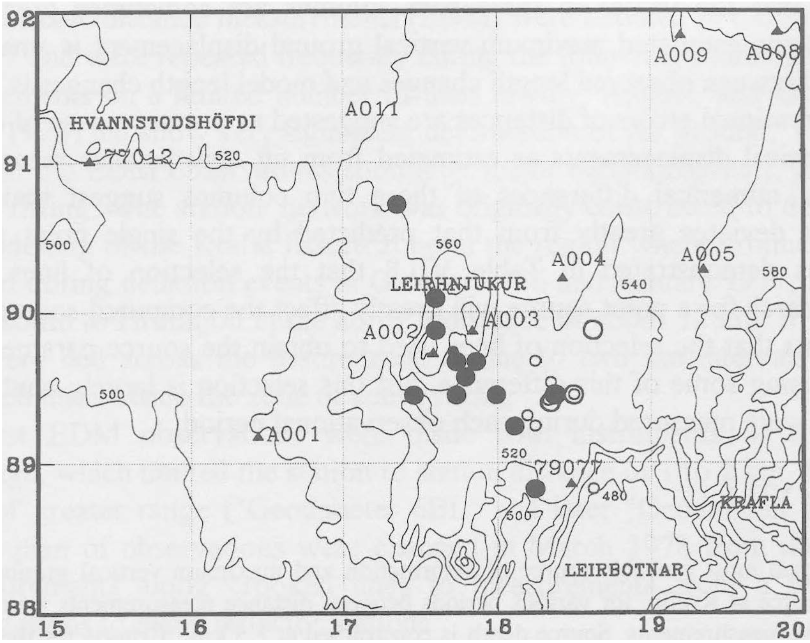

Fig. VII,1 The most probable point source of deformation at Krafla during the 1978-1995 period of volcanic and tectonic activity. Plotted are data of Table VII,3, based on distance measurements made at different times. Solid circles are computed source points based on measurements made before the last eruption of Krafla in September 1984, open circles are based on measurements made after September 1984. Large symbols are computed point sources based on observed distance changes during periods of inflation of the Krafla volcano, small symbols are based on distance changes during periods of deflation.

Table VII,2

This table shows the result of an experiment to determine how computed center of deformation and computed maximum vertical ground displacement varies if different number of lines are used in the model computation. The change of observed distance between March 1983 (average time March 20) and March 1984 (average time March 15) is used. A total of 34 measured lines are included in the experiment, but these are all the measured lines which are believed to be affected by inflations or deflations of Krafla. First calculation is based on all 34 lines. Then four lines with greatest deviation in observed length change from model length change are removed from the data and remaining 30 lines are used to compute new values of source parameters. Similar removal of four or five lines of worst fit is repeated two more times.

Number of Lines	Constrained depth km	X0 km	Y0 km	DH0 mm	Standard deviation mm
34	2.5	18.07	89.35	167.1	23.9
34	3.0	18.13	89.35	161.8	22.5
34	3.2	18.10	89.35	159.3	22.4*
30	2.5	18.32	89.35	181.7	19.9
30	2.8	18.32	89.35	176.1	19.6*
30	3.0	18.32	89.35	172.6	19.8
26	2.5	18.32	89.45	186.3	18.8
26	3.0	18.32	89.45	179.7	17.6*
26	3.5	18.32	89.45	174.0	18.6
21	2.5	18.32	89.35	186.7	18.3
21	3.0	18.32	89.45	181.9	16.0*
21	3.5	18.26	89.45	176.1	16.8

*) Best fit between observation and model for each group of computations.

Comments on Table VII,2: This table shows that removal of lines of worst fit to the Mogi model, causes only a small change of the computed source parameters. The standard deviation of observed from model distance changes decreases from 22 mm to 16 mm by removing 13 worst fitted lines from the computation. This standard deviation is not much greater than observational error of the EDM measurements. Therefore, it appears as if the Mogi model is a good representation of the observed distance changes of the 34 lines used in obtaining the data of Table VII,2.

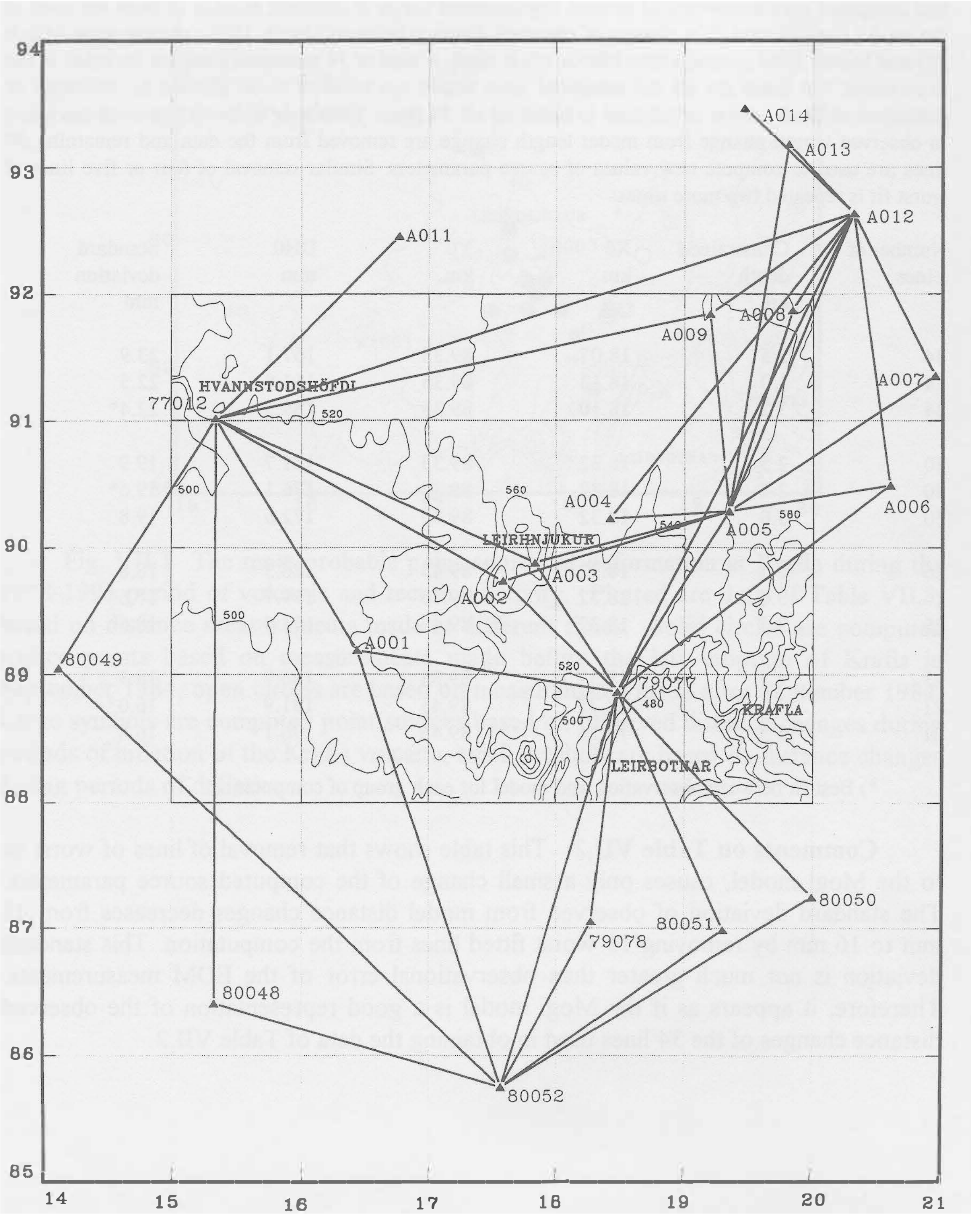

Fig. VII,2. A map showing the 40 lines used to obtain the data in the last four lines of Table VII,3. Other results in Table VII,1 and VII,3 are based on measurements of some of the same lines, and possibly of lines not shown here, depending on which lines were measured at each time

Table VII,3

Computed most probable point source parameters for deformation at Krafla during the 1978-1995 period of volcanic and tectonic activity. The minimum standard deviation of observed from model distance changes is taken as criteria for most probable source parameters. This table is partly based on computations using the same observational data as used in Table VII,1, but the data are treated differently. In Table VII,1, maximum correlation between observed and model length changes is used as a criteria for the best solution, while in the present table, minimum standard deviation is used as criteria for the best solution. Source depth is constrained at 2.5 km.

First date	Last date	X0 km	Y0 km	DH0 mm	st. dev. mm	R^2	N
78 03 12	78 06 25	17.79	89.57	567.1	35.9	0.8300	21
78 06 26	78 07 21	17.71	89.74	-553.7	31.3	0.8921	16
78 07 21	78 08 10	17.60	90.09	263.0	12.3	0.8612	7
78 07 21	78 08 29	17.86	89.67	446.1	26.8	0.8975	14
78 08 10	78 08 29	17.73	89.45	179.5	12.3	0.6621	10
79 08 04	79 08 24	17.35	90.72	108.3	37.9	0.1691	24
79 08 04	79 11 21	17.99	89.45	218.3	26.4	0.6964	23
79 08 24	79 10 06	17.60	89.88	145.0	22.9	0.4257	17
79 10 06	79 11 21	18.24	88.82	124.7	24.0	0.4832	16
80 03 17	80 04 15	17.86	89.67	336.0	32.9	0.7582	18
81 02 08	81 04 05	17.46	89.45	480.3	13.8	0.9829	12
81 04 05	81 07 05	17.73	89.67	167.9	26.2	0.4964	42
82 04	83 03	18.37	89.45	207.9	28.1	0.5022	33
83 03	84 03	18.11	89.24	168.1	24.4	0.4845	34
84 10	89 03	18.49	89.45	633.8	53.1	0.8786	22
84 10	85 03	18.37	89.45	252.0	20.8	0.8862	14
85 03	86 03	18.32	89.41	-51.7	13.7	0.1295	14
86 03	87 03	18.34	89.40	177.0	13.2	0.9191	16
87 02	88 04	18.62	89.88	106.9	11.2	0.8007	29
88 04	89 03	18.37	89.45	147.9	14.8	0.8138	30
89 03	90.03	18.34	89.53	-96.3	8.4	0.8624	31
90 03	92 03	18.37	89.45	-60.0	7.0	0.7534	31
92 03	93 03	18.49	89.45	-46.9	6.9	0.7179	22
93 03	94 03	18.62	88.82	-42.4	9.3	0.3216	40
89 03	94 03	18.24	89.24	-282.4	26.3	0.7553	40
94 03	95 03	18.24	89.67	-41.7	7.8	0.2740	40
89 03	95 03	18.19	89.31	-316.9	26.6	0.7969	40

Comments on Table VII,3: This table contains computation of apparent point source based on electronic distance measurements (EDM) in the Krafla region during the period March 1978 to March 1995. Lines used for the period March 1994 to March 1995 are shown on Fig VII,2, and similar distribution of lines are used for most calculations of periods after 1980. Many of the southern markers (80048, 80049, 80050, 80051, 80052) were constructed in 1980, and additional two markers (79077, 79078) were constructed in 1979. A few markers were destroyed during eruptions. Therefore, different groups of lines were used for source estimates during different periods.

Table VII,3 is considered to contain solutions for all periods when reliable point source parameters can be obtained from EDM measurements in the Krafla area during the 1975-1995 sequence of volcanic and tectonic activity. It is considered that reliable solutions can be obtained only if the period between EDM measurements is characterised by either continuous inflation or continuous deflation, according to recording tiltmeters or other continuous observations. One period of rapid deflation of Krafla is included in Table VII,3, June 26 to July 21, 1978. This period includes large deflation event of July 10 to 14, 1978, and rapid inflation during the week of July 14 to 21 and much slower inflation during the first two weeks. The total inflation during these three weeks (June 26 to July 10 and July 14 to 21) amounted to approximately 106 mm while the deflation of July 10 to 14 amounted to about 620 mm at the point of maximum inflation/deflation according to the water tube tiltmeter at the Krafla power station. Thus the inflation amounted to about 17 per cent of the deflation, meaning that deflation dominated during the period between EDM measurements of June 26 and July 21, 1978.

The computed geographic coordinates of the most probable point source appear to have drifted eastward and southward with time (Fig. VII,1), from an average location of 17.51 km E, 89.65 km N before 1982 to 18.16 km E, 89.49 km N between 1982 and 1989 to the average location of 18.17 km N, 89.35 km E after 1989. The standard error of these average values are about 0.1 km, so the eastward drift appear significant but the southward drift is hardly significant. There appear to be no significant difference between computed source location of inflations and deflations.

The southern stations which were added in 1980 were regularly occupied thereafter. This means that there is considerable difference in the distribution of measured lined before and after 1980. This may possibly cause the apparent eastward shift in average location of the source of deformation.

Table VII,4

Computed "most probable" point source and how it changes as constrained source depth is varied. Used are distance measurements of 17 lines of March 1986 and March 1987.

Constrained depth, km	X0 km	Y0 Km	DH0 mm	St. dev. mm	R^2
2.0	17.85	89.65	224.7	29.1	0.5765
2.2	17.90	89.57	218.6	27.0	0.5863
2.4	17.95	89.57	213.8	25.7	0.5890
2.6	18.00	89.57	209.9	25.2	0.5809
2.8	18.05	89.48	207.4	25.3	0.5630
3.0	18.05	89.48	204.1	25.9	0.5378
3.2	18.05	89.48	201.1	26.7	0.5055
3.4	18.05	89.48	198.5	27.8	0.4677
3.6	18.05	89.48	196.3	28.9	0.4265
3.8	18.05	89.48	194.6	30.0	0.3842
4.0	18.00	89.48	192.6	31.1	0.3431

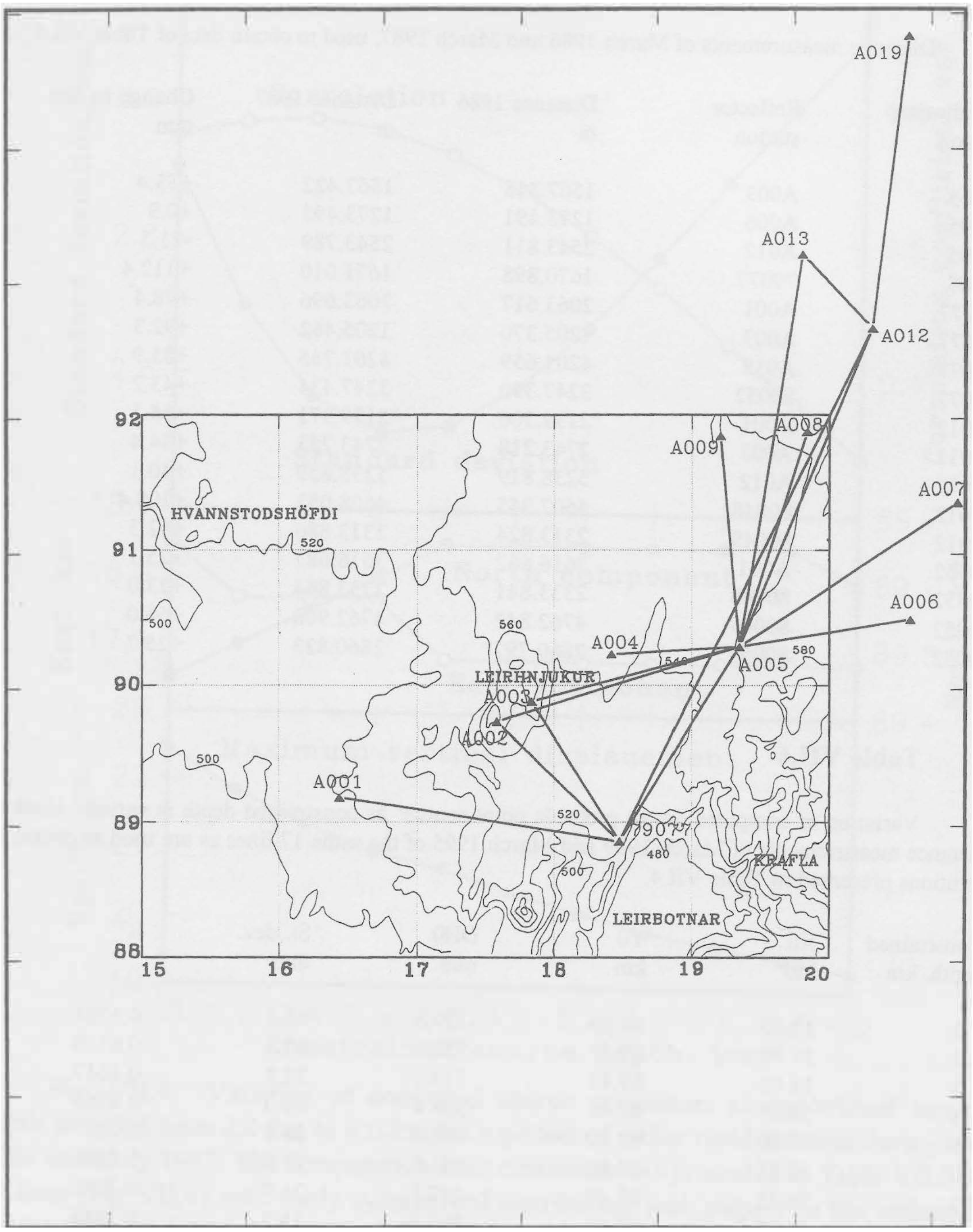

Fig. VII,3. An example of lines used to obtain the solutions presented in Table VII,3 for the period March 1986 to March 1987. In many cases, observations were made on limited number of lines, frequently of lines to the east or north-east of the center of deformation. Because of this, the distribution of lines which are used to obtain the solutions of table VII,3 is quite variable.

Table VII,5

Distance measurements of March 1986 and March 1987, used to obtain data of Table VII,4

Geodimeter station	Reflector station	Distance 1986 m	Distance 1987 m	Change in dist. mm
A005	A003	1567.348	1567.422	+73.4
A005	A006	1273.491	1273.492	+0.9
A005	A012	2543.811	2543.789	-21.5
A005	79077	1670.898	1671.010	+112.4
79077	A001	2063.617	2063.696	+78.4
79077	A003	1205.370	1205.462	+92.3
79077	A012	4201.659	4201.745	+85.9
79077	80052	3247.390	3247.434	+43.2
77012	A001	2139.306	2139.371	+65.1
77012	A003	2743.218	2743.253	+34.4
77012	A012	5238.819	5238.859	+40.1
77012	80048	4607.945	4608.053	+108.4
77012	80049	2313.824	2313.886	+62.5
80052	A001	3616.662	3616.687	+25.1
80052	80048	2333.841	2333.864	+23.0
80052	80049	4762.842	4762.908	+66.0
80052	80050	2860.797	2860.823	+25.7

Table VII,6

Variation of computed "most probable point source" as constrained depth is varied. Used are distance measurements of March 1989 and March 1995 of the same 17 lines as are used to obtain the solutions presented in Table VII,4.

Constrained depth, km	X0 km	Y0 km	DH0 mm	St. dev. mm	R^2
2.0	17.85	89.65	-329.0	43.3	0.5704
2.2	17.90	89.57	-320.0	37.8	0.6160
2.4	18.00	89.48	-314.0	32.8	0.6647
2.6	18.05	89.48	-308.7	29.0	0.6963
2.8	18.10	89.40	-305.5	26.3	0.7177
3.0	18.15	89.40	-301.6	25.0	0.7284
3.2	18.15	89.40	-297.1	24.7	0.7266
3.4	18.15	89.40	-293.1	25.2	0.7142
3.6	18.15	89.40	-289.8	26.2	0.6923
3.8	18.15	89.40	-287.1	27.5	0.6632
4.0	18.15	89.40	-285.0	28.9	0.9290

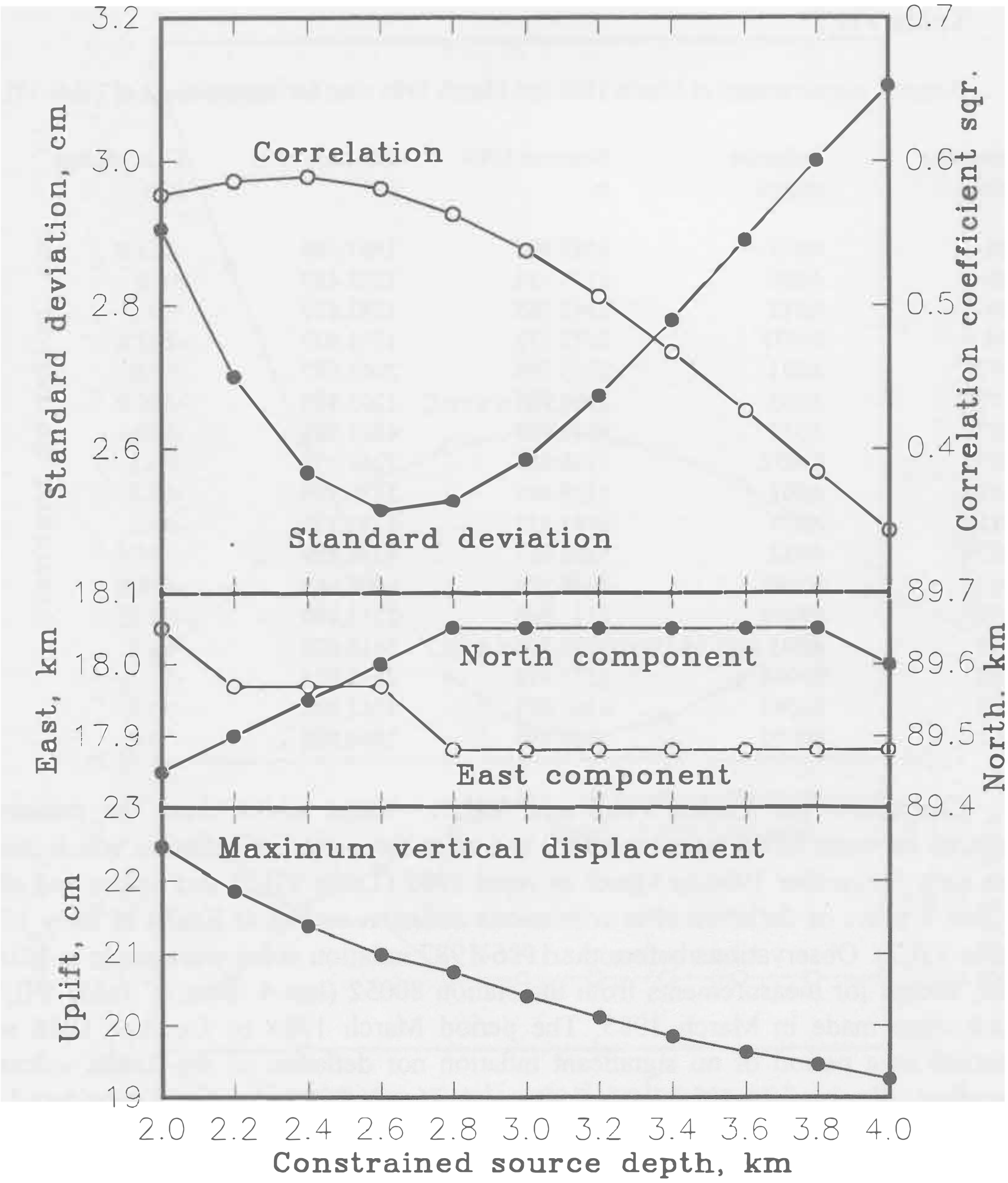

Fig. VII,4. Variation of computed source parameters as constrained source depth is varied from 2.0 km to 4.0 km for a period of rather rapid inflation during late 1986 and early 1987. The computation uses measurements presented in Table VII,5 of 17 lines (Fig VII,6) with fairly symmetrical distribution with respect to the estimated source. Measurements before the inflation were made in March 1986 or March 1985. Measurements after the inflation were made in March 1987. As both distance measurements and tilt measurements suggest almost no ground deformation in the Krafla area between March 1985 and March 1986 (Tryggvason 1984) it is considered justifiable to combine these observations. The minimum standard deviation (top) between observed length changes and those predicted by the Mogi model are found for constrained depth of 2.6 km.

Table VII,7

Distance measurements of March 1989 and March 1995 used for computations of Table VII,6

Geodimeter station	Reflector station	Distance 1989 m	Distance 1995 m	Dist. change mm
A005	A003	1567.502	1567.390	-111.9
A005	A006	1273.491	1273.497	+6.6
A005	A012	2543.785	1543.816	+31.7
A005	79077	1671.172	1671.029	-143.4
79077	A001	2063.795	2063.697	-98.6
79077	A003	1205.595	1205.495	-100.0
79077	A012	4201.923	4201.783	-140.1
79077	80052	3248.453	3248.377	-76.1
77012	A001	2139.485	2139.396	-89.3
77012	A003	2743.327	2743.273	-54.2
77012	A012	5238.997	5238.890	-107.5
77012	80048	4608.204	4608.065	-138.8
77012	80049	2313.965	2313.890	-74.7
80052	A001	3616.766	3616.679	-86.2
80052	80048	2333.912	2333.854	-57.7
80052	80049	4763.021	4762.930	-90.7
80052	80050	2860.896	2860.816	-79.0

Comments on Tables VII,5 and VII,7: These tables show the measured distances between EDM stations before and after the period of inflation which lasted from early November 1986 to March or April 1987 (Table VII,5) and before and after the first 6 years of deflation after continuous deflation started at Krafla in early 1989 (Table VII,7). Observations before the 1986-1987 inflation event were made in March 1986, except for measurements from the station 80052 (last 4 rows of Table VII,5) which were made in March 1985. The period March 1985 to October 1986 was observed as a period of no significant inflation nor deflation of the Krafla volcano. Therefore, observations of March 1985 and March 1986 are both considered to represent the condition immediately before the inflation which commenced in early November 1986.

The distribution of distance changes is very similar as shown in the last column of these tables, with the difference that increased length is generally seen in Table VII,5 while decreasing length is seen in Table VII,7. Exception is line A005 to A012 but that is caused by its location and orientation.

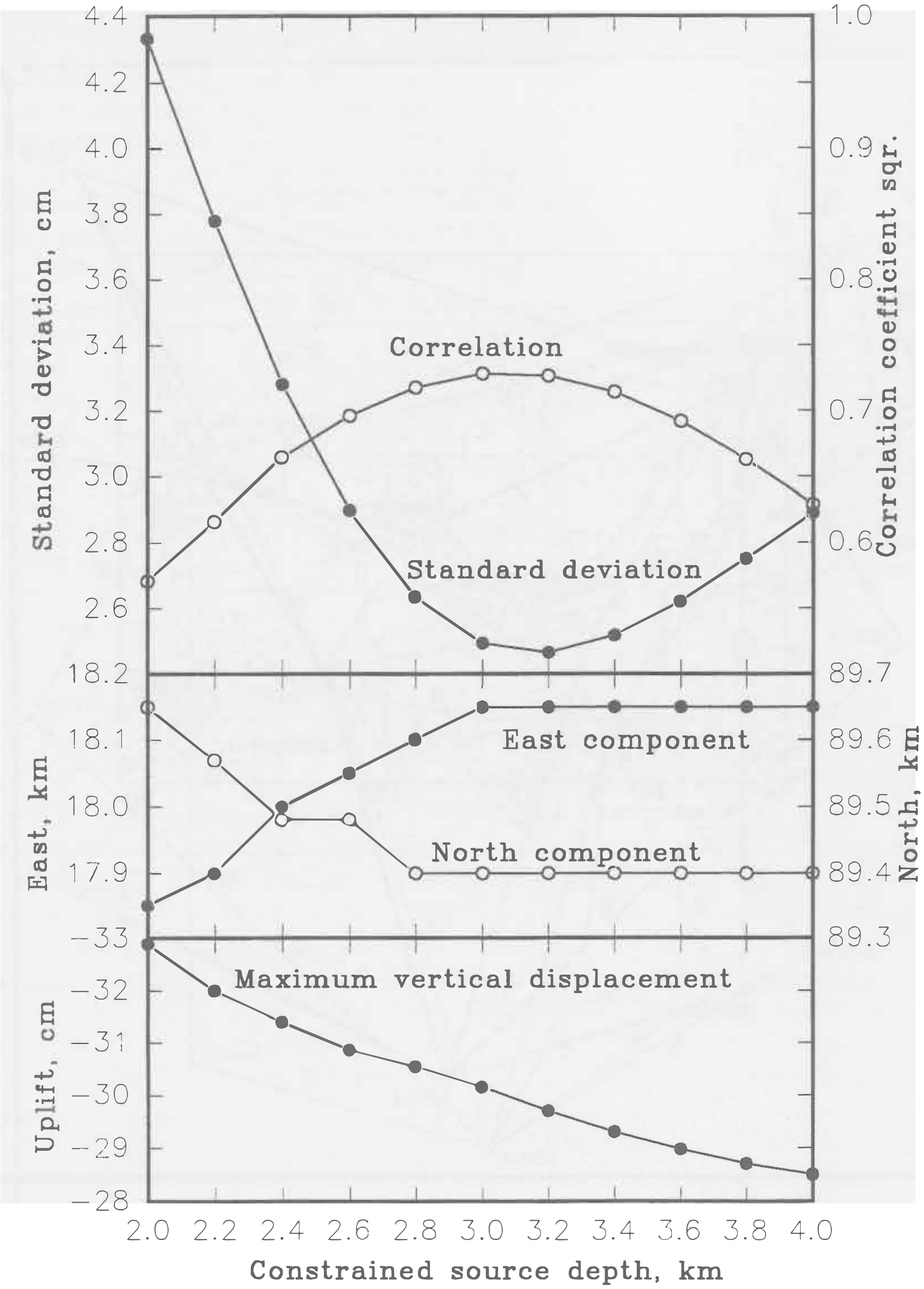

Fig. VII,5. Variation of computed source parameters as constrained source depth is varied from 2.0 km to 4.0 km for an extended period of deflation. The observational data are length measurements in March 1989 and March 1995 (Table VII,7) of the same 17 lines as used to obtain data presented in Fig. VII,4. Note that the minimum standard deviation is found for source depth of 3.2 km.

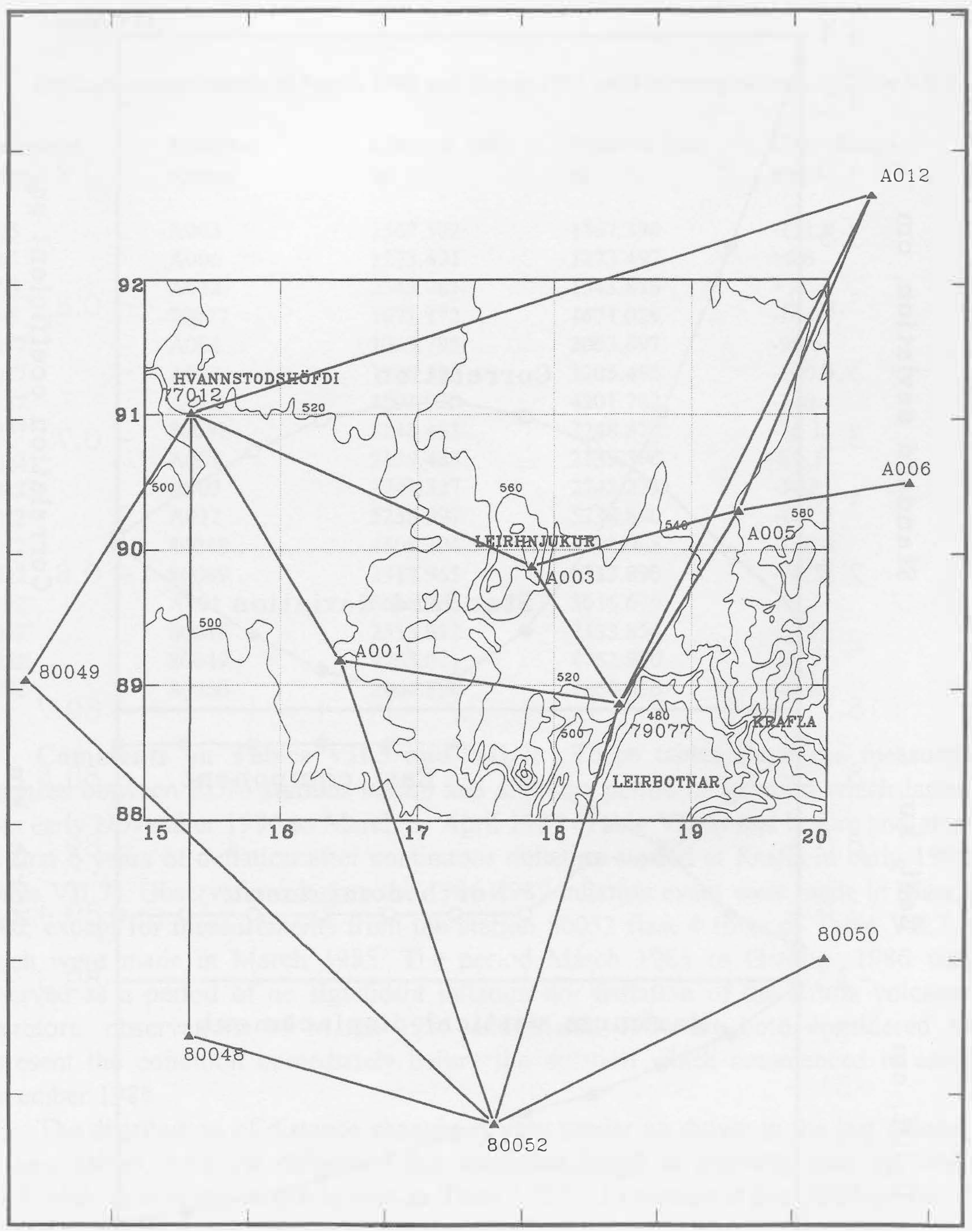

Fig. VII,6. Map showing the 17 lines of EDM used to obtain the results presented in Figs VII,4 and VII,5 and Tables VII,4 and VII,6.

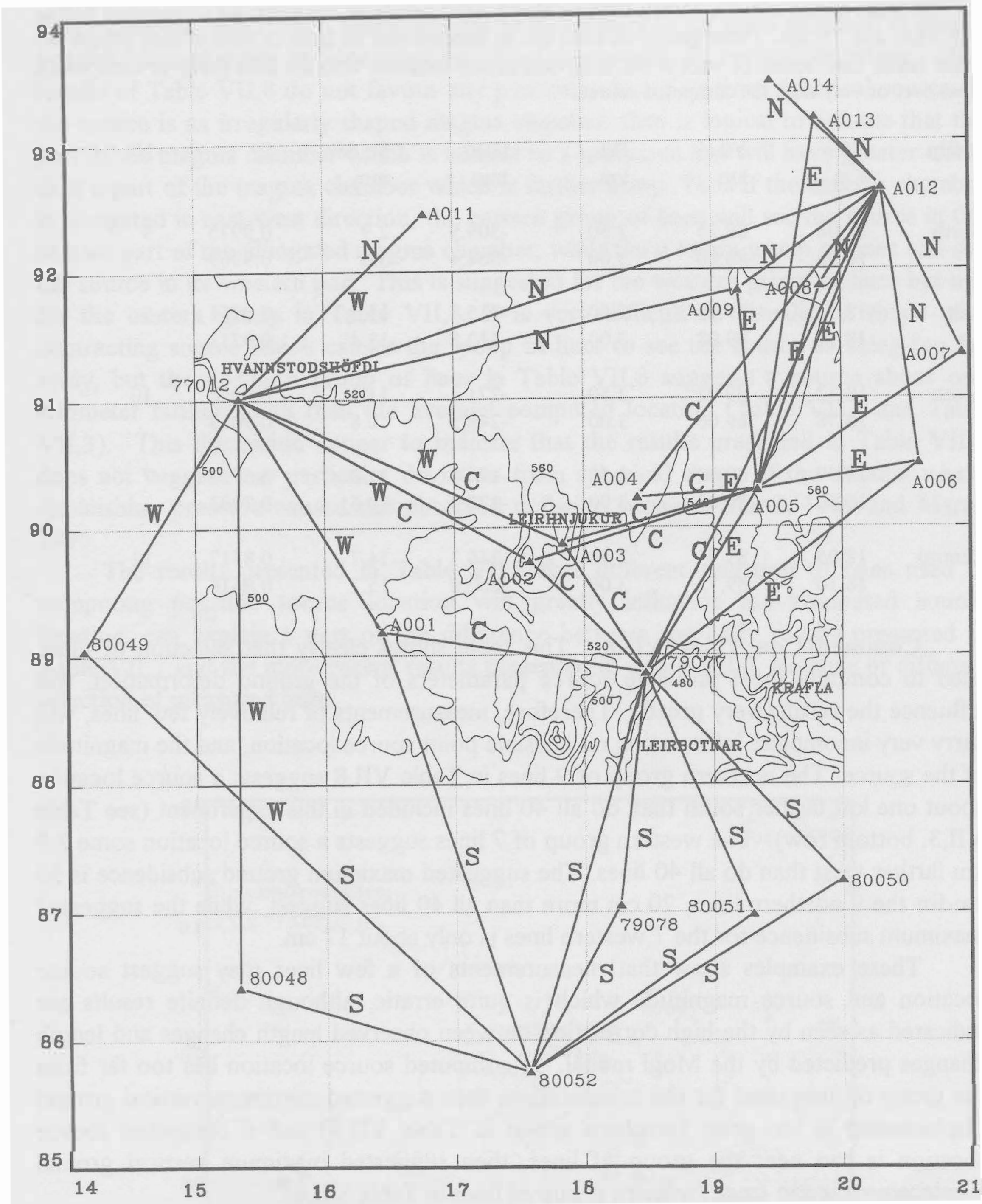

Fig. VII,7. A map showing the lines used to obtain data of Fig. VII,8 and Table VII,8. Groups of lines are marked with capital letters, **N** for the northern group, **E** for the eastern group, **S** for the southern group, **W** for western group and **C** for the central group. Five lines are included in two groups each.

Table VII,8

Computed source parameters by using length changes of five selected groups of lines observed over the same period of time, March 1989 to March 1995 Solutions are given for constrained depths of 2.5 km and 3.0 km. These groups of lines are so selected that all lines in each of four groups are either north, east, south, or west of the computed source location, with the fifth group of lines which cross over or very near the computed source.

Group	X0 Km	Y0 km	H0 km	DH0 mm	St. dev. mm	R^2	N
North	17.08	88.25	2.50	-509.9	2.9	0.9975	9
	16.98	88.00	3.00	-504.4	3.6	0.9969	
East	18.34	89.34	2.50	-315.7	11.5	0.9761	9
	18.10	89.08	3.00	-412.8	13.4	0.9713	
South	18.32	89.02	2.50	-271.1	11.1	0.8998	10
	18.38	89.06	3.00	-249.5	10.8	0.9033	
West	15.57	89.00	2.50	-176.0	21.8	0.6798	7
	15.50	89.08	3.00	-170.7	19.6	0.7093	
Central	18.05	89.93	2.50	-246.3	14.7	0.8717	12
	18.10	89.72	3.00	-260,0	15.7	0.8616	

Comments on Table VII,8: This table shows clearly that selection of lines, used to compute most probable source parameters of the ground deformation, will influence the results very greatly. Therefore, measurements of relatively few lines, will carry very incomplete information on possible point source location, and the magnitude of the source. The northern group of 9 lines in Table VII,8 suggests a source location about one km farther south than do all 40 lines included in this experiment (see Table VII,3, bottom row). The western group of 7 lines suggests a source location some 2.5 km farther west than do all 40 lines. The suggested maximum ground subsidence is 50 cm for the 9 northern lines, 20 cm more than all 40 lines suggest, while the suggested maximum subsidence for the 7 western lines is only about 17 cm.

These examples show that measurements of a few lines may suggest source location and source magnitude which is quite erratic, although definite results are indicated as seen by the high correlation between observed length changes and length changes predicted by the Mogi model. If computed source location lies too far from the group of lines used for the computation, then suggested maximum vertical ground displacement is too great (northern group in Table VII,8) and if computed source location is too near the group of lines, then suggested maximum vertical ground displacement is too small (western group of lines in Table VII,8).

The reason for these erratic solutions for possible point source parameters is poorly known. It is quite certain that the strain field in case of either inflation or deflation is somewhat irregular because of irregularity of elastic parameters in the near-surface formation, and also because of the topography of the immediate vicinity of the stations. The fissures or ground cracks are known to respond to both inflations and deflations differently from unbroken ground surface, so if a observing station is near a ground fissure, its horizontal displacement depends on which side of the fissure the station is located.

A possible reason for this anomalous computed location of a source of ground deformation, is that the source itself is irregular. It has been suggested (Ewart et al. 1991) that the source consists of two or several separate magma chambers, possibly interconnected. Also that a single magma chamber may be far from spherical in shape, possibly disk-shaped, or elongated in either horizontal or vertical direction. The results of Table VII,8 do not favour any particular deviation from spherical source. If the source is an irregularly shaped magma chamber, then is logical to assume that the part of the magma chamber which is nearest to a measured line will have greater effect than a part of the magma chamber which is farther away. Thus if the magma chamber is elongated in east-west direction, the eastern group of lines will see the source in the eastern part of the elongated magma chamber, while the western group of lines will see the source in its western part. This is suggested for the western group of lines but not for the eastern group in Table VII,8. It is very difficult to visualise a shape of a contracting source which causes the group of lines to see the source as being too far away, but the northern group of lines in Table VII,8 suggests a source about one kilometer farther south than the average computed location (Table VII,1 and Table VII,3). This discussion appear to indicate that the results presented in Table VII,8 does not suggest any particular deviation from spherical shape of the volume where diminishing pressure caused the observed deflation between March 1989 and March 1995.

The results presented in Table VII,8 that different selection of lines used in computing possible source location will greatly influence the computed source location, can explain a part of the difference between the early results presented in Table VII,1 and the more recent results presented in Table VII,3, because of different selection of measured lines.

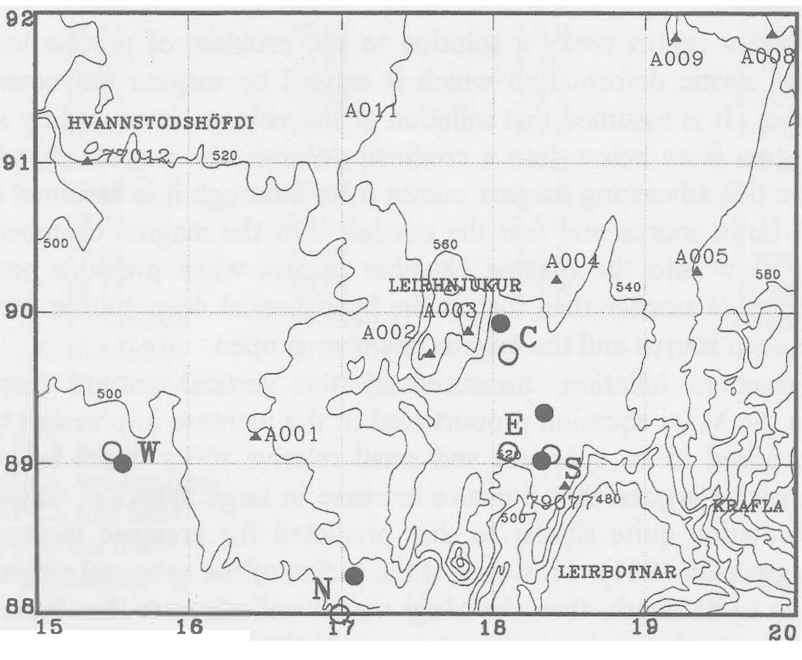

Fig. VII,8. Map of the computed source parameters as obtained from the groups of lines presented in Fig. VII,7. Solid circles are solutions for constrained depth of 2.5 km and open circles for constrained depth of 3.0 km.

DISCUSSION AND CONCLUSION

This report deals with the application of single source point model, the Mogi model, to analyse and search for a source of deformation at Krafla volcano, Iceland. It may be questioned if the point source model should be applied, in stead of some more complex model. It is well known that the observed ground deformation in the Krafla region is quite complex, and only a fraction of it is purely elastic, but the Mogi model assumes a perfectly elastic deformation. Most of the clearly visible deformation in the Krafla region is non-elastic and related to fault displacements and opening of fissures of the Krafla fissure zone, an elongated narrow zone of dense ground fissures and fault scarps extending from the Krafla volcano northwards to the north coast of Iceland, and southwards some 20 km.

The non-elastic ground deformation in the Krafla fissure zone is related to plate tectonics, as the east flank of the fissure zone is displaces eastward, relative to its west flank, representing widening of the fissure zone amounting to several meters during the 9 year period December 1975 to September 1984 (Tryggvason 1984, 1994). At the same time vertical fault displacements caused the fissure zone to subside and its flanks to be uplifted.

The elastic ground deformation is usually not clearly visible and is observed with more or less sophisticated equipment and techniques. It appear to be related to two different processes, plate tectonics and magma movement, although these processes cannot always be separated. The plate tectonics part of the elastic deformation includes horizontal east-west contraction of the flanks of the Krafla fissure zone during events of rifting, and associated ground tilt down away from the fissure zone. The magmatic part of the elastic deformation includes inflation and deflation of a near circular region, centred near the center of the Krafla volcanic complex. The deflation of the Krafla volcano was usually associated with some ground rifting somewhere along the Krafla fissure zone.

The present report seeks a solution to the problem of precise location of the source of the elastic deformation which is caused by magma movement within the Krafla volcano. It is assumed that inflation of the volcano is caused by a flow of low viscosity magma from below into a confined volume, the magma chamber. It is not known where this advancing magma comes from although it is assumed that it comes from a deep large source and that the conduit into the magma chamber is relatively narrow. The flow into the magma chamber occurs when pressure potential in the magma chamber is smaller than that in the hypothetical deep source and the conduit between the deep source and the magma chamber is open.

The observed inflation, measured by the vertical ground displacement, is according to the Mogi equation proportional to the increase in pressure at the source, which is supposed to be spherical and small relative to its depth below the earth's surface. It may be argued that pressure increase in large spherical volume will cause surface deformation quite similar to that predicted for pressure increase in a small volume (Tryggvason 1981). However, if the radius of the spherical magma chamber is great, relative to its depth, then the Mogi model will estimate the depth to its center wrongly in the way that estimated depth is smaller than true depth. This error in depth estimate will amount to about 10% of the true depth, if the radius of the magma chamber is 50 % of the depth to its center. If the radius of the magma chamber is 70% of the depth, then the Mogi model will estimate the depth to its center about 20%

smaller than true depth. In these cases the shape of the inflation bulge will be very similar to that predicted by the Mogi model for a small source volume.

The Mogi equation is claimed to be correct only for a model of perfectly elastic and homogenous half-space. When it is applied to the real earth, none of these claims are fulfilled. The term "half-space" means that its surface is flat, which is not true for the real earth. The effect of topographic features on the displacement of the earth's surface will not be discussed here, although it can certainly be quite significant, and it will cause individual measurements, be it either ground tilt, ground elevation or lateral displacement, to deviate from that predicted by the Mogi model.

The requirement of homogenous perfectly elastic material is far from being fulfilled in the real earth. The elastic properties of the earth change greatly with depth, and also laterally in the near surface formations. It is likely that the change of elastic properties with depth in the earth will cause systematic errors in estimated depth of a source of ground deformation, although this has not been studied by the present author.

Table VIII,1

Average location of apparent or most probable center of deformation at Krafla for several periods for which several solutions are available. The average location is obtained by attaching weight to each solution, this weight is proportional to the square of the product of computed maximum vertical ground displacement and the correlation coefficient squared. The apparent source depth is usually constrained (R in the depth column) at either 2.5 or 3.0 km below ground surface.

Period	X0, km	Y0, km	Depth, km	Remarks
1977-1979	17.36	89.59	2.5 R	4 stations, 1)
1977-1979	16.79	89.41	3.0 R	4 stations, 1)
1977-1979	17.56	89.69	2.5 R	3 stations, 2)
1977-1979	17.41	89.64	3.0 R	3 stations, 2)
1977-1979	17.51	89.42	3.0 R	12 stations, 3)
1981-1983	16.83	89.43	2.42	6-10 stations, 4)
1981-1983	16.93	89.43	2.5 R	6-10 stations, 5)
1981-1983	16.75	89.34	2.5 R	5-9 stations, 6)
1981-1983	16.78	89.42	3.0 R	5-9 stations, 6)
1984-1989	17.27	89.47	2.5 R	9-11 stations, 7)
1989-1994	17.93	89.11	2.5 R	9-11 stations, 8)
1989-1994	17.09	89.18	2.5 R	8 stations, 9)
1989-1994	18.13	89.53	2.5 R	11 stations, 10)
1977-1979	17.33±0.28	89.55±0.12		Average, 11)
1981-1983	16.82±0.06	89.40±0.04		Average, 11)
1984-1994	17.60±0.44	89.32±0.18		Average, 11)

1) From Table IV,5, two last lines.
2) From Table IV,6, two last lines.
3) From Table IV,2, first line.
4) From Table V,2, last line.
5) From Table V,3, last line.
6) From Tables V,5 and V,6, last line.
7) Calculated from inflation data of Table VI,1.
8) Calculated from deflation data of Table VI,1, omitting the period 84 06 09 to 84 10 03.
9) From Table VI,17, line 5.
10) From Table VI,18, line 5.
11) Direct average of four or five lines above with standard deviation.

No effort has been made to combine distance measurements and tilt measurements into a single solution for parameters of the central source of deformation at Krafla. This is partly because the two types of observations were rarely made at the same time, and with the rapid deformation in progress, measurements made at different times could not easily be combined into a single solution. Also, if two different families of data are combined into a single solution, the relative importance or weight of each family need to be included into the analysis.

Table VIII,1 shows the result of some representative solutions for location of hypothetical point (or spherical) source of deformation at Krafla, based on tilt observations. No obvious shift in the computed source location is evident, although some drift towards south-east is vaguely suggested.

Table VIII,2

Probable source of inflation or deflation at Krafla, based on tilt observation at 3 optical levelling tilt stations for periods between observations, when either inflation or deflation has dominated the deformation.

First Observation	Last observation	X0, km	Y0, km	DH0 mm	St. dev. µrad	R^2
77 06 14	77 07 18	16.97	89.29	203.7	8.16	1.0000
77 07 18	77 08 16	17.08	89.21	147.2	10.09	0.5633
77 08 16	77 09 11	20.32	89.93	-987.0	51.50	0.9828
77 09 11	77 12 02	17.18	89.42	635.7	14.15	0.9170
77 12 02	78 01 11	17.10	89.34	-767.4	21.89	0.8750
78 01 11	78 05 19	17.46	89.42	703.6	27.51	0.9622
78 05 19	78 06 28	16.65	90.08	160.5	29.27	0.9182
78 06 28	78 08 05	16.65	89.56	-347.5	20.66	0.8475
78 08 05	78 09 30	16.95	89.64	352.1	14.73	0.9088
78 09 30	78 11 12	17.18	89.50	-570.4	15.97	0.9244
78 11 12	79 02 16	17.56	89.42	692.4	11,58	0,9609
79 08 02	79 11 22	16.92	89.08	224.5	6.07	0.9160
80 05 09	80 06 30	15.10	89.92	162.9	17.10	0.8525
80 06 30	80 07 14	16.54	89.21	-456.0	28.89	0.7237
81 06 19	81 11 06	17.79	89.77	122.4	11.82	0.8025
81 11 06	81 11 21	16.21	89.29	-442.2	36.37	0.6300
81 11 21	82 02 21	17.00	89.42	417.6	14.92	0.8942
82 02 21	83 06 24	16.56	89.56	168.2	17.27	0.7695
83 06 24	84 06 10	17.25	89.42	94.7	9.82	0.9804
84 06 10	84 09 06	16.52	89.34	-534.6	38.81	0.6254
84 10 04	84 12 02	17.20	89.64	233.4	10.72	0.8063
86 10 22	87 04 28	16.98	89.56	213.6	9.63	0.9638
87 04 28	89 06 23	16.98	89.34	106.2	6.41	0.4767
89 06 23	94 07 05	17.05	89.50	-209.2	11.37	0.6072
1977-1979	Inflation	17.10±0.29	89.44±0.29	N = 8		
1977-1979	Deflation	17.81±1.46	89.58±0.22	N = 4		
1980-1984	Inflation	16.74±0.91	89.62±0.20	N = 5		
1980-1984	Deflation	16.42±0.15	89.28±0.05	N = 5		
1984-1994	Inflation	17.05±0.10	89.50±0.13	N = 3		
1984-1994	Deflation	17.05	89.50	N = 1		

The results presented in Table VIII,1 are based on observational data of variable quality, as the station network was gradually being expanded and improved. Therefore, results obtained at different times are not fully comparable. This is particularly disturbing as individual tilt stations appear to observe tilt, due to the central source of deformation, with consistent deviation from that predicted (Tryggvason 1995). An effort to avoid this problem was made by computing the apparent source parameters by using only three tilt stations, which were established in 1976 and 1977, were frequently observed and were observed to respond to inflations and deflations with well detected tilt. These stations (0000, 0080, and 0090 see Table I,1) are located at 3 to 5 km distance from the center of inflation/deflation towards north-west, west, and south. Table VIII.2 shows the result of this experiment. This table is based on the same data as Table IV,6 but the difference is that in Table IV,6 the correlation between model tilt and observed radial component of tilt is maximised while in Table VIII,2 the standard deviation between the observed tilt vector and the model tilt vector is minimised. Further, Table VIII,2 includes several periods which are not included in Table IV,6.

The period 77 08 16 to 77 09 11 includes subsidence event on September 8, 1977. Extensive rifting occurred in the vicinity of Leirhnjukur during this event, suggesting major non-elastic deformation, which again suggests that obtained apparent source parameters are invalid.

All periods including subsidence events, also include some period of inflation, but Table VIII,2 contains only those deflation events where period between tilt observations contains much more deflation than inflation, as judged by daily observations at the Krafla power station water tube tiltmeter. Deflations of November 1981, and September, 1984 caused significant non-elastic deformation (ground rifting) near the center of deformation, making the obtained source parameters rather uncertain.

The average values of coordinates of the computed "most probable" point source at the bottom of Table VIII,2 do not show any definite movement of this source. Comparison of average values for the first period, 1977 to 1979, and the last period, 1984 to 1994 show the same source location for inflation periods, and the difference found in location of source of deflation events is mostly caused by the computed location for the deflation event of September 1977, which is not reliable because of large scale non-elastic deformation in the near-source area.

The average computed source location for the period 1980 to 1984 appear to lie about 0.5 km farther west than that for the previous or succeeding periods. This can not be considered significant as the standard deviation of the east coordinate of 0.91 km suggest that observed tilt has been erratic during this period, probably to large extend caused by processes other than the Krafla central inflation

It has been mentioned earlier in comments on Table VII,3 that the "most probable" source location had apparently drifted towards south-east according to solutions based on EDM observations.

As the solutions based on tilt observations do not suggest any significant change in location of the source of deformation, it seems that the apparent drift in this location based on solutions using EDM observations may be the result of different selection of lines of measurements during different periods.

Table VIII,3. Comparison of computed location of hypothetical point source of ground deformation at Krafla. The solutions for tilt measurements are taken from Table VIII,2 and those based on EDM observations are taken from discussion on Table VII,3.

Type of observations	Period	Average X0 km	Average Y0 km
Tilt during inflations	1977 to 1979	17.10 ± 0.29	89.44 ± 0.29
Tilt during inflations	1980 to 1984	16.74 ± 0.91	89.62 ± 0.20
Tilt during inflations	1984 to 1994	17.05 ± 0.10	89.51 ± 0.13
EDM	1978 to 1981	17.51	89.65
EDM	1982 to 1989	18.16	89.49
EDM	1989 to 1995	18.17	89.35

The conclusion of this report is that the source of deformation at Krafla remained at the same location throughout the period of volcanic and tectonic activity 1975 to 1989. The absolute location of this center is not well established, as the EDM observations place it about one km farther east than do the tilt measurements. The average location, using all values of Table VIII,3 is 17.45 ± 0.55 km east, 89.50 ± 0.10 km north in the rectangular coordinate system used here, which is equivalent to:

65° 42' 53" ± 4" N

16° 47' 59" ± 44" W

This location is about 0.5 km to the south-west of the EDM station A003 on Leirhnjúkur. The large error limit on the east coordinate is caused by different solutions for EDM observations and tilt observations. This may be the result of different distribution of this two types of stations. Most tilt observations are from the region south-west of the center of deformation while most distance measurements were made to the north-east of the center.

The depth to the hypothetical point source is not well established. This is partly because the depth is considered poorly determined by the Mogi model as the earth deviates greatly from the strict requirements of the Mogi model, and these deviations (large source volume, variation of elastic properties with depth) will cause an error in the estimate of the source depth. Therefore, all source depth estimates, based on the Mogi model, should be considered as uncertain.

Table VIII,4 shows several depth estimates based on tilt observations. Many of these estimates are uncertain but it appears that depth of between 2 and 3 km is favoured if the estimate is based on tilt observations at the tilt stations nearest to the apparent center of deformation. If however, the nearest stations are not included in the computation of probable source of deformation, then the depth estimate becomes 4 to 8 km, but at the same time, this estimate becomes less trustworthy because the observed tilt at the more distance stations is small, and may be greatly influenced by observational errors and by processes other than those of the source of inflations and deflations of Krafla volcano.

This increase of estimated depth of the source of deformation as more distant tilt stations are used can be explained by large vertical dimension of the source (or magma chamber) The near tilt stations will see the effect of the top of the magma chamber while stations at greater distance will be more affected by deeper part of the source. This can not be used to estimate the vertical extend of the magma chamber, but it should amount to several kilometers.

The distance measurements appear to favour 2.6 to 3.2 km source depth (Table VII,2, Figs. VII,4 and VII,5). No effort has been made to study if the estimated depth depends on the distance from the center of deformation to the stations used in the analysis of source parameters.

All the treatment in this report related to the source of deformation at Krafla uses the single source model of Mogi (1958), which implies that the source is treated as a spherical body of increased or decreased pressure. The size of this spherical body need to be small relative to its depth below the earth's surface for the Mogi equations to be correct, but it can be argued that the surface effect of a large body, with radius as large as 50% to 70% of the depth to its center, will be observed as near identical to those of smaller source (Tryggvason 1981). Because of this, the volume of the source can not be estimated from the observational data here considered. The various estimates of the depth to the center of hypothetical spherical source of deformation at Krafla are listed in Table VIII,4.

Table VIII,4.

Estimates of source depth based on Mogi model treatment of tilt observations.

Years	Depth, km	Reference	comments
1977-1979	3.0	Table IV,3	7 tilt stations
1977-1979	2.5	Table IV,4	6 tilt stations
1977-1979	2.5	Table IV,5	4 stations, 2.5 km rather than 3.0
1977-1979	2.5	Table IV,6	3 stations, 2.5 km rather than 3.0
1977-1979	3.0	Fig. IV,5	11 tilt stations
1981-1983	2.42	Table V,2	Weighted average
1983-1984	4.0	Table VI,2	7 tilt stations
1984	2.4	Table VI,3	During eruption of 1984
1984-1985	2.4	Table VI,4	8 tilt stations
1986-1987	2.8	Table VI,5	8 tilt stations
1988-1989	2.4	Table VI,6	8 tilt stations
1989-1990	2.4	Table VI,7	8 tilt stations
1990-1992	2.4	Table VI,8	8 tilt stations
1986-1987	2.7	Table VI,9	11 tilt stations
1984-1985	2.9	Table VI,10	18 tilt stations
1984-1985	4.5 to 5.0	Table VI,11	13 distant (> 4.5 km) stations
1984-1985	6.5	Table VI,12	7 stations at 4.5 - 10 km distance
1984-1985	2.8	Table VI,13	10 nearest (< 7.5 km) stations
1985-1989	4.0	Table VI,15	10 tilt stations
1985-1989	(8.0)	Table VI,16	6 distant (> 5 km) stations
1984-1994	5.0	Table VI,20	6 tilt stations at medium distance

REFERENCES

Björnsson, A., Johnsen, G., Sigurdsson, S., Thorbergsson, G., and Tryggvason, E.: Rifting of the plate boundary in North Iceland 1975-1978. J. Geophys. Res. **84**, 3029-3038, 1979.

Björnsson, A. and Eysteinsson, H.: Breytingar á landhæð við Kröflu 1974-1995: Samntekt á landhæðarmælingum. Orkustofnun **OS-98002**; Nordic Volcanological Institute **9801**, 1-161, 1998

Czubik, E: Präzisionshöhenmessungen in Island 1986. Das Markscheidewesen **95**, 89-92, 1988.

Ewart, J.A., Voigt, B., and Björnsson, A.: Elastic deformation models of Krafla volcano, Iceland, for the decade 1975 through 1985. Bull Volcanol. **53**, 436-459, 1991

Mogi, K.: Relations between the eruptions of various volcanoes and the deformation of the ground surfaces around them. Bull. Earthq. Res. Inst. **36**, 99-134, 1958.

Möller, D., and Ritter, B.: Geodetic measurements and horizontal crustal movements in the rift zone of NE-Iceland. J. Geophys. **47**, 110-119, 1980

Rymer, H., and Tryggvason, E.: Gravity and elevation changes at Askja, Iceland. Bull. Volcanolog. **55**, 362-371, 1993.

Spickernagel, H: Results of height measurements in northern Iceland 1965/1977. J. Geophys. **47**, 120-124, 1980.

Torge, W.: Gravity and height variations connected with the current rifting episode in northern Iceland, Tectonophysics, **71**, 227-240, 1981

Tryggvason, E.: Distance measurements in 1977 in the Krafla-Mývatn area and observed ground movements, Nordic Volcanological Institute **7810**, 1-47, 1978.

Tryggvason, E.: Tilt observations in the Krafla-Mývatn area, progress report. Nordic Volcanological Institute **7907**, 1-55, 1979.

Tryggvason, E.: Pressure variations and volume of the Krafla magma reservoir. Nordic Volcanological Institute **8105**, 1-17, 1981.

Tryggvason, E.: Accuracy of tilt observations through optical leveling. Nordic Volcanological Institute **8302**, 1-32, 1983.

Tryggvason, E.: Widening of the Krafla fissure swarm during the 1975-1981 volcano-tectonic episode. Bull. Volcanol. **47**, 47-69, 1984.

Tryggvason, E.: Myvatn lake level observations and ground deformation during a Krafla eruption. J. Volcanol Geotherm. Res., **31**, 131-138, 1987.

Tryggvason, E.: Distance measurements in the Krafla-Gjástykki area 1983-1993. Nordic Volcanological Institute **9302**, 1-200, 1993

Tryggvason, E.: Surface deformation at the Krafla volcano, north Iceland, 1982-1992. Bull. Volcanol. **56**, 98-107, 1994

Tryggvason, E: Optical levelling tilt stations in the vicinity of Krafla and the Krafla fissure swarm, observations 1976 to 1984. Nordic Volcanological Institute **9505**, 1-218, 1995.